TRAINING COURSE ON RADIATION DOSIMETRY:

A monolithic silicon telescope for solid state microdosimetry

Andrea Pola, Politecnico di Milano

Abstract

- **The detection system**
- **Microdosimetry of neutron fields: numerical studies and experimental characterizations.**
- **Quality assessment of clinical proton beams: microdosimetric characterization and direct comparison with TEPCs.**
- **Microdosimetry of carbon beams: preliminary tests.**
- **A silicon microdosimeter integrated into a nanodosimeter.**

MONOLITHIC SILICON TELESCOPE ΔE-E (ST-Microelectronics)[10]

Sensitive area: 1 mm^2

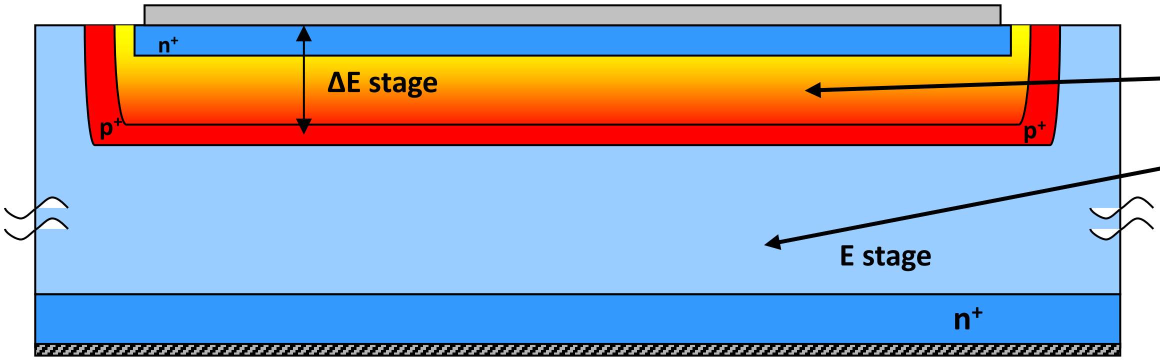

ΔE thickness: ~2 μm

E thickness: ~500 μm

Schematics

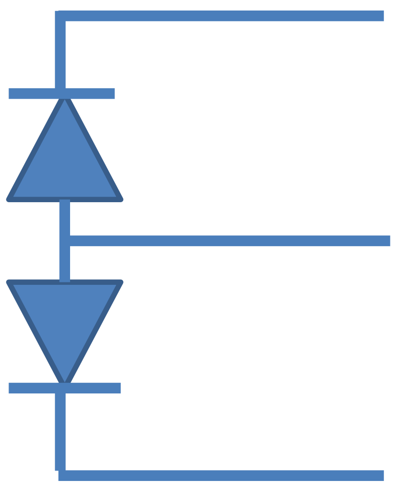

ΔE stage

E stage

Monolithic Si - ΔE/E detector
(ST-Microelectronics & LNS INFN)

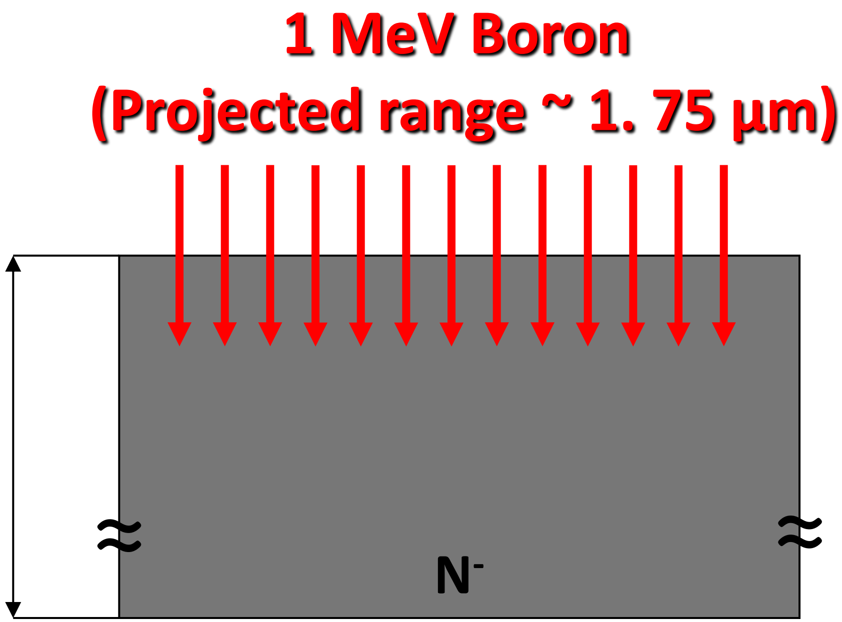

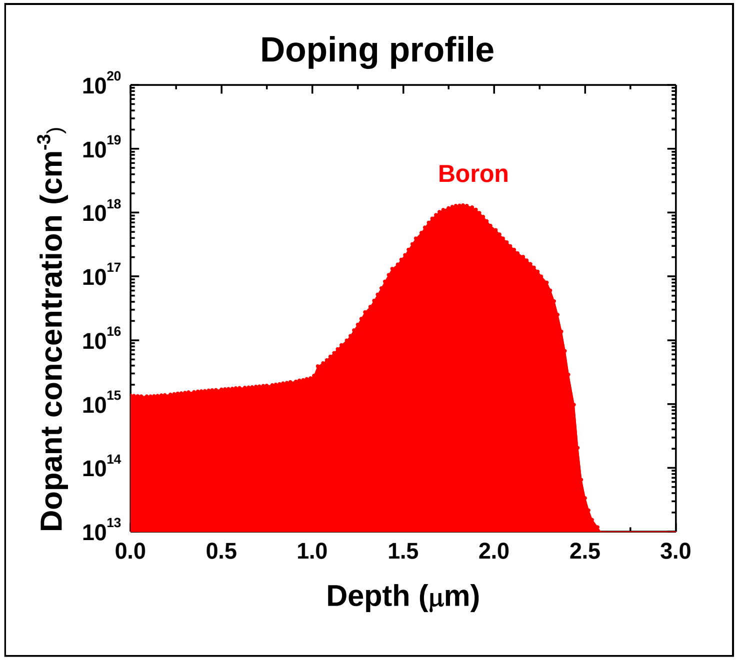

Monolithic Si - ΔE/E detector

Process (ST-Microelectronics & LNS INFN - 1996)

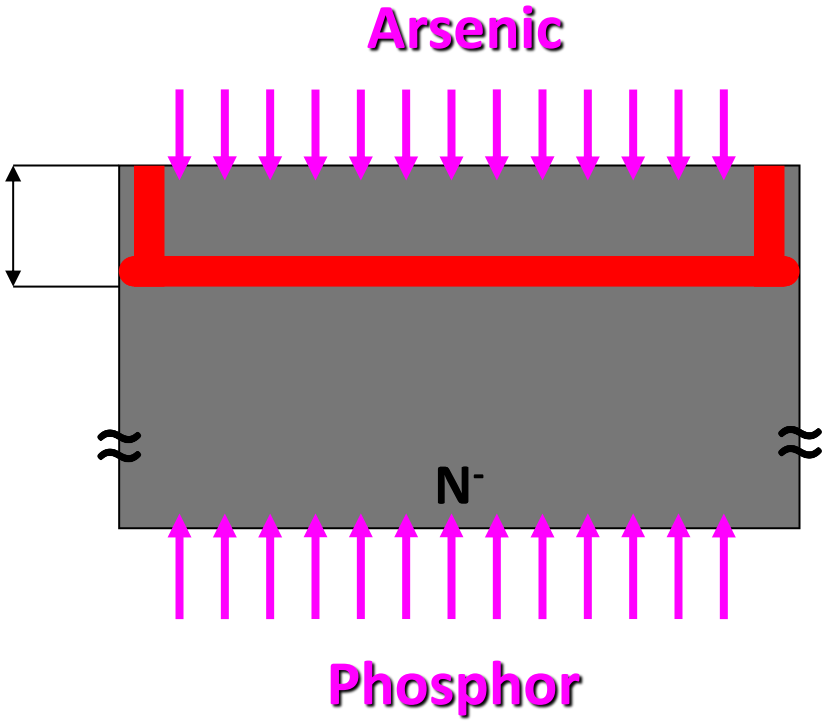

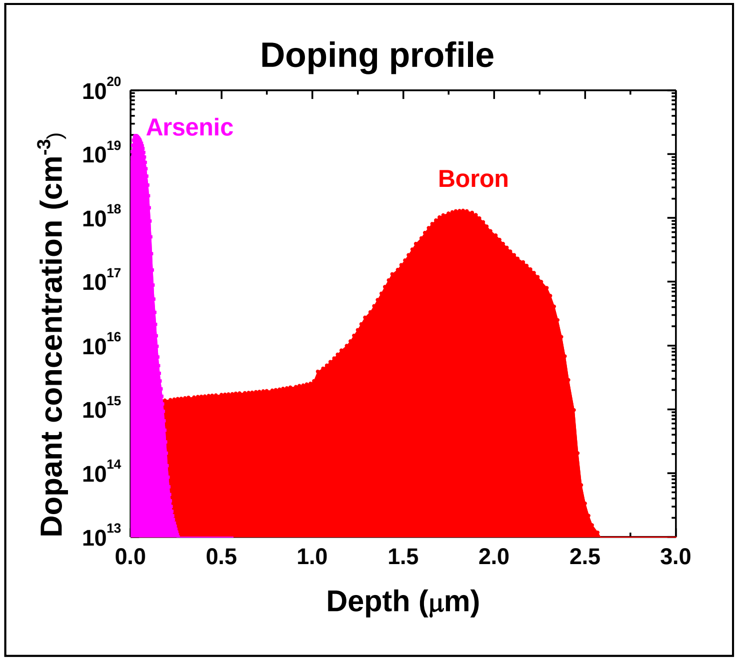

Monolithic Si - ΔE/E detector

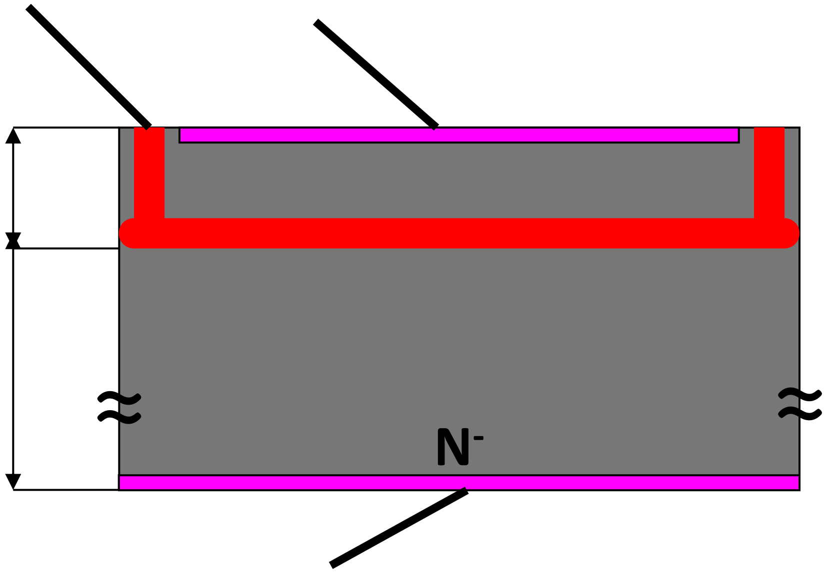

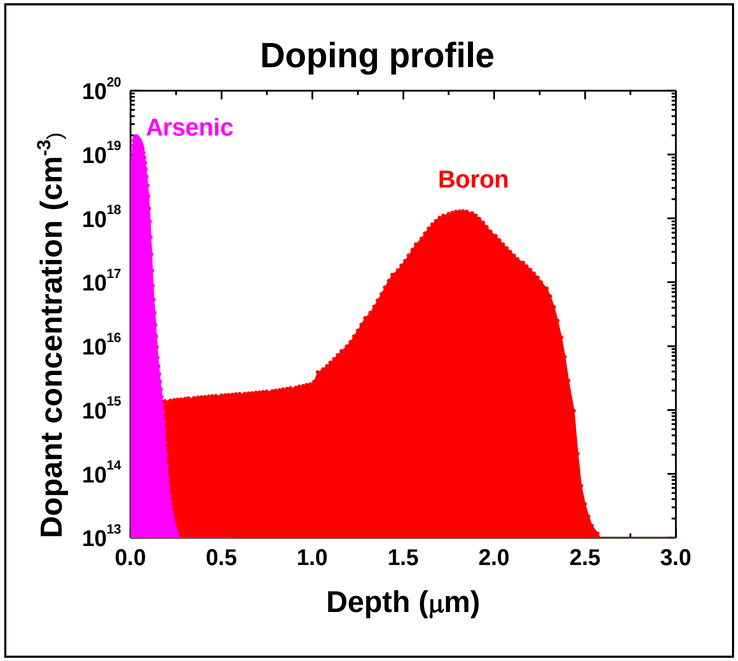

Monolithic Si - ΔE/E detector

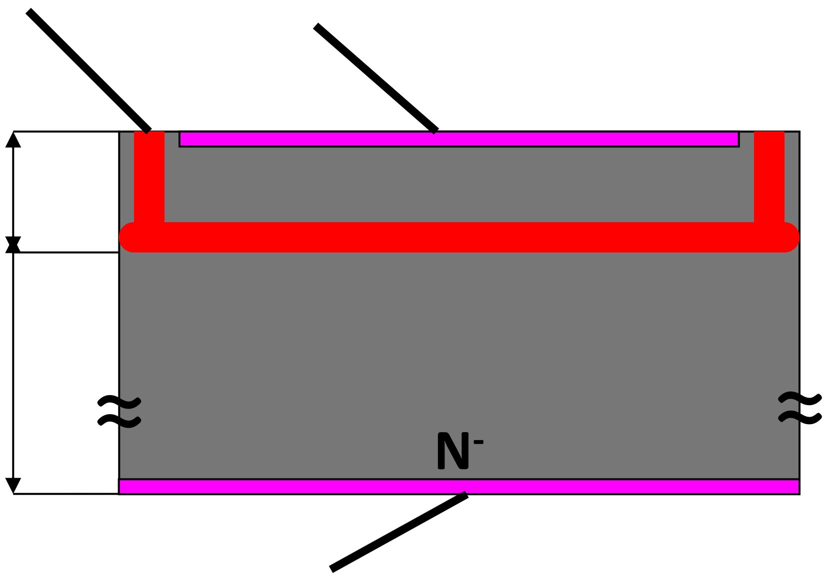

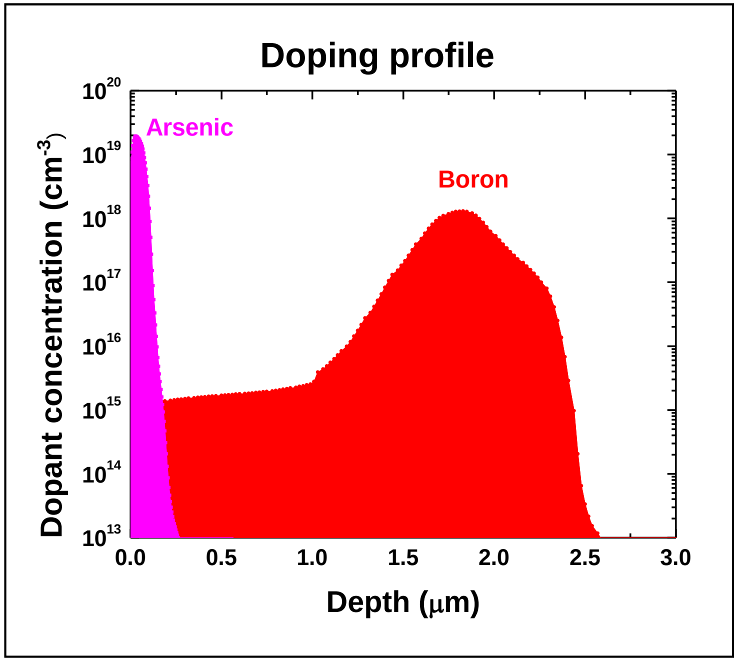

Monolithic Si - ΔE/E detector

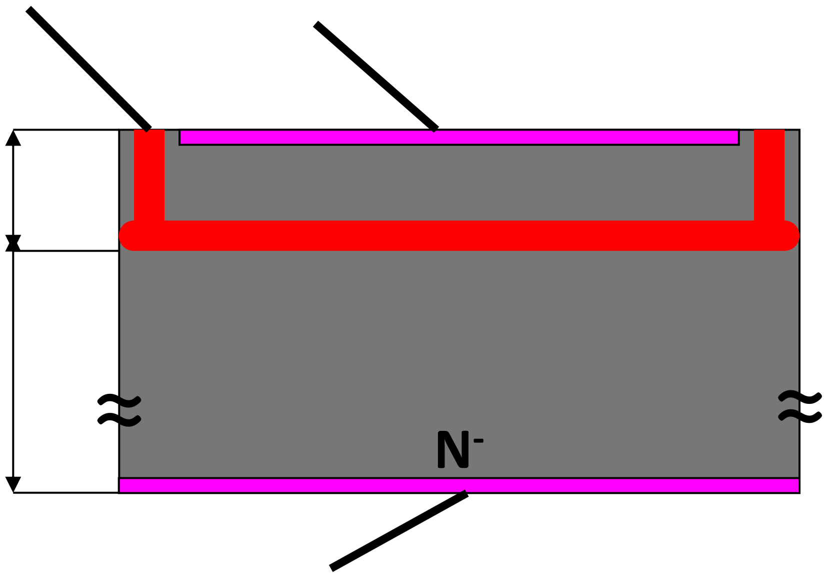

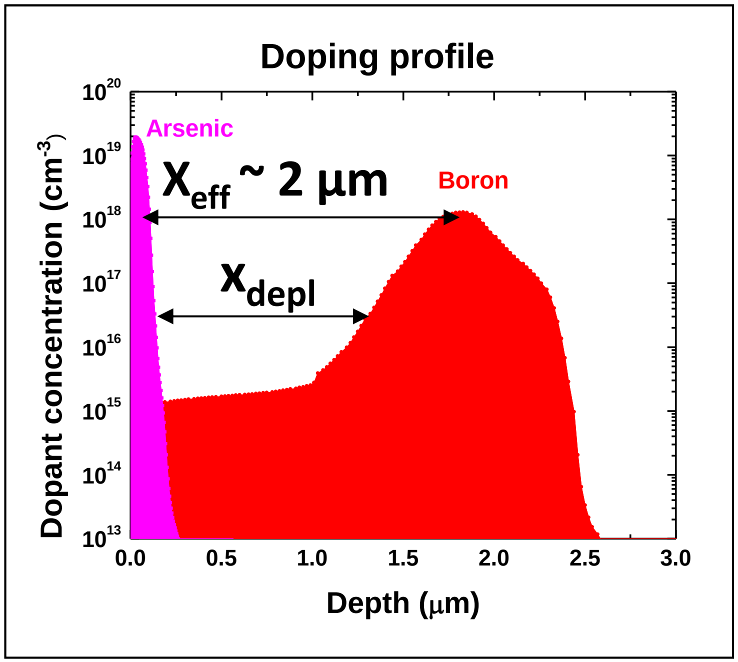

E stage: PIN diode substrate, x ~ 500 µm

ΔE stage: N on P diode micrometric thickness, x_{depl}~ 1 µm
Capacitance ~ 10 nF cm^{-2}

Charge collection: fast vertical drift
charge division x_{eff} ~ 2 µm

MONOLITHIC SILICON TELESCOPE ΔE-E (ST-Microelectronics)[10]

Device geometrical structure:

Sensitive area: 1 mm^2

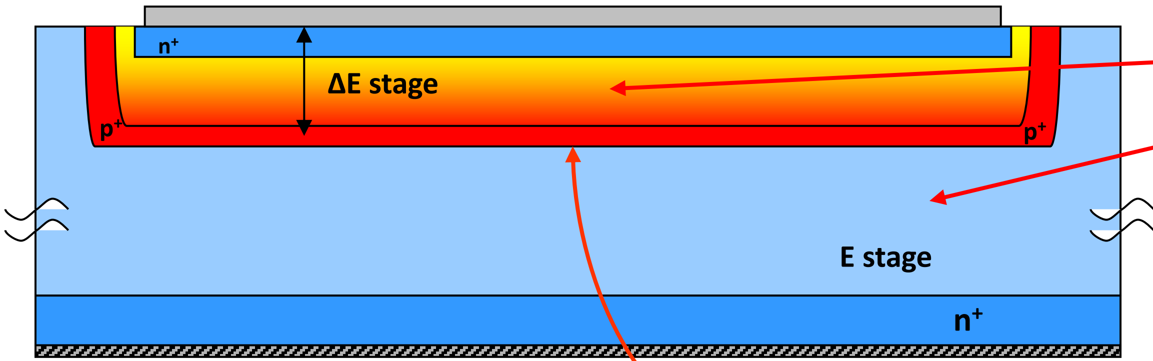

ΔE thickness: ~2 μm
E thickness: ~500 μm

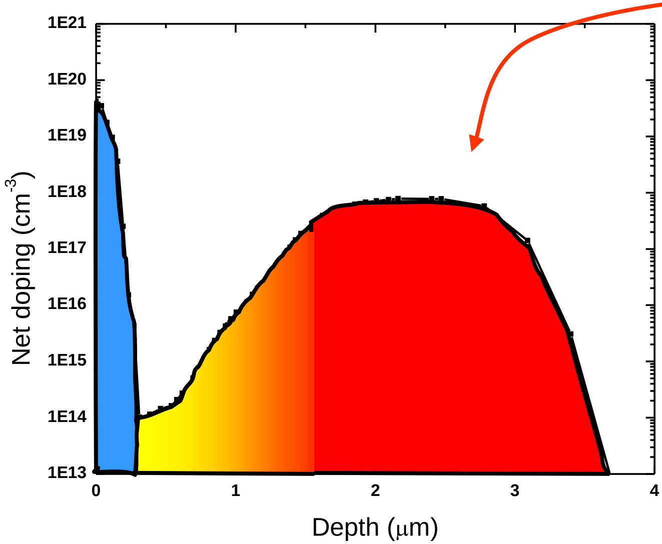

The p+ cathode acts as a "watershed" for the charge collection

Minimization of the "field-funneling effect" [11]

[10] Tudisco, S., et al. A new large area monolithic silicon telescope. Nucl. Instrum. Meth. A 426, 436-445 (1999).
[11] Agosteo, S., Fallica P.G., Fazzi, A., Pola, A., Valvo, G., Zotto, P. A feasibility study of a solid-state microdosimeter. Applied Radiation Isotopes. 63, (5-6) 529-535 (2005).

IRRADIATION WITH
2.7 MeV MONOENERGETIC NEUTRONS

ΔE and E biased and acquired by a 2-channel ADC in coincidence mode

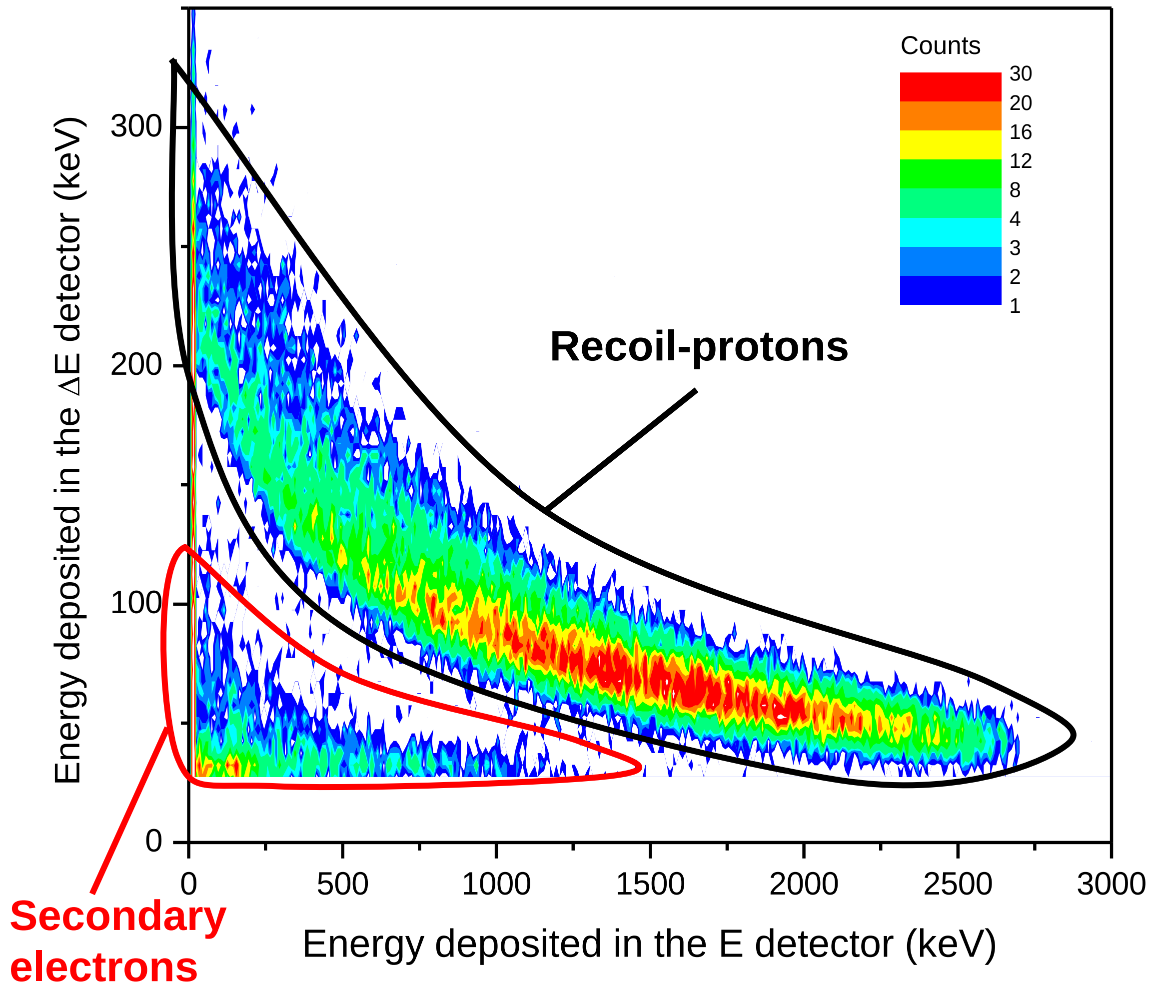

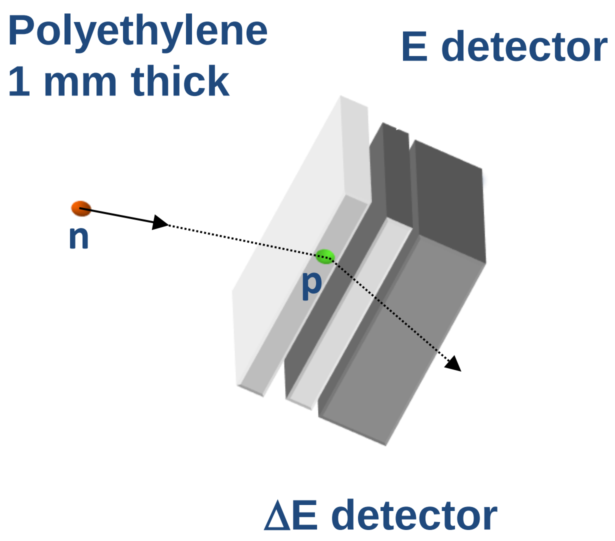

Distributions well-discriminated

Recoil-protons only

IRRADIATION WITH
2.7 MeV MONOENERGETIC NEUTRONS

ΔE stage spectrum

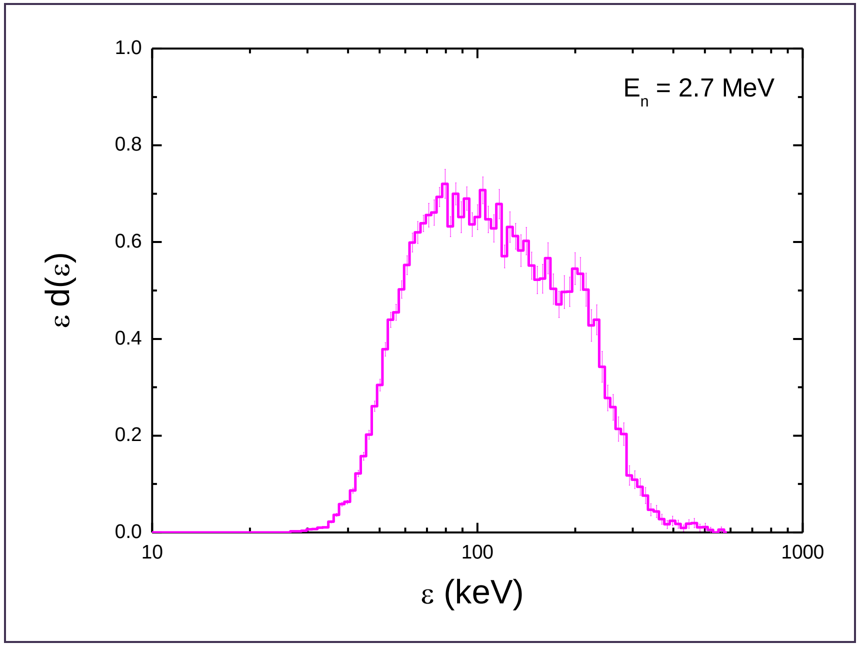

E stage spectrum

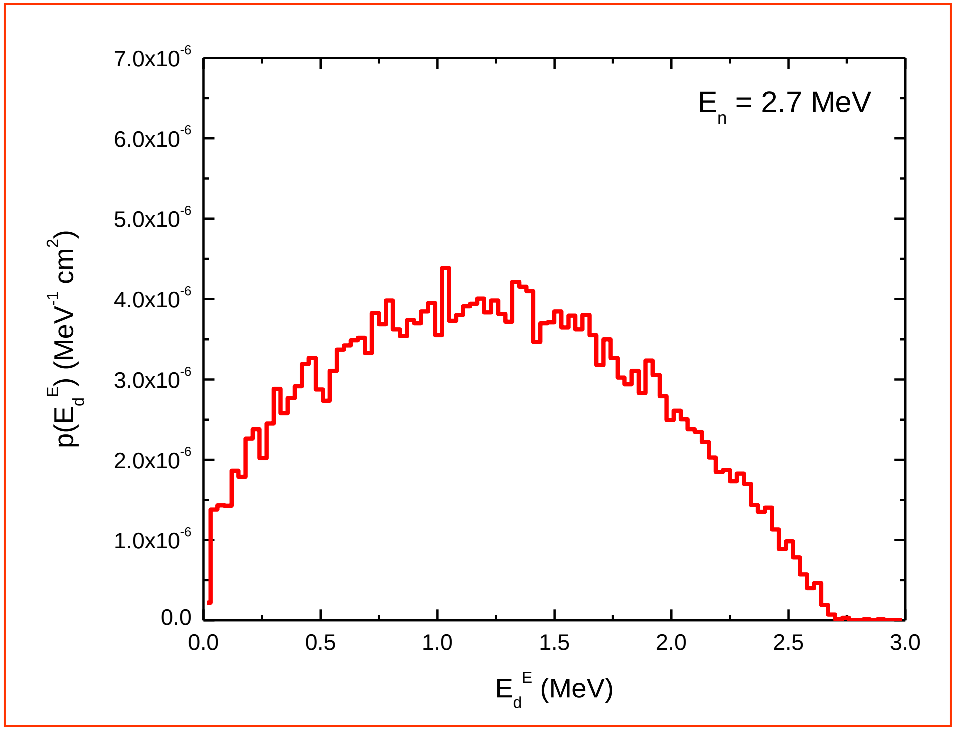

MONOLITHIC SILICON TELESCOPE:
ANALYTICAL MODEL of RESPONSE FUNCTIONS

1. **Assumptions:**
- **elastic scattering isotropic in the centre-of-mass system;**
- **a parallel beam of monoenergetic neutrons;**
- **a uniform probability of interaction in the polyethylene;**
- **the contribution of recoil carbon ions is neglected at the energies accounted for**

2. **Taking into account the actual geometrical structure of the telescope (dead layer 0.4 μm, ΔE stage 1.9 μm and E stage)**

3. **Starting from range-energy and stopping power –energy relations taken from ICRU report n° 49**

Bivariate probability density distribution per unit neutron fluence of the energy $Ed_{\Delta E}$ and Ed_E deposited in the ΔE and E stage, respectively

$$Prob(Ed_{\Delta E}, Ed_E)$$

MONOLITHIC SILICON TELESCOPE: ANALYTICAL MODEL of RESPONSE FUNCTIONS

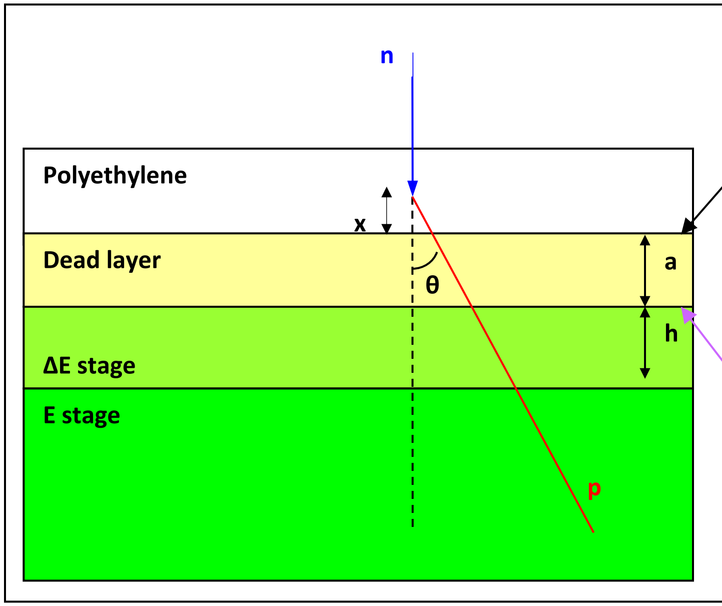

Radiator-detector interface

$$p(E_p^{int}) = \frac{2}{3}\cdot\left[1-\left(\frac{E_p^{int}}{E_n}\right)^{\frac{3}{2}}\right]\cdot\left[R^{poly}(E_n)\cdot S^{poly}(E_p^{int})\right]^{-1}$$

ΔE stage surface

$$p(E_d^{tot}) = \frac{2}{3}\cdot\left[1-\cos(\theta_{max}\,|\,E_d^{tot})^3\right]\cdot\frac{1}{R^{poly}(E_n)}\cdot\frac{S^{Si}\left(E^{Si}\left(R^{Si}(E_d^{tot})+a\right)\right)}{S^{poly}\left(E^{Si}\left(R^{Si}(E_d^{tot})+a\right)\right)}\cdot\frac{1}{S^{Si}(E_d^{tot})}$$

ΔE – E interface

$$p(E_d^{E}) = \frac{2}{3}\cdot\left[1-\cos(\theta_{max}\,|\,E_d^{E})^3\right]\cdot\frac{1}{R^{poly}(E_n)}\cdot\frac{S^{Si}\left(E^{Si}\left(R^{Si}(E_d^{E})+a+h\right)\right)}{S^{poly}\left(E^{Si}\left(R^{Si}(E_d^{E})+a+h\right)\right)}\cdot\frac{1}{S^{Si}(E_d^{E})}$$

MONOLITHIC SILICON TELESCOPE: ANALYTICAL MODEL of RESPONSE FUNCTIONS

$$p(E_d^{\Delta E},E_d^{E}) = \frac{2\cdot h^3}{R^{poly}(E_n)}\cdot\frac{1}{\left(R^{Si}(E_d^{\Delta E}+E_d^{E})-R^{Si}(E_d^{E})\right)^4}\cdot\frac{S^{Si}\left(E^{Si}\left(R^{Si}(E_d^{E})+\frac{a+h}{h}\cdot\left(R^{Si}(E_d^{\Delta E}+E_d^{E})-R^{Si}(E_d^{E})\right)\right)\right)}{S^{poly}\left(E^{Si}\left(R^{Si}(E_d^{E})+\frac{a+h}{h}\cdot\left(R^{Si}(E_d^{\Delta E}+E_d^{E})-R^{Si}(E_d^{E})\right)\right)\right)}\cdot\frac{S^{Si}(E_d^{\Delta E}+E_d^{E})}{S^{Si}(E_d^{E})}$$

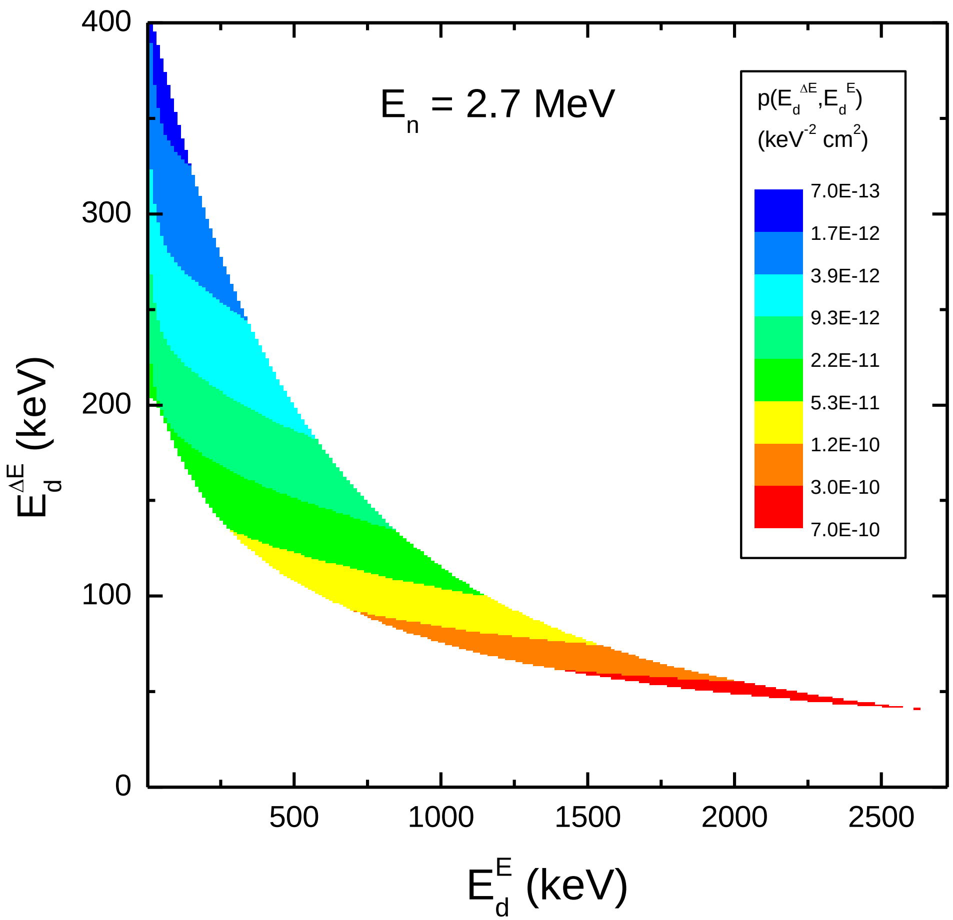

Bivariate distribution normalized to unit neutron fluence

MONOLITHIC SILICON TELESCOPE: FLUKA SIMULATIONS

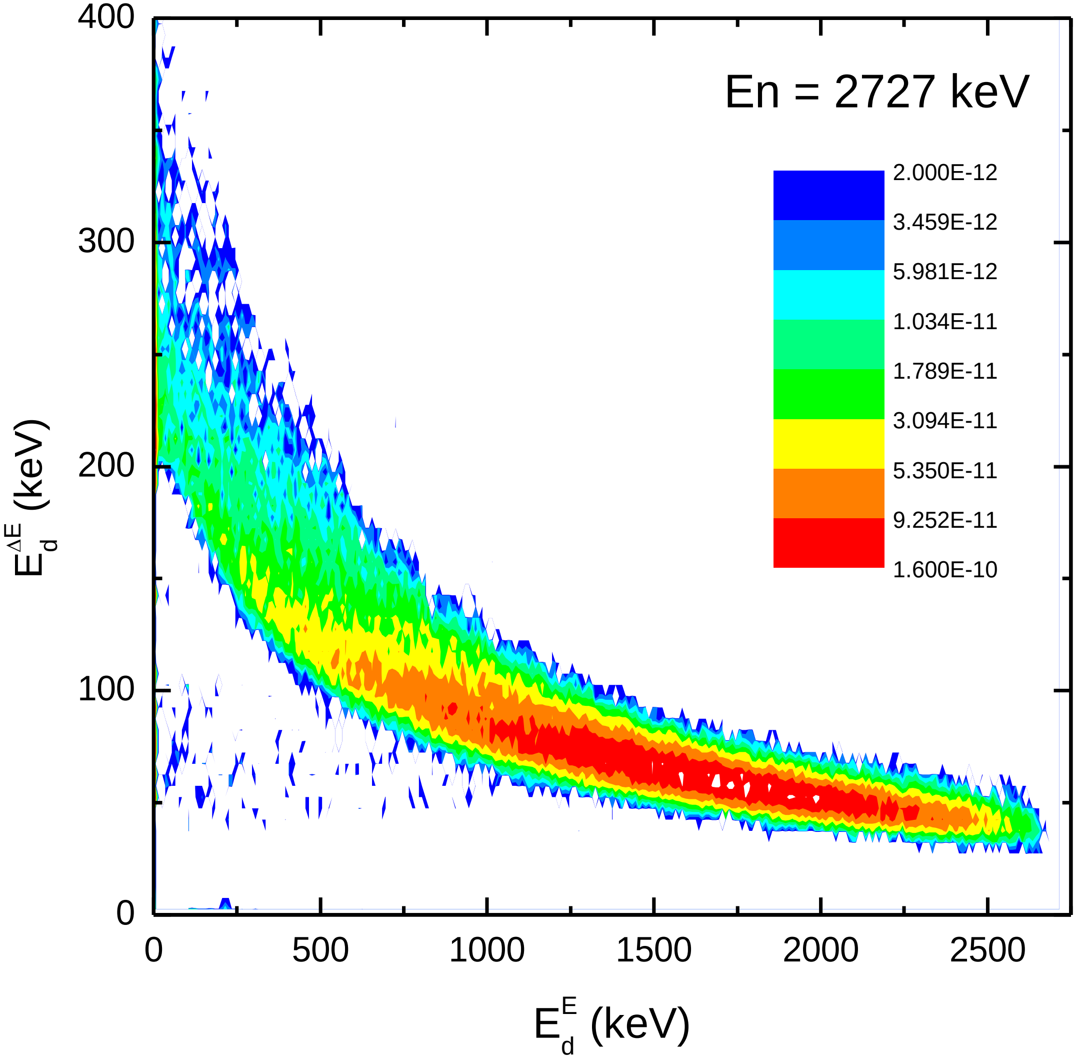

MONOLITHIC SILICON TELESCOPE:
FLUKA simulation and analitycal model

Comparison between analytical model and simulation

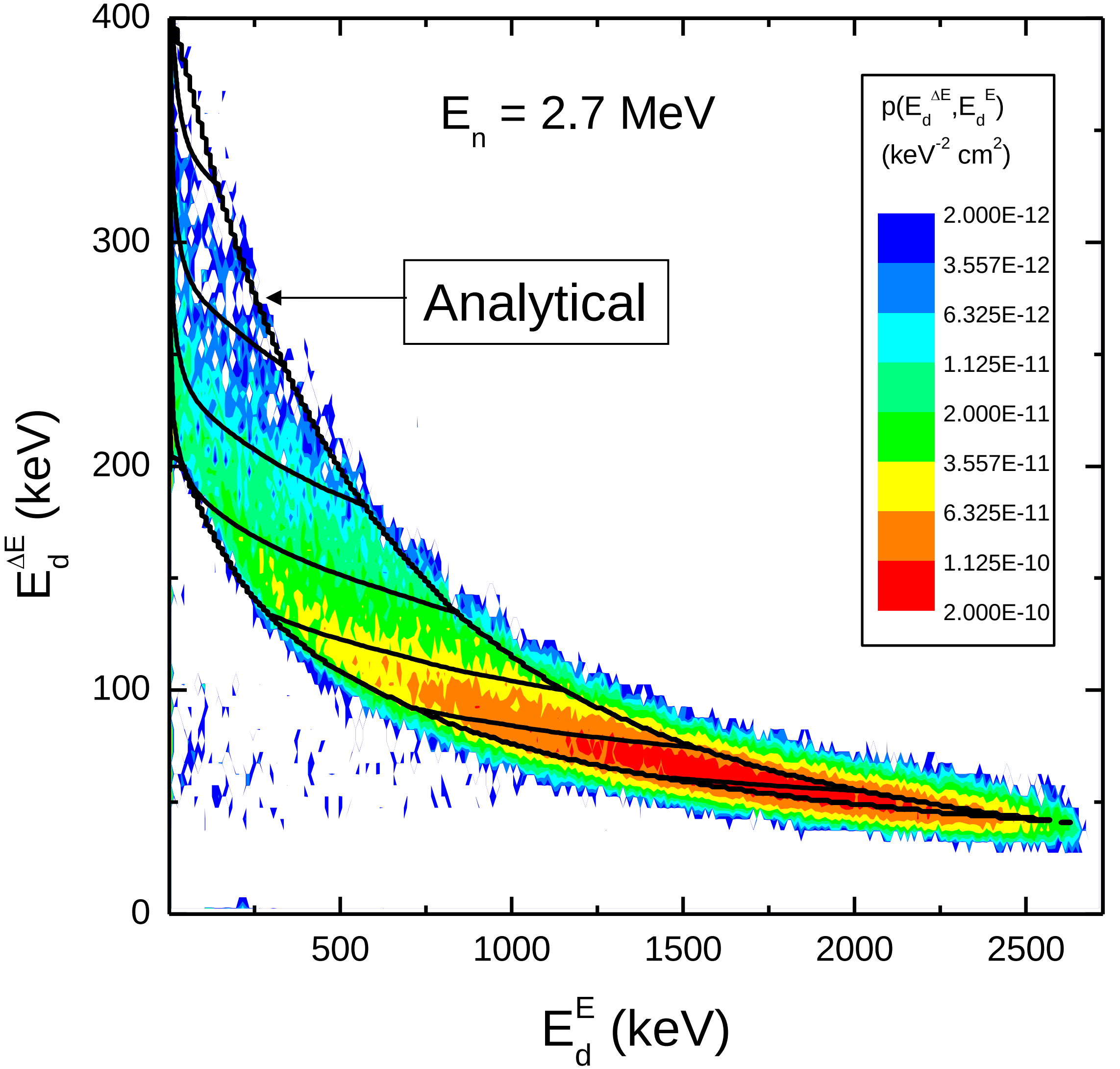

IRRADIATIONS WITH MONOENERGETIC NEUTRONS
(at INFN LNL - Padova):
comparison with simulations and analytical model

Marginal distributions of $p(E_d^{\Delta E}, E_d^{E})$: response functions of the two stages

ΔE stage response

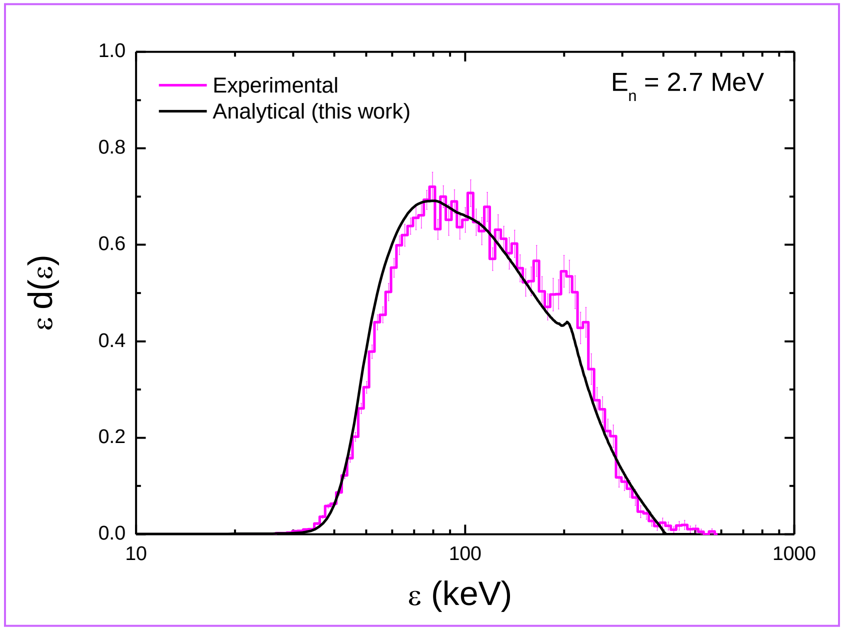

E stage response

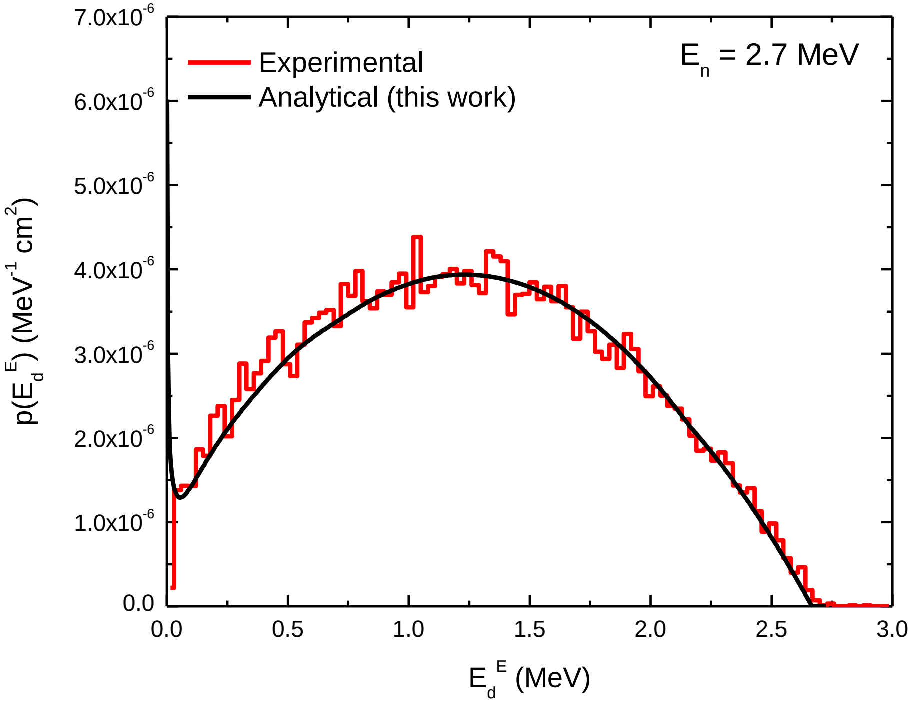

IRRADIATIONS WITH MONOENERGETIC NEUTRONS
(at INFN LNL - Padova):
comparison with simulations and analytical model

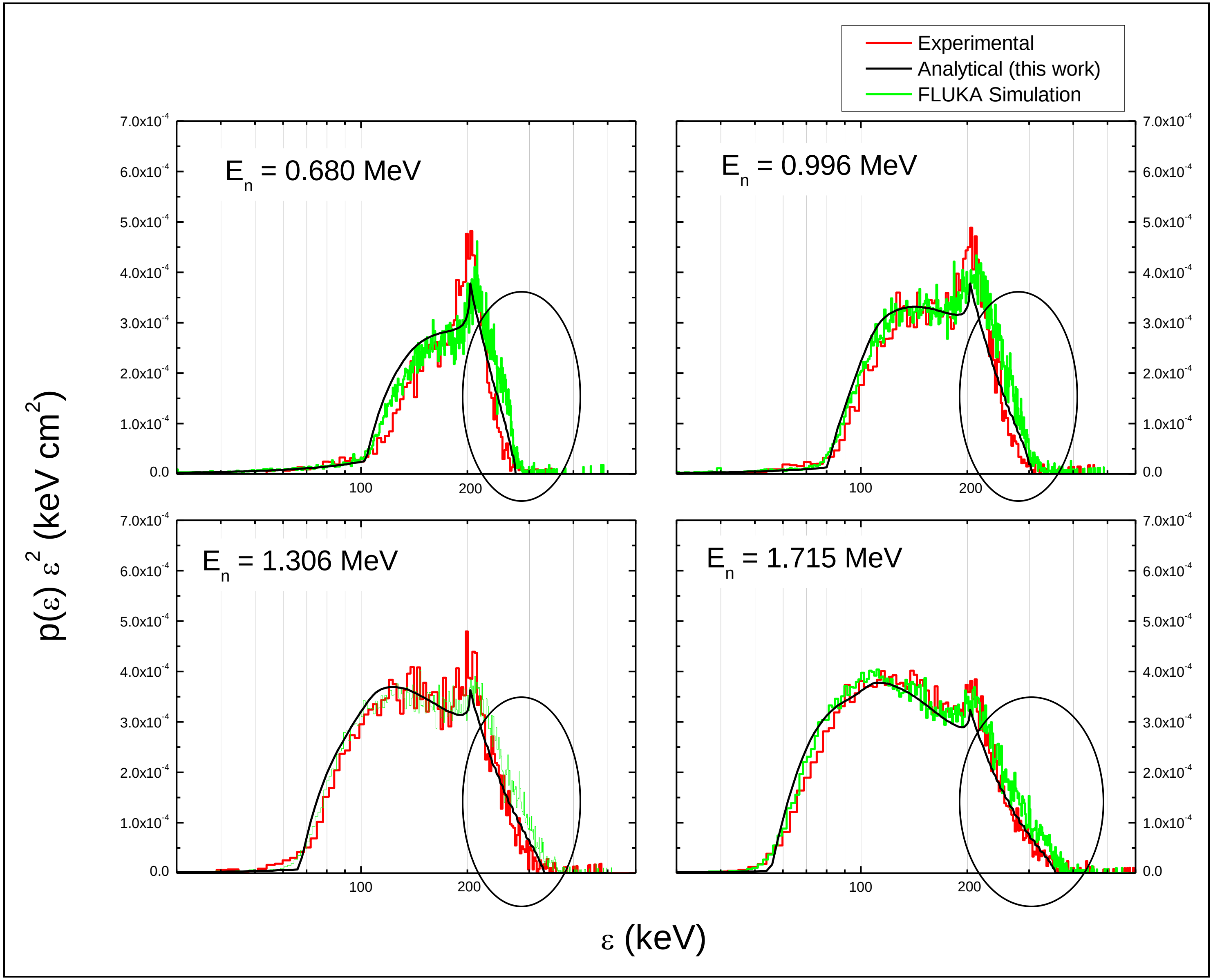

IRRADIATIONS WITH MONOENERGETIC NEUTRONS
(at INFN LNL - Padova):
comparison with simulations and analytical model

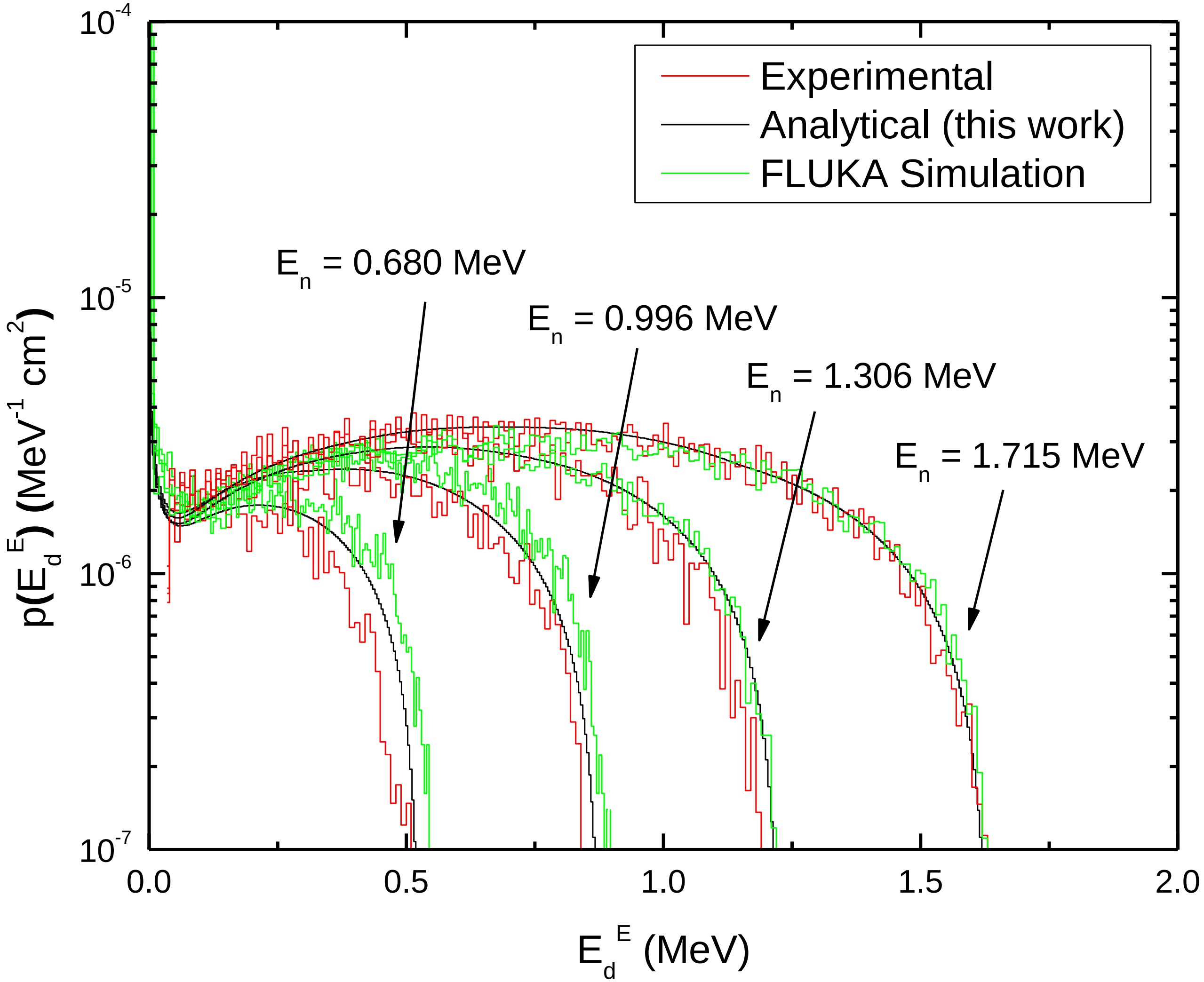

SILICON MICRODOSIMETRY

Besides the "Field Funneling Effect", the realization of a silicon microdosimeter involves other problems, mainly:

- **<u>Silicon</u> is not tissue** → **Tissue-equivalence correction**
- **<u>The sensitive volume</u> is usually a rectangular parallelepiped** → **Shape-equivalence criteria and correction**
- **<u>The electronic noise</u> imposes a minimum detectable energy higher than TEPC** → **Noise - efficiency trade off (⇒ detector & ampli segmentation)**

TISSUE EQUIVALENCE CORRECTION

The tissue equivalence of silicon requires:

1. the minimization of the contribution of secondaries generated by direct interactions of neutrons with silicon, i.e. most events should be crossers or stoppers

Relevant reactions that can generate starters or insiders:

Fast neutrons → Elastic scattering with silicon nuclei — One order of magnitude lower than the one due to recoil-protons

Fast neutrons → $^{28}Si(n,\alpha)^{25}Mg$, $^{28}Si(n,p)^{28}Al$ — In commercial PIN diodes the contribution is of the order of a few percent

Thermal neutrons → $^{10}B(n,\alpha)^{7}Li$ — Implantation of pure ^{11}B

The spectrum of the energy imparted in the ΔE detector is due to the secondaries generated in the converter

TISSUE EQUIVALENCE CORRECTION

The tissue equivalence of silicon device requires:

2. **a suitable correction of the measured distribution in order to obtain a spectrum equivalent to that acquired with an hypothetical tissue ΔE detector**

Analytical procedure for tissue-equivalence correction

$$E_d^{Tissue}(E_p, l) = E_d^{Si}(E_p, l) \cdot \frac{S^{Tissue}(E_p)}{S^{Si}(E_p)}$$

Energy deposited along a track of length l by recoil-protons of energy E_p in a tissue-equivalent ΔE detector

Scaling factor : stopping powers ratio

Calculated energy deposited by protons in silicon and in tissue for a fixed track length l (based on the range-energy relation)

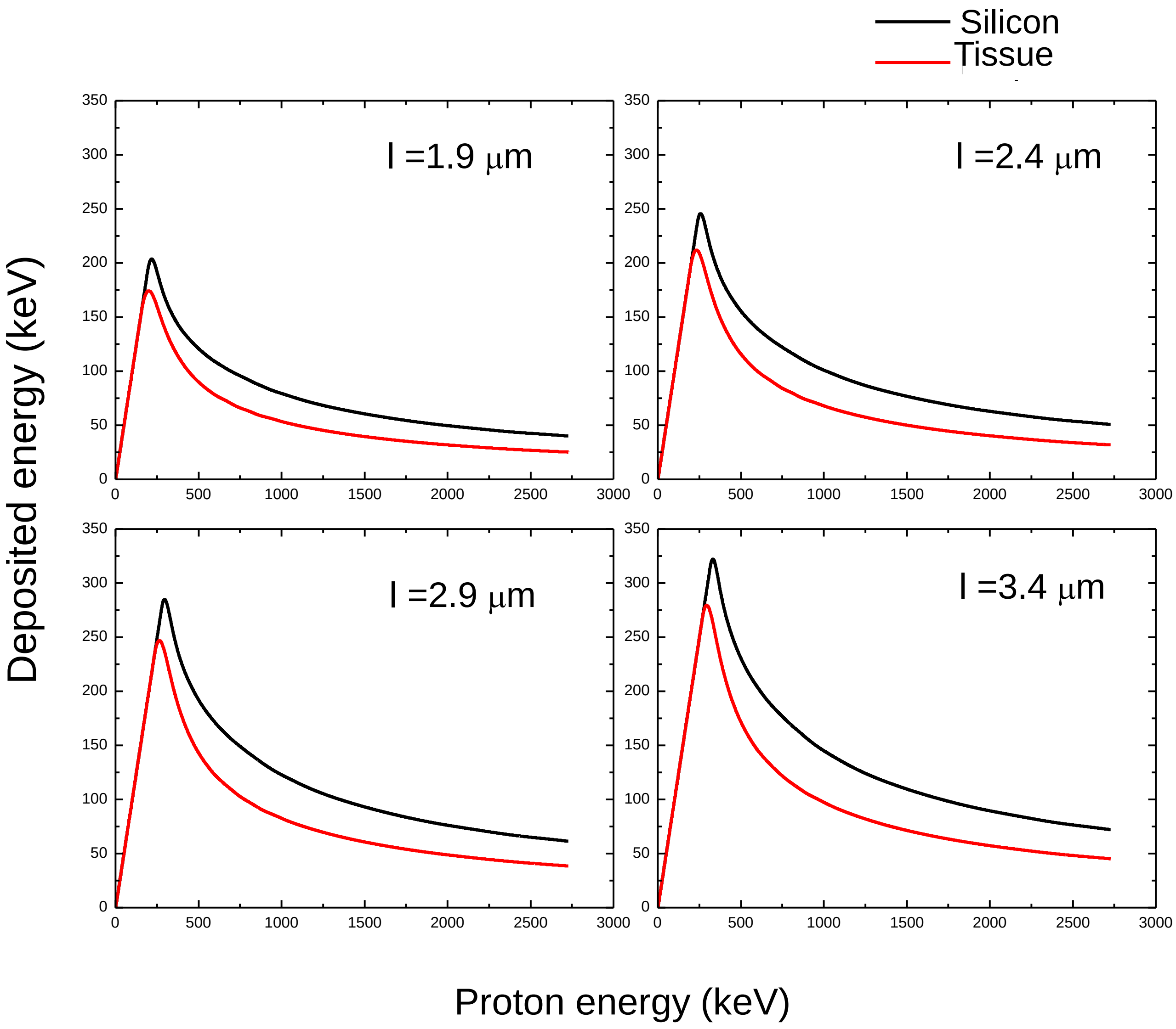

TISSUE EQUIVALENCE CORRECTION

Calculated energy deposited by recoil-protons in silicon and in tissue for a fixed track length l (based on range-energy relation)

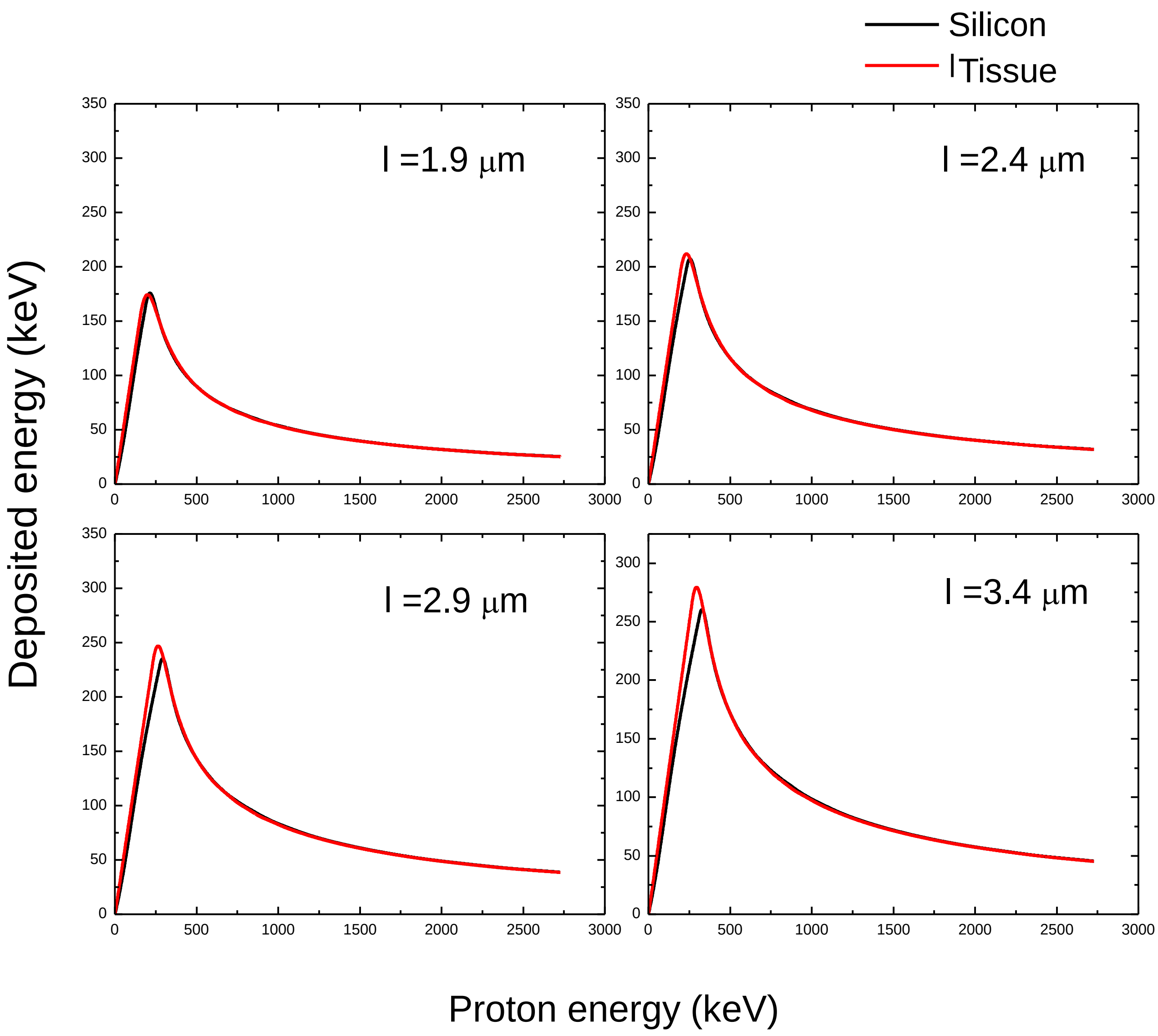

TISSUE-EQUIVALENCE CORRECTION

The scaling factor $\frac{S^{Tissue}(E_p)}{S^{Si}(E_p)}$ depends on the energy E_p of recoil-protons

E_p can be measured event-by-event by exploiting the E-stage of the telescope

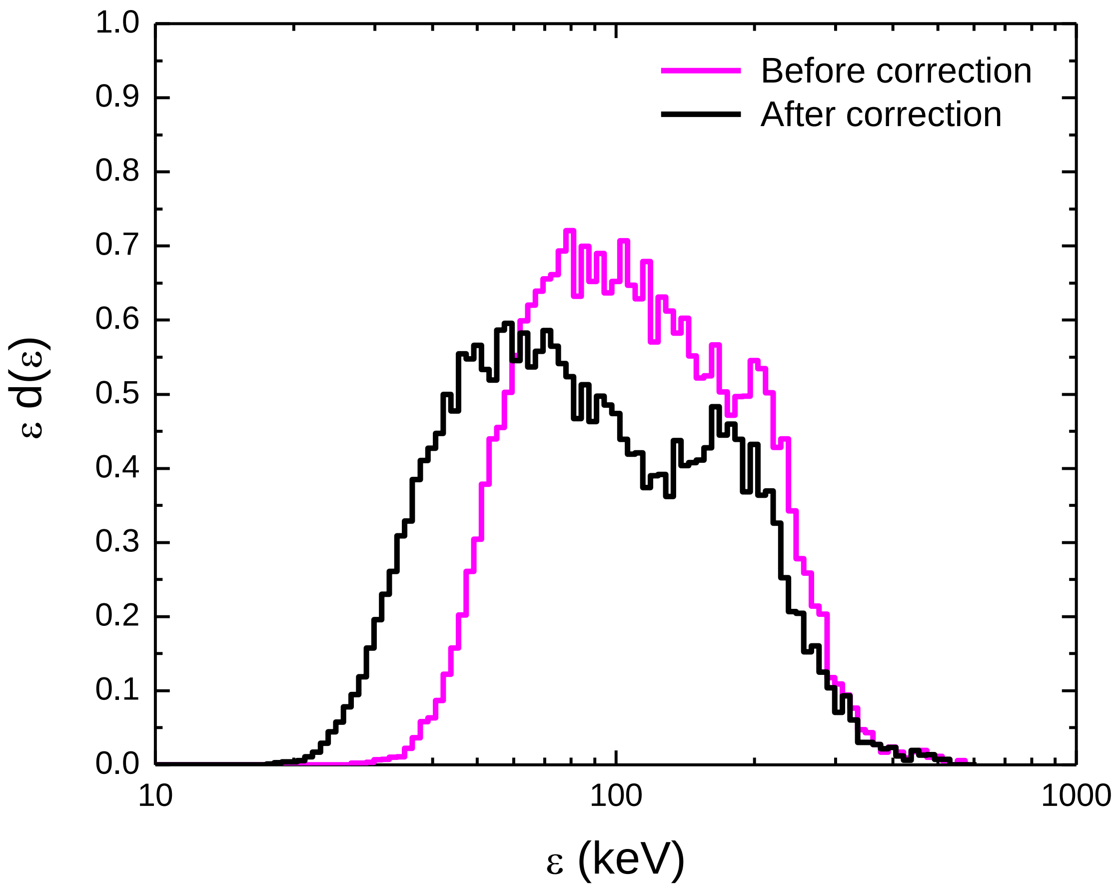

COMPARISON WITH SIMULATIONS (FLUKA code)

A tissue-equivalent detector with the same geometrical structure of the monolithic silicon telescope was modelled and irradiated with a parallel beam of 2.7 MeV neutrons.

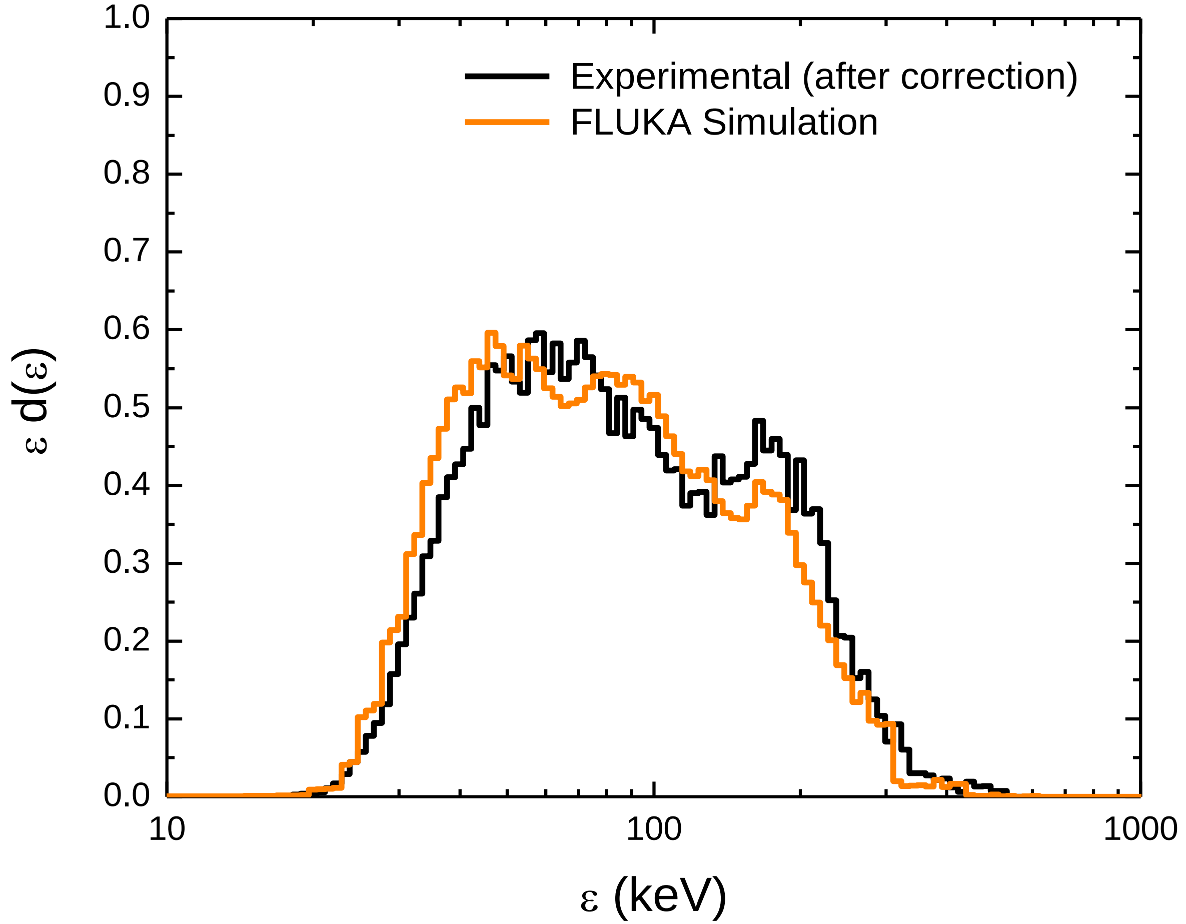

Higher Limit: the thickness of the E stage restricts the TE correction to neutrons below 8 MeV

SHAPE ANALYSIS

Objective: compare the distributions measured with the monolithic silicon telescope and with a cylindrical TEPC

It's necessary to adopt some criteria for choosing the dimensions of simulated tissue cylinder

The equivalent cylindrical dimensions are calculated by equating the dose-mean energy imparted per event [Kellerer].

Assuming a constant linear energy transfer L:

$$\bar{\varepsilon}_D = L \cdot \frac{\int_0^\infty l^2 \cdot p(l)\,dl}{\bar{l}}$$

Ratio of the first and second moments of the track length distributions

SHAPE ANALYSIS and CORRECTION CRITERIA

Equating the dose-mean track length for the two track length distributions it is possible to estimate an equivalent cylinder dimension of about <u>2.67 μm</u> (unit elongation)

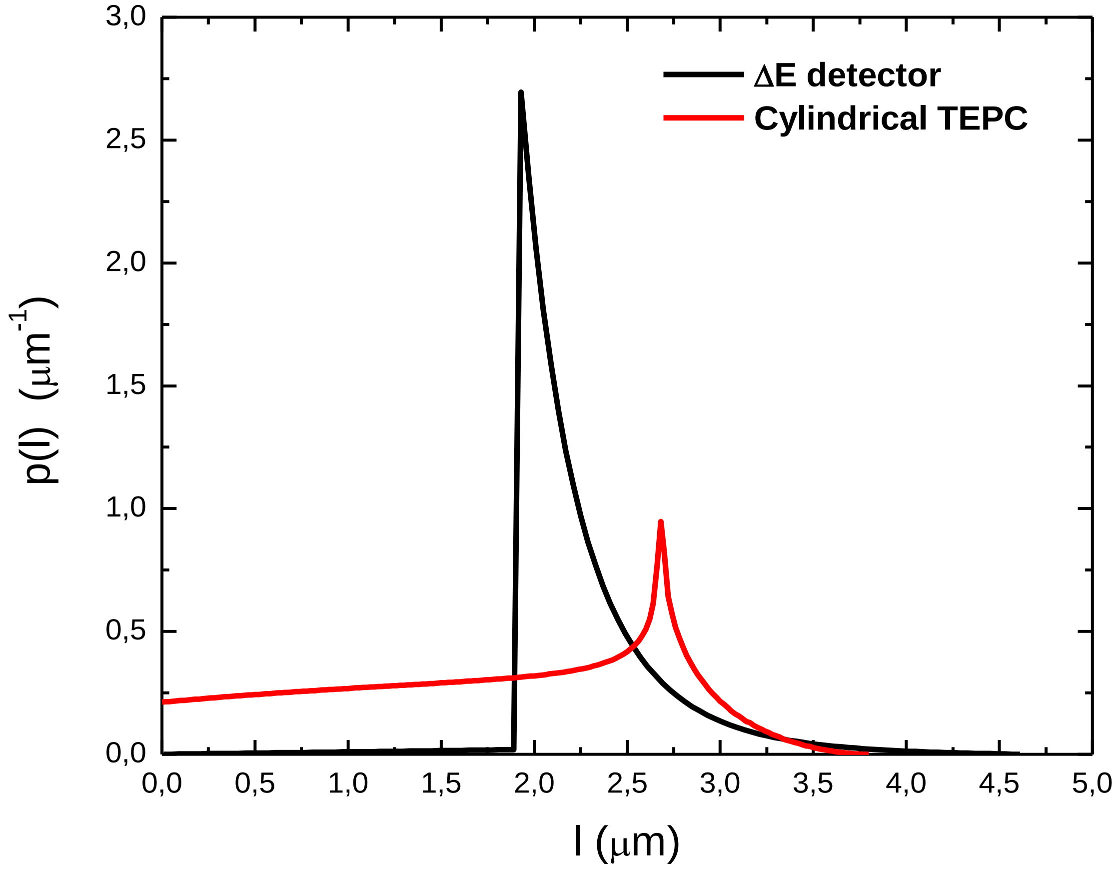

This estimation is valid for neutron energies above 1 MeV

INTER-COMPARISON WITH A CYLINDRICAL TEPC

Preliminary results of the irradiation with 2.7 MeV mono-energetic neutrons (INFN-LNL Van De Graaff accelerator)

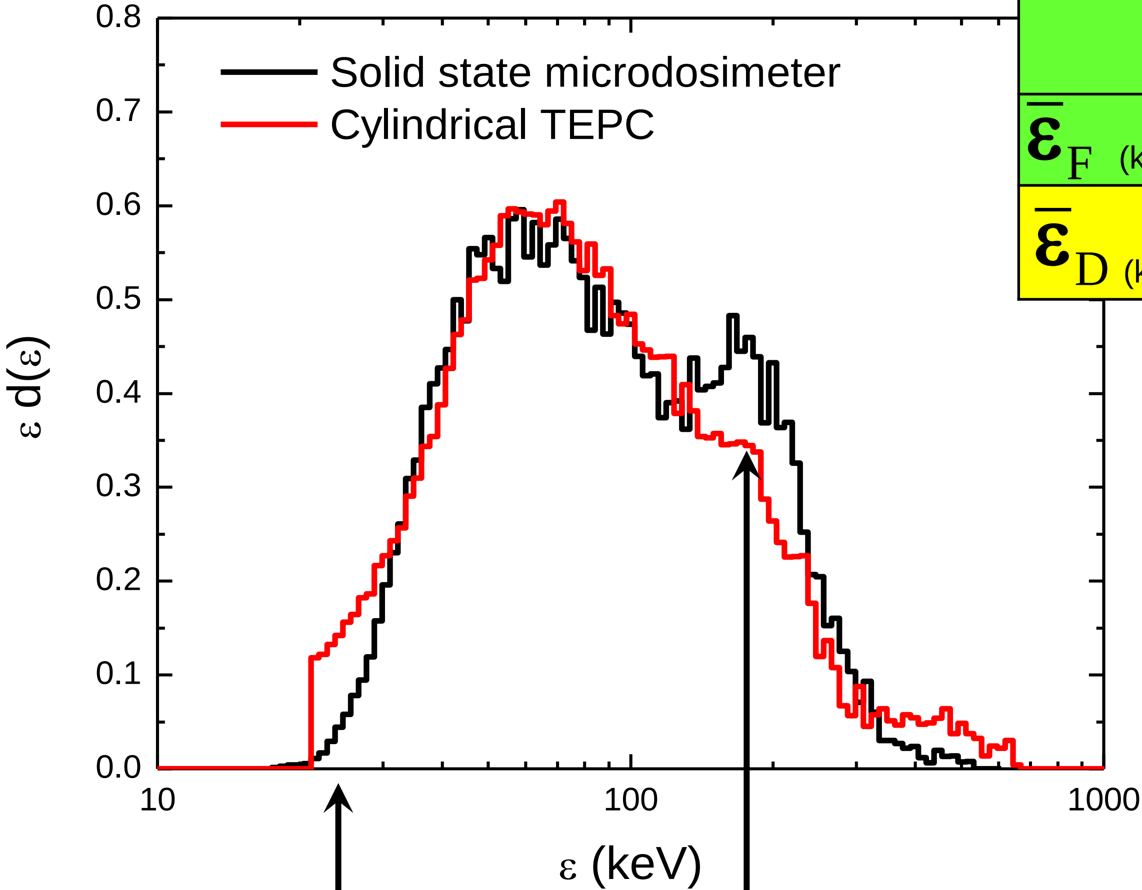

	TEPC	Si-Telescope
$\bar{\varepsilon}_F$ (keV)	66.8 ± 2.7	71.6 ± 4.3
$\bar{\varepsilon}_D$ (keV)	104.2 ± 4.2	105.5 ± 6.3

Despite the shape equivalence correction, the inherent difference in the track length distributions still subsists

MONOLITHIC SILICON TELESCOPE: NEW DETECTOR DESIGN

A matrix of cylindrical ΔE elements (about 2 μm thick) implanted on a single E stage (500 μm thick) was designed and constructed.

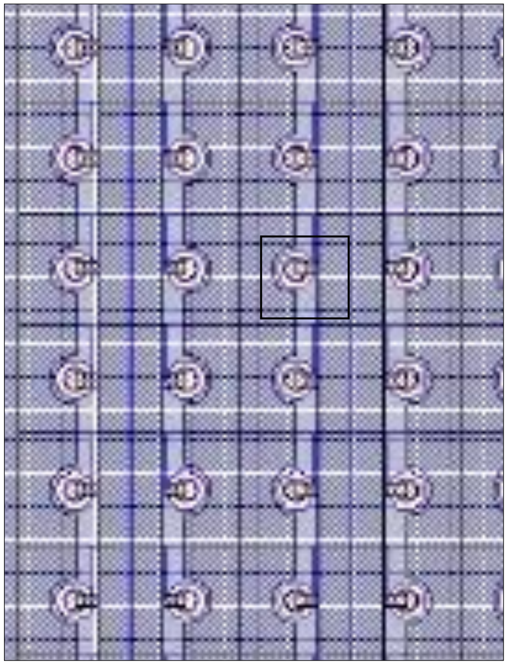

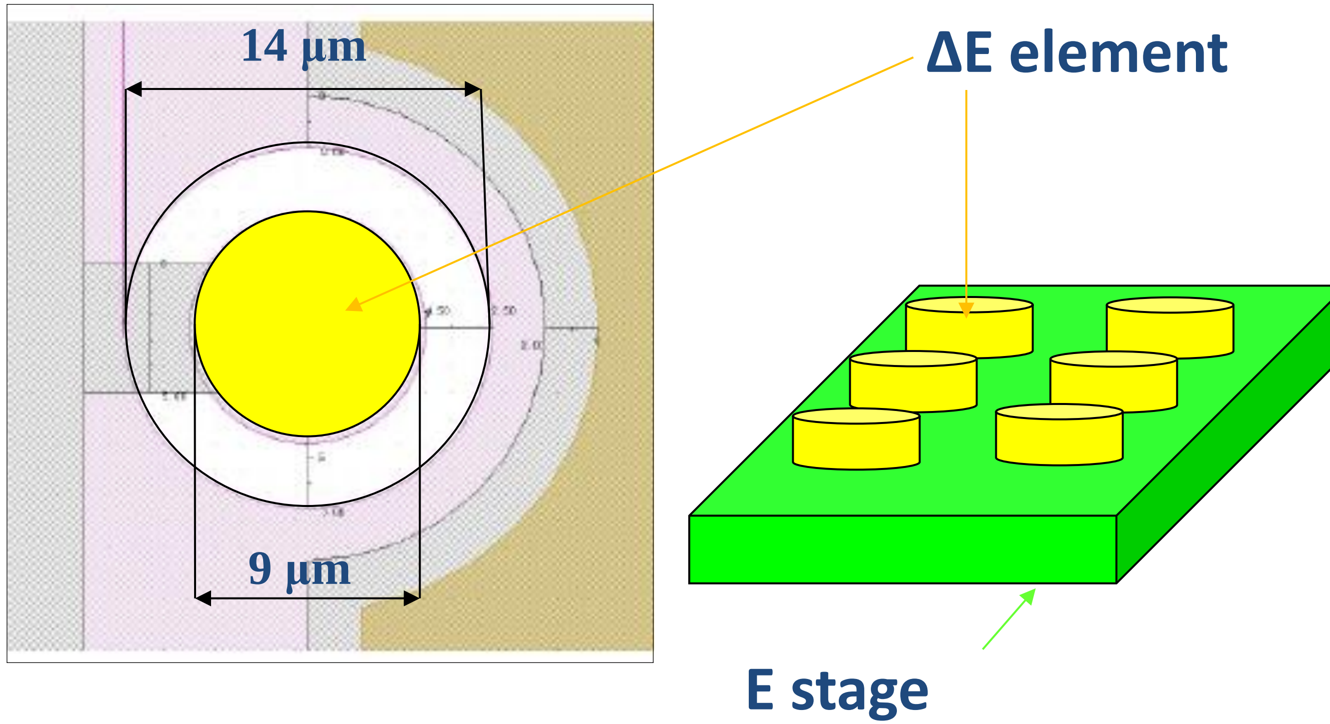

More than 7000 pixels are connected in parallel to give an effective detection area of the ΔE stage of about 0.5 mm^2

Pictures of the device at SEM

(by NEMAS – Nano Engineered MAterials and Surfaces - PoliMi)

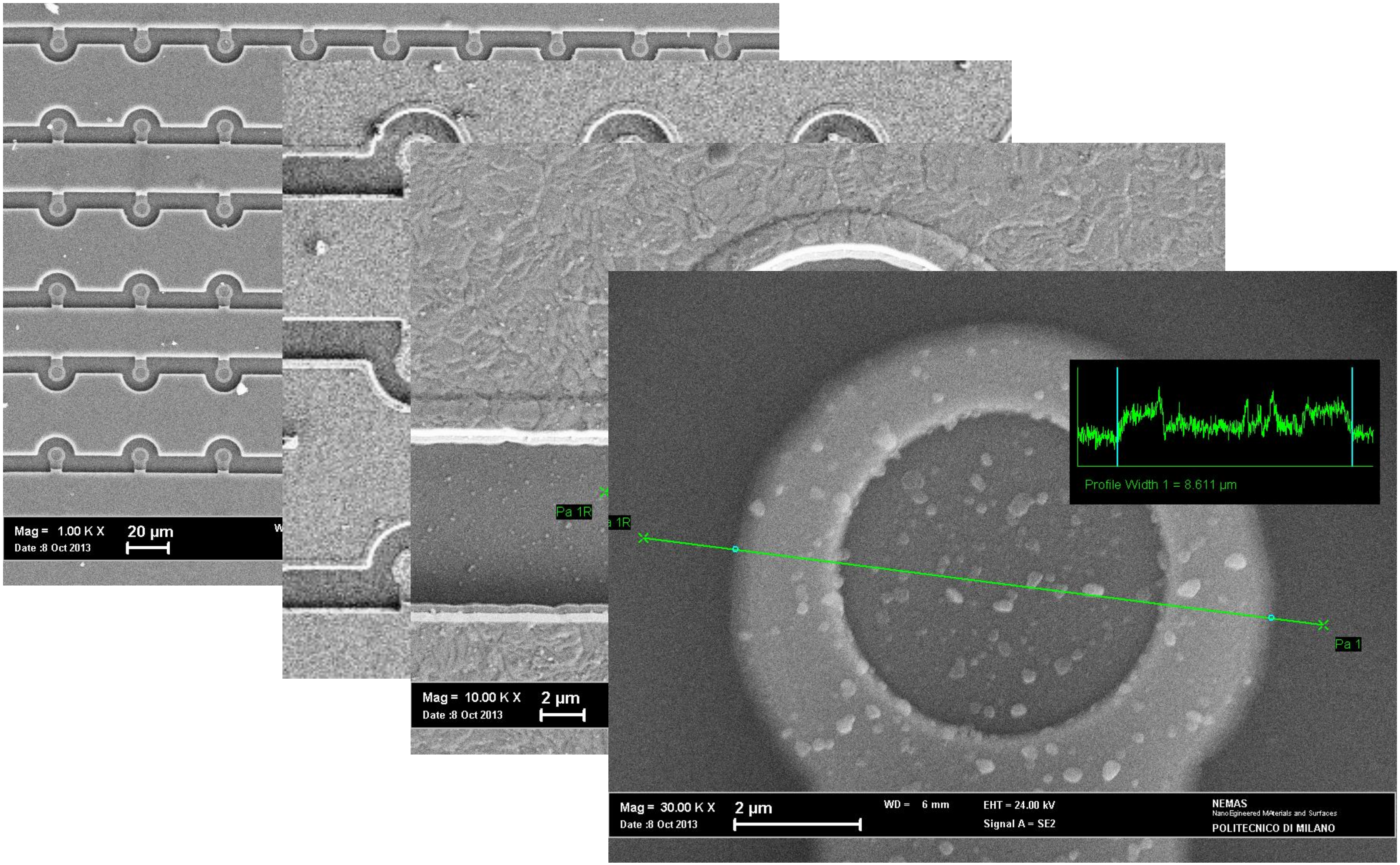

MONOLITHIC SILICON TELESCOPE: NEW DETECTOR DESIGN

Device packages

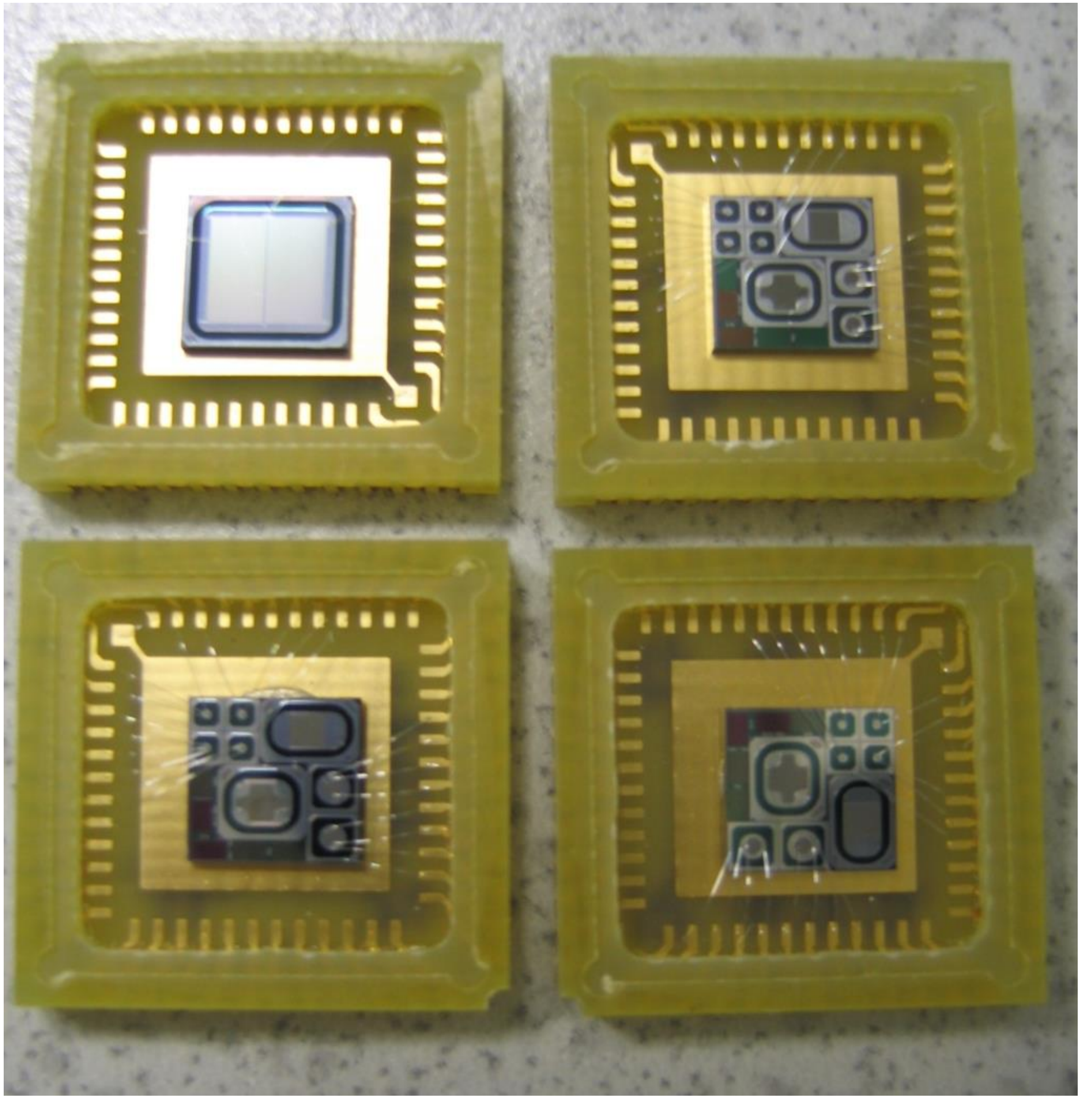

IRRADIATION WITH 2.7 MeV MONOENERGETIC NEUTRONS

ΔE stages and E stage were acquired by a 2-channel ADC in coincidence mode

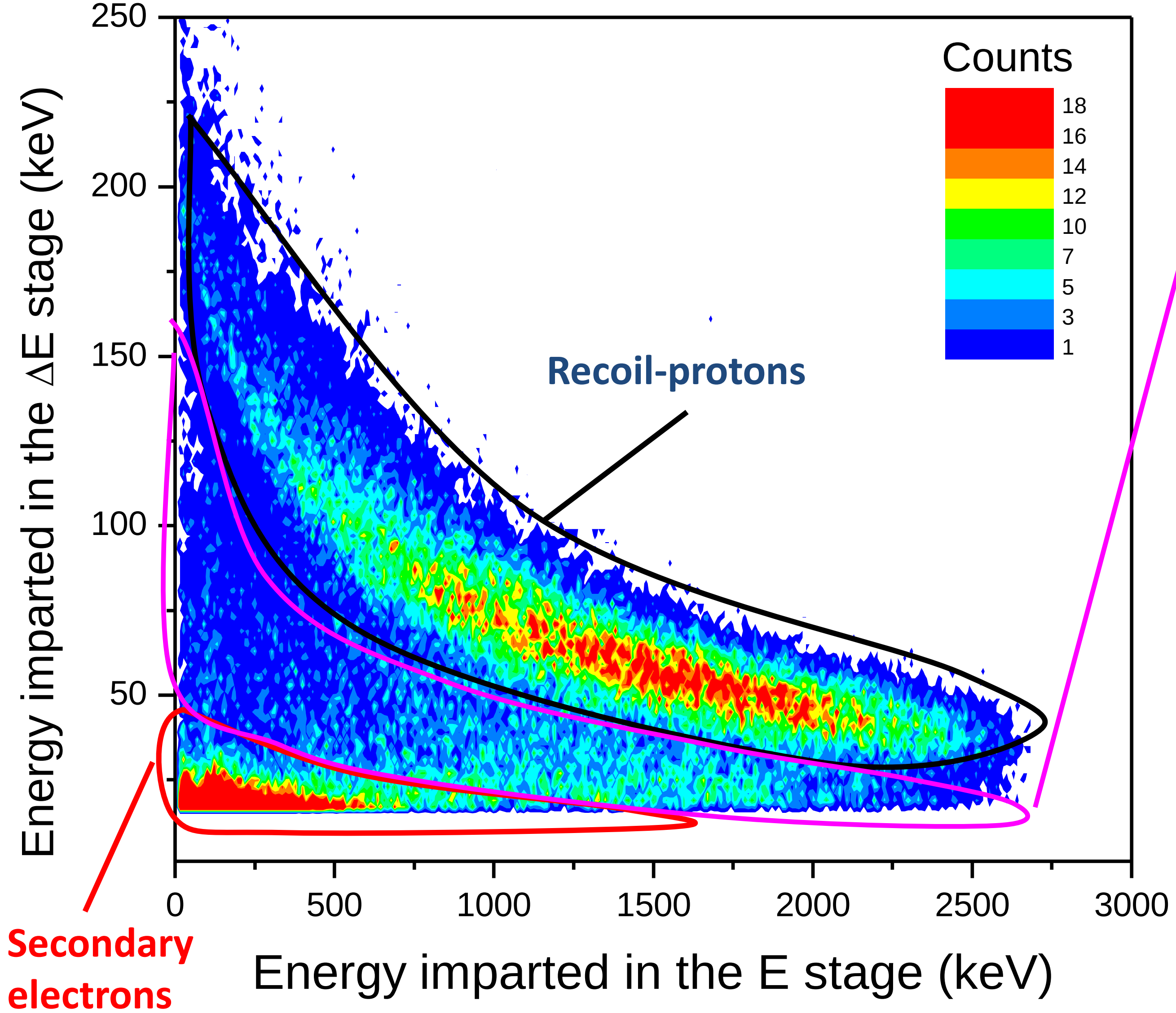

Recoil-protons due to track length distribution

RESULTS OF THE COMPARISON WITH A CYLINDRICAL TEPC

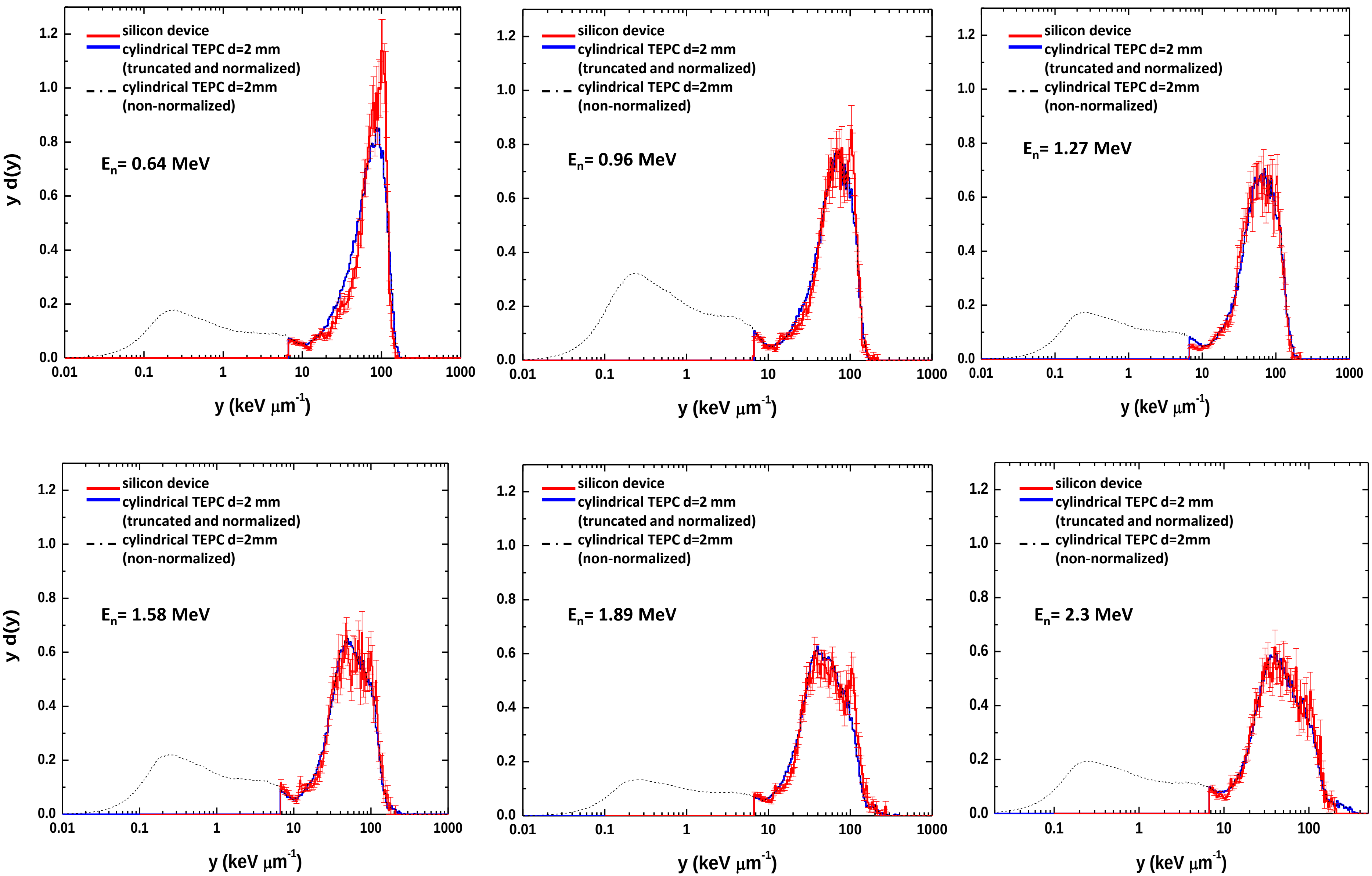

CLINICAL BEAM QUALITY & TREATMENT PLANNING

Effectiveness of a radio therapeutic treatment

Accurate knowledge of the local distribution of energy

Beam quality assessment

Absorbed dose gives a macroscopic description

CLINICAL BEAM QUALITY & TREATMENT PLANNING

Accurate knowledge of local energy deposition

Beam quality assessment from both physical and biological point of view

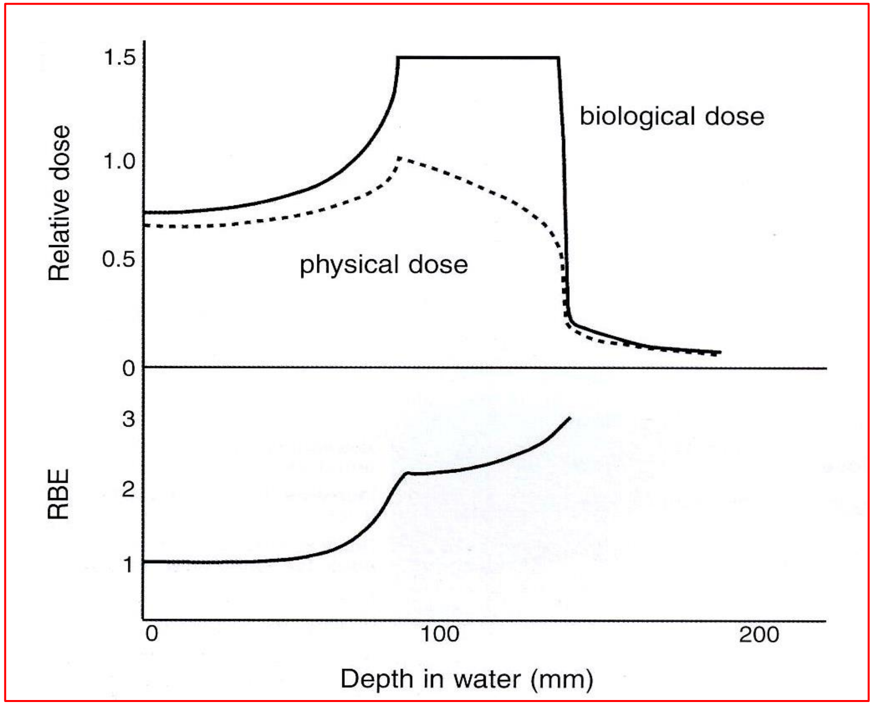

Locally (micrometric or nanometric size) the absorbed dose becomes inadequate…

MICRODOSIMETRIC APPROACH:
STUDIES OF CLINICAL PROTON BEAMS

Studies concerning the characterization of the quality of proton beams by exploiting microdosimetric measurements performed with Tissue Equivalent Proportional Counters (TEPC) were recently presented.

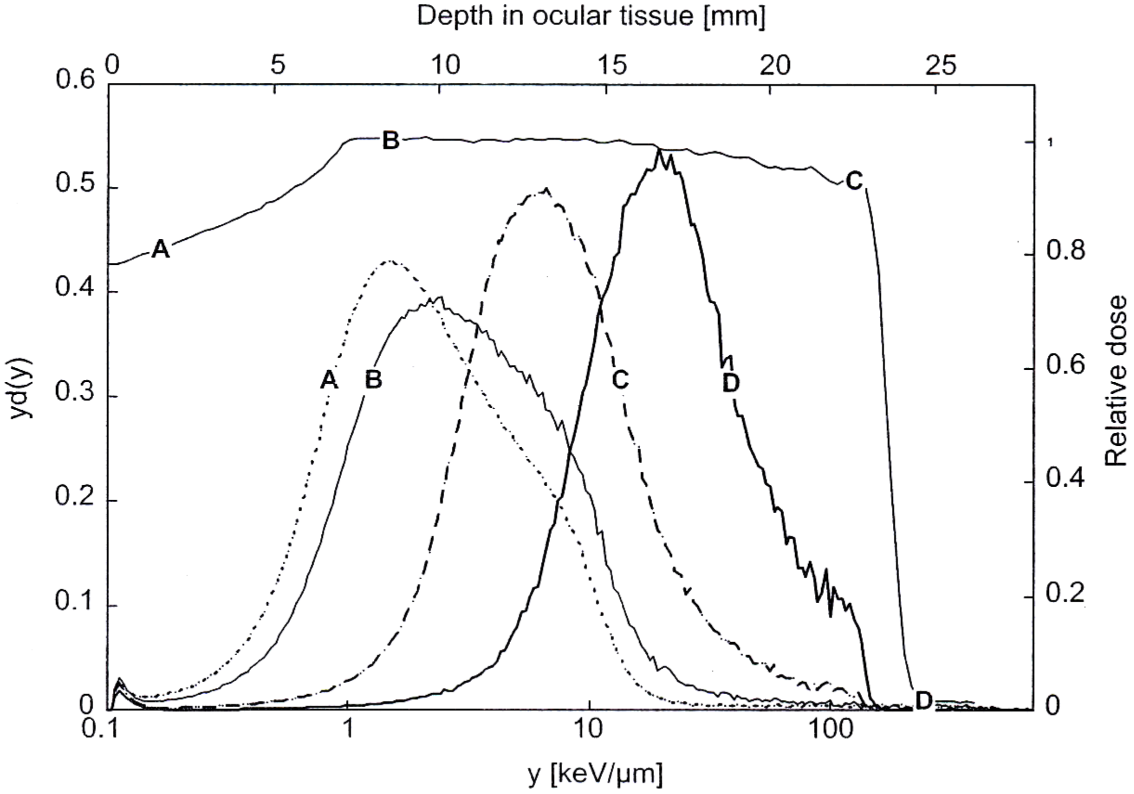

CATANA facility

[1] L. De Nardo, D, Moro, P. Colautti, V. Conte, G. Tornielli and G. Cuttone, "Microdosimetric investigation at the therapeutic proton beam facility of CATANA", Radiat. Prot. Dosim. 110, 681-686 (2004).

Irradiations with a 62 MeV modulated proton beam at CATANA facility (LNS-INFN Catania)

Measurement set-up

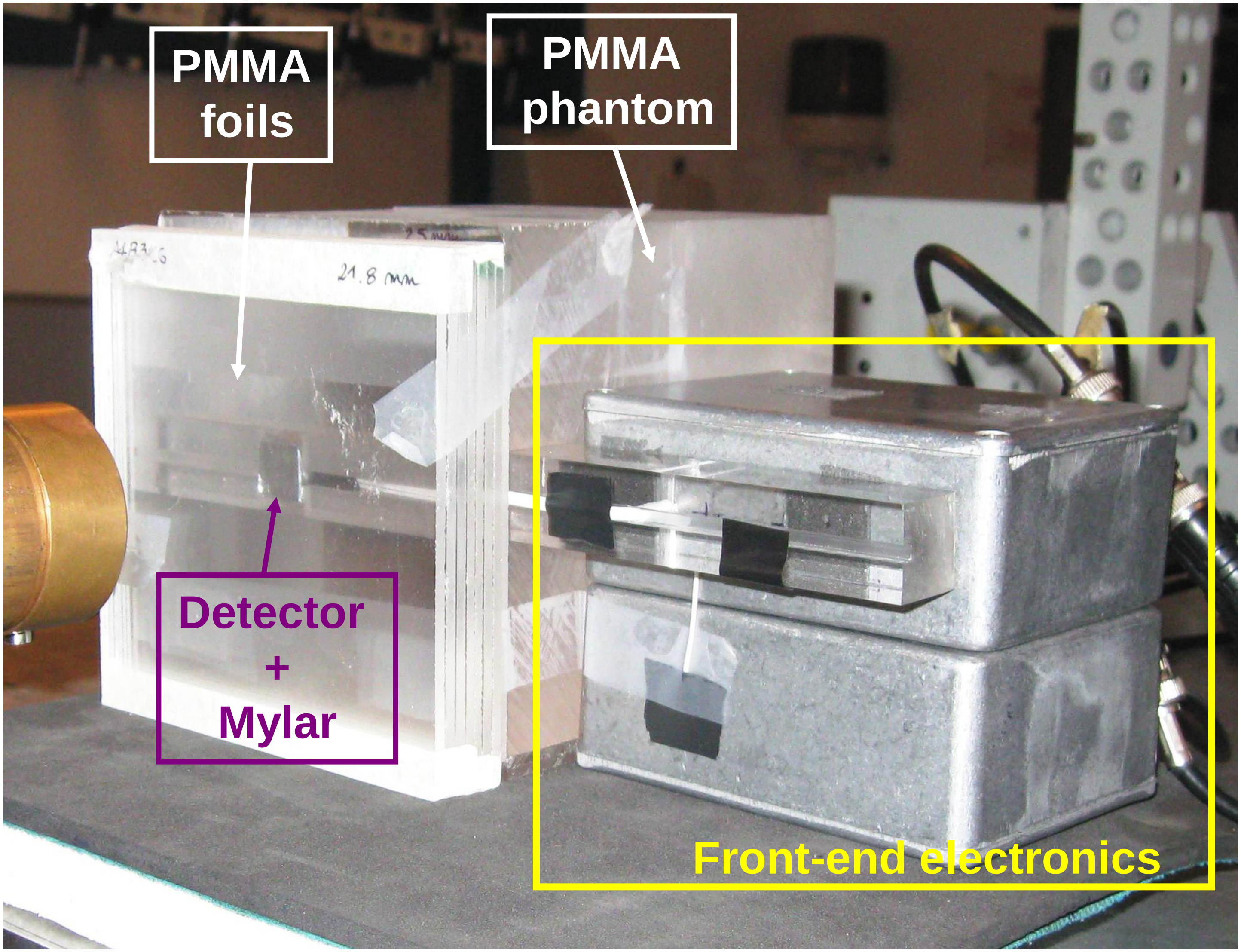

Measurements of the 62 MeV modulated proton beam (CATANA)

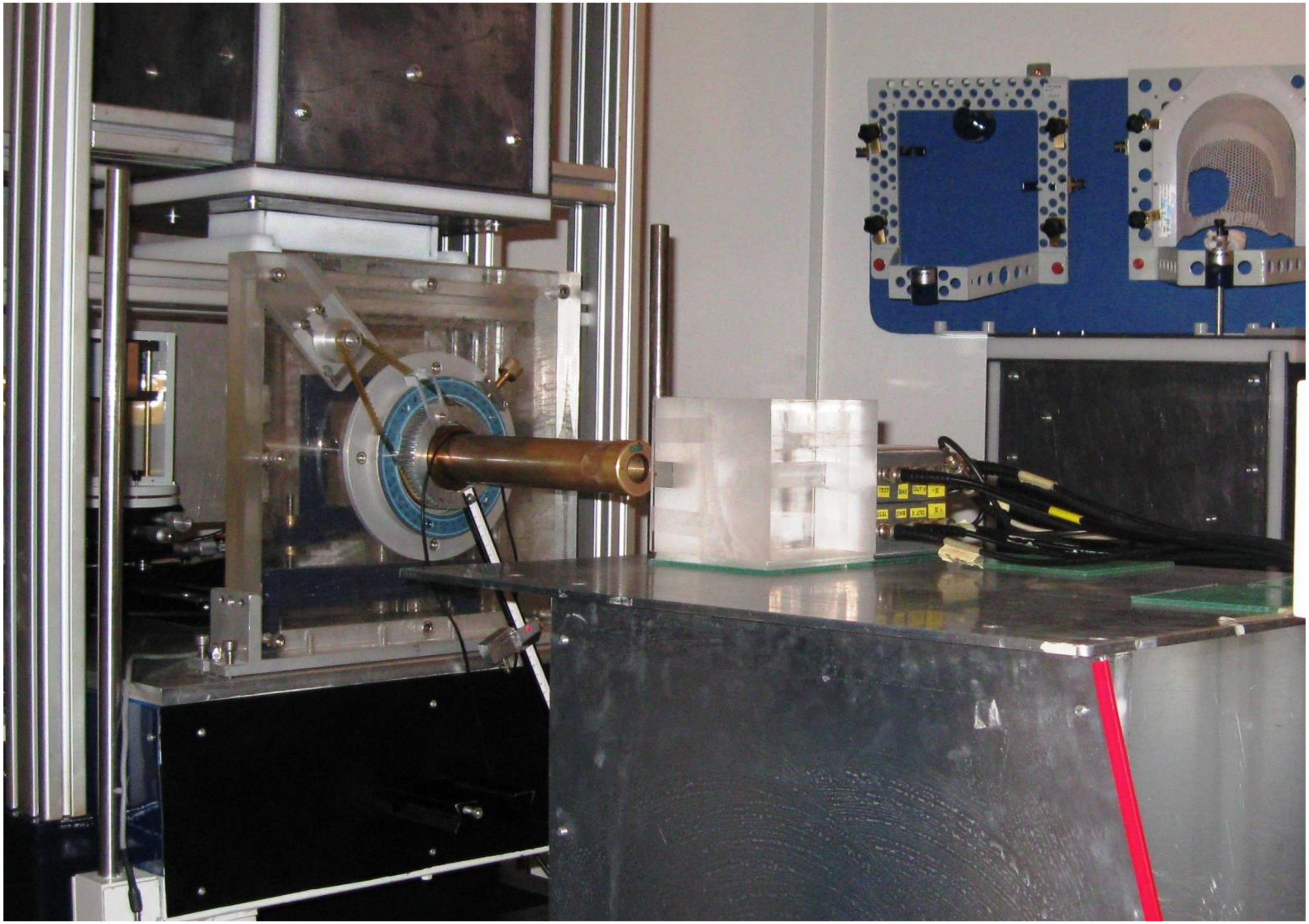

Measurement set-up

62 MeV protons

Range Shifter (4.58 mm PMMA)

Range Modulator (13.4 mm PMMA)

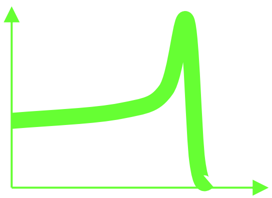

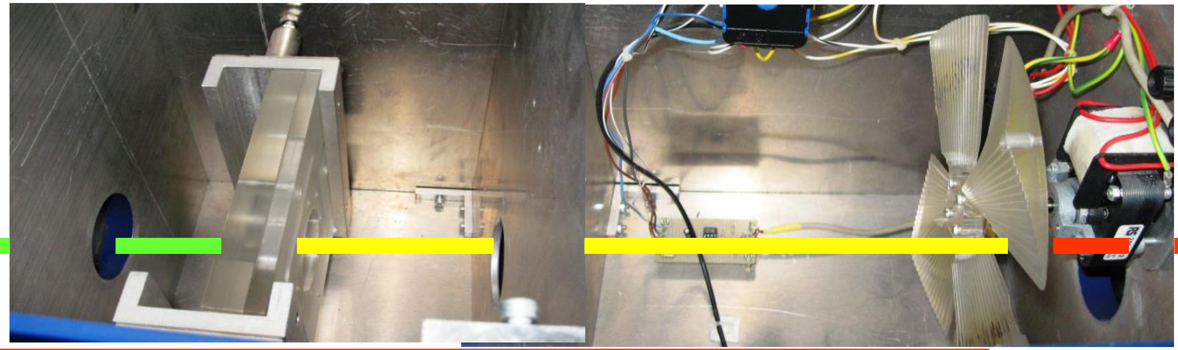

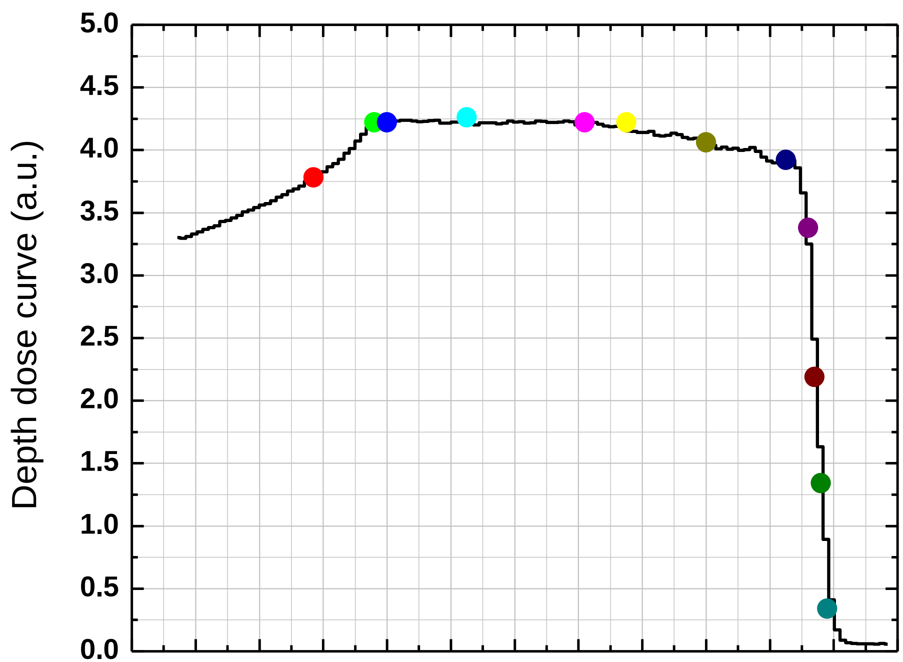

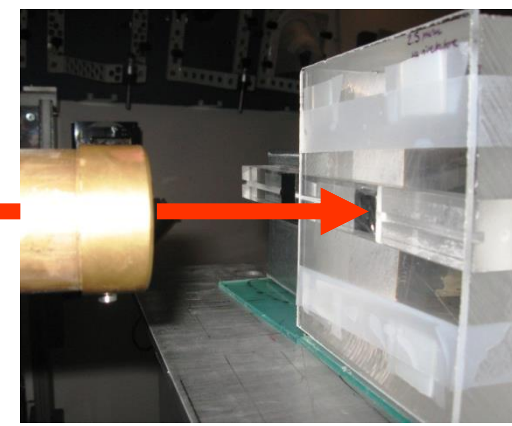

Same experimental set-up of Colautti et al. (with TEPC)

After exciting night measurements ...

Experimental results: ΔE – E scatter plots

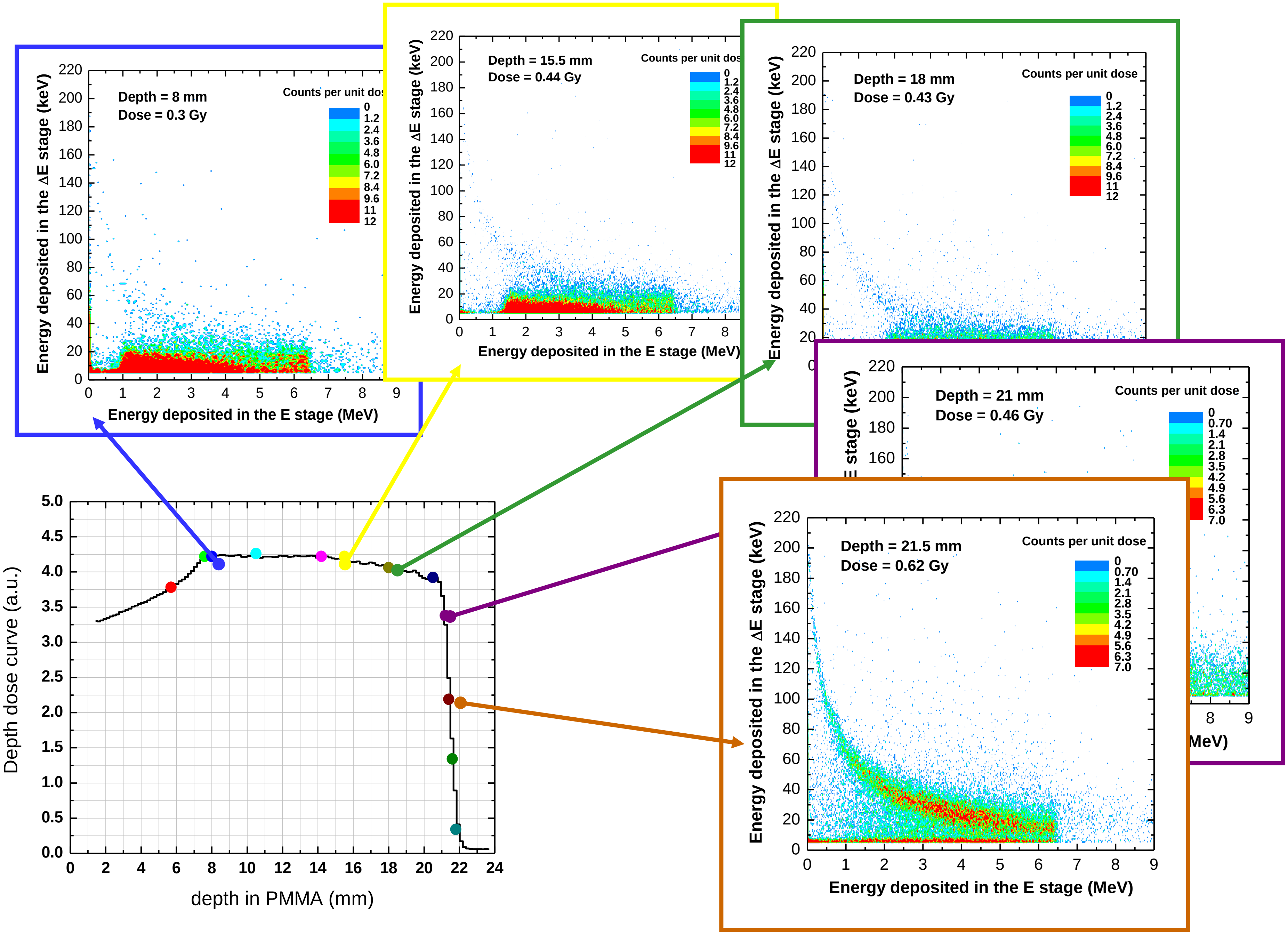

CATANA 62 MeV proton beam:
comparison of microdosimetric spectra measured by the silicon device with those obtained with a cylindrical TEPC

L. De Nardo, D. Moro, P. Colautti,
V. Conte, G. Tornielli and G. Cuttone.
Radiation Protection Dosimetry 110, 1 - 4 (2004)

In order to perform a direct comparison with the microdosimetric spectra acquired by a TEPC, the distributions of the energy imparted per event measured by the silicon detector were corrected for:

1) **Tissue-equivalence**

   Since protons cross both stages, the simplest correction procedure consists of applying a scaling factor given by:

$$\varepsilon_{\Delta E}^{Tissue}(E) = \varepsilon_{\Delta E}^{Si}(E)\cdot \frac{1}{E_{max}}\int_{0}^{E_{max}} \frac{S^{Tissue}(E)}{S^{Si}(E)}\,dE$$

$$\varepsilon_{\Delta E}^{Tissue}(E) = \varepsilon_{\Delta E}^{Si}(E)\cdot 0.574$$

2) **Shape equivalence**

   By equating the dose-mean energy imparted per event for the two different shapes considered:

$$\bar{\varepsilon}_{D}^{\Delta E} = L\cdot \bar{l}_{D}^{\Delta E} = \bar{\varepsilon}_{D}^{TEPC} = L\cdot \bar{l}_{D}^{TEPC}$$

$$\eta = \frac{\bar{l}_{D}^{TEPC}}{\bar{l}_{D}^{\Delta E}} = 0.533$$

1. S. Agosteo, P. Colautti, A. Fazzi, D. Moro and A. Pola, "**A Solid State Microdosimeter based on a Monolithic Silicon Telescope**", Radiat. Prot. Dosim. 122, 382-386 (2006).
2. S. Agosteo, P.G. Fallica, A. Fazzi, M.V. Introini, A. Pola, G. Valvo, "**A Pixelated Silicon Telescope for Solid State Microdosimeter**", Radiat. Meas., 43 (2-6) (2008), 585-589.

Comparison with cylindrical TEPC: proximal part of the SOBP

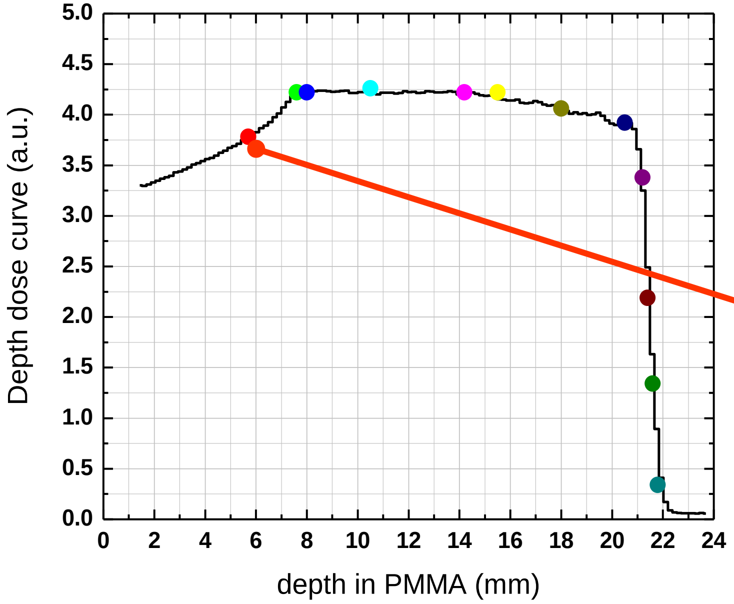

Constant TE scaling factor

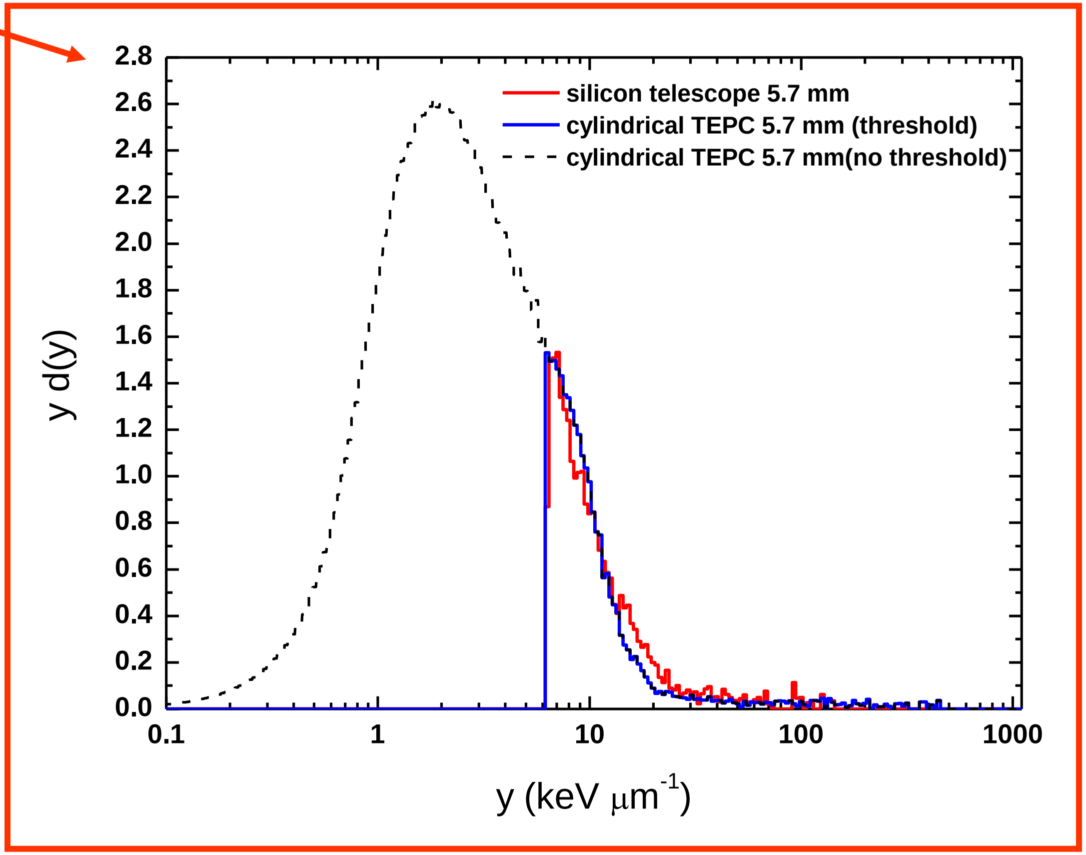

Comparison with cylindrical TEPC: proximal part of the SOBP

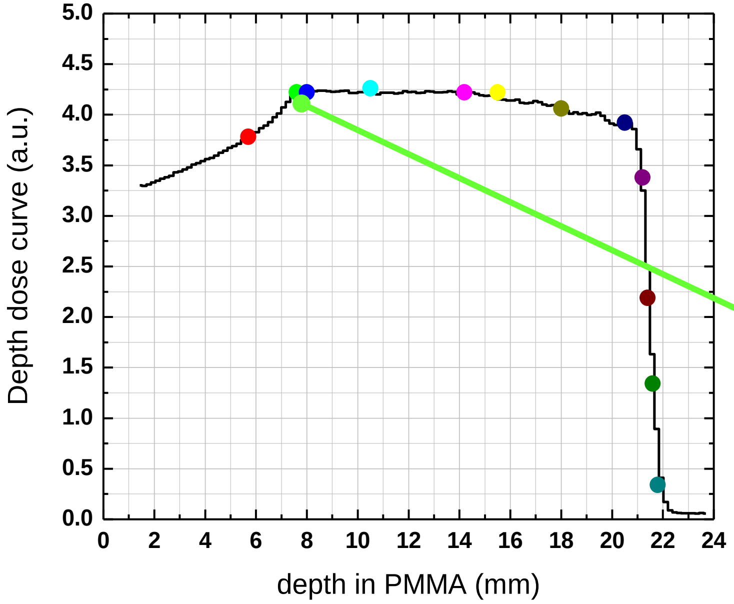

Constant TE scaling factor

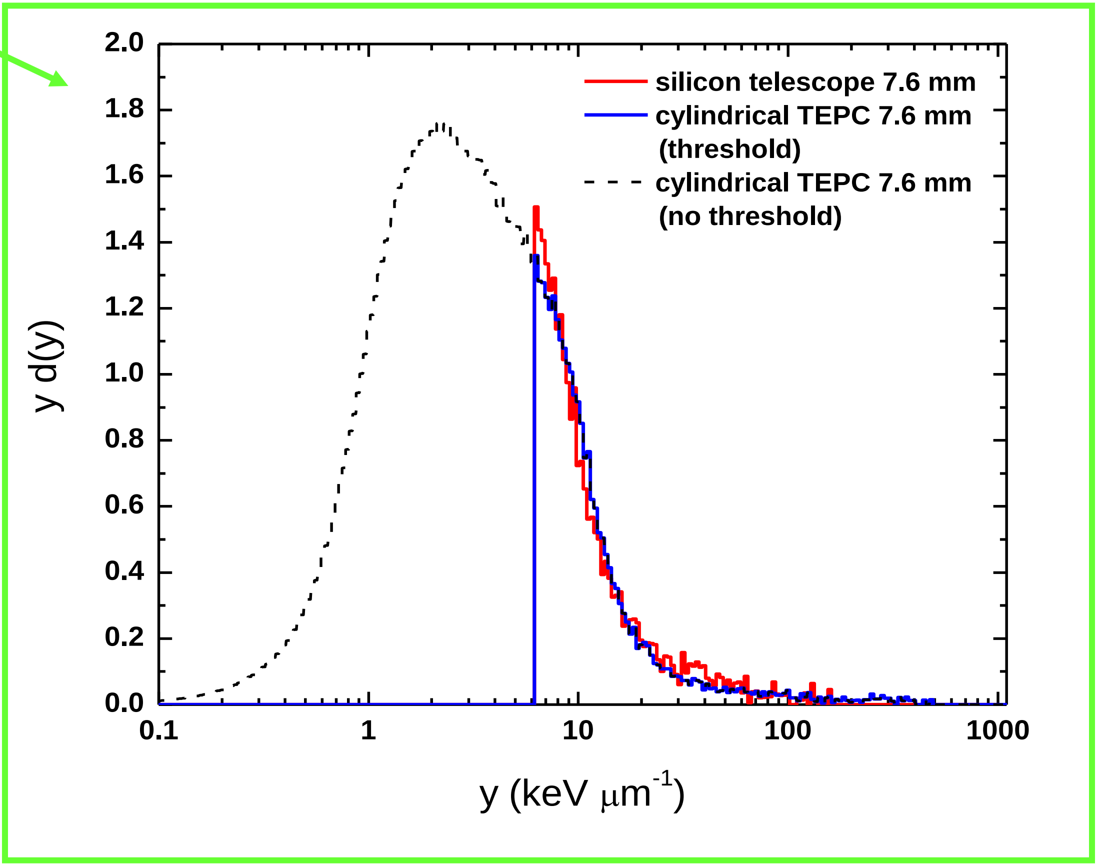

Comparison with cylindrical TEPC: proximal part of the SOBP

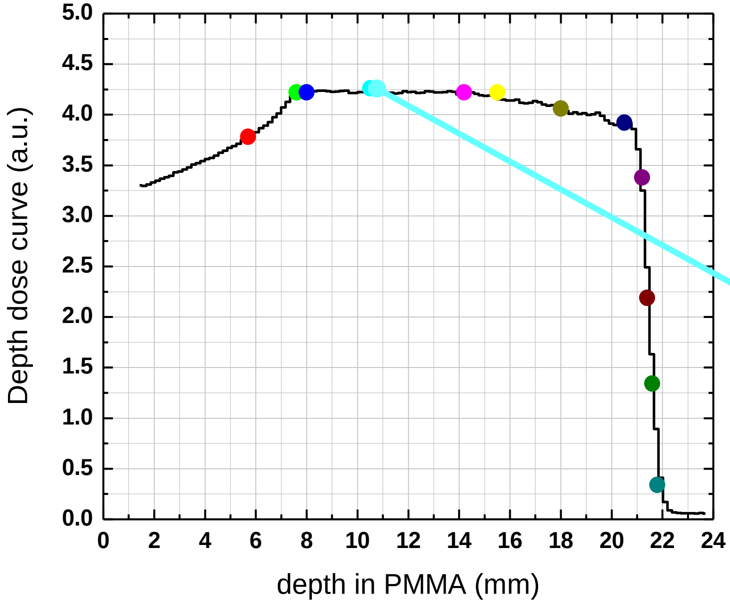

Constant TE scaling factor

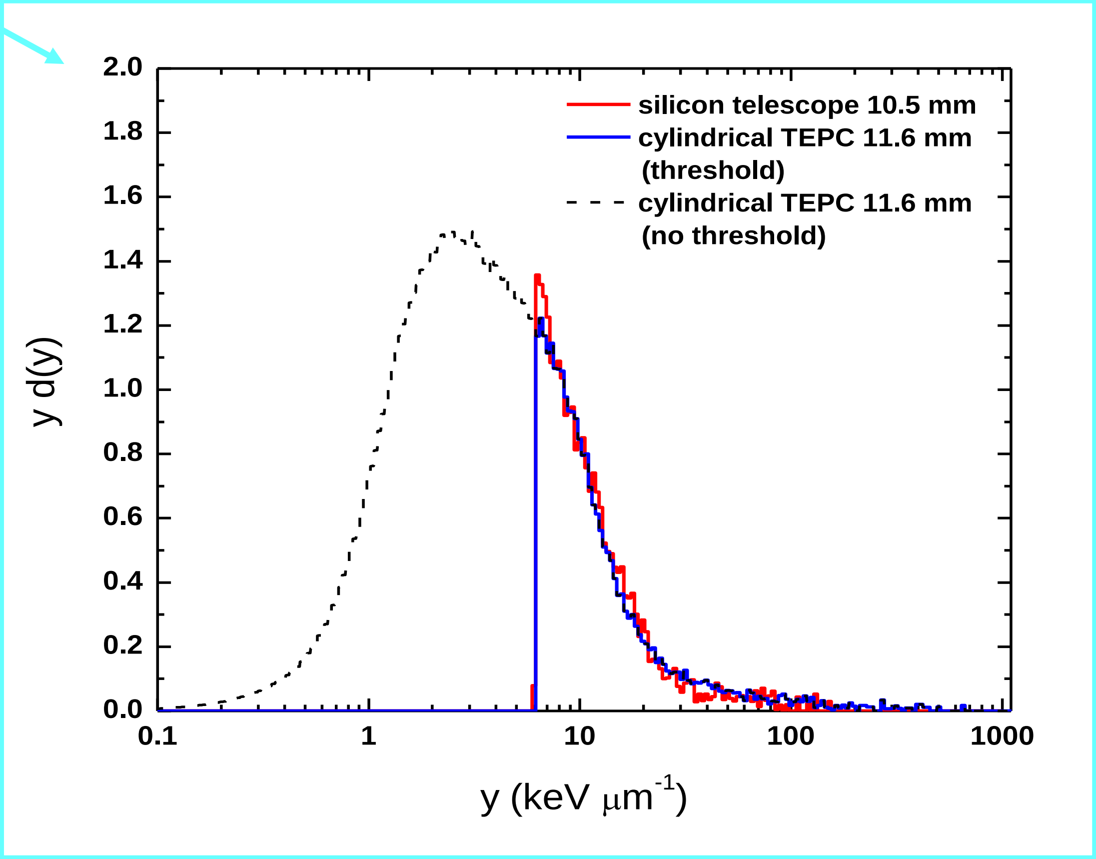

Comparison with cylindrical TEPC: proximal part of the SOBP

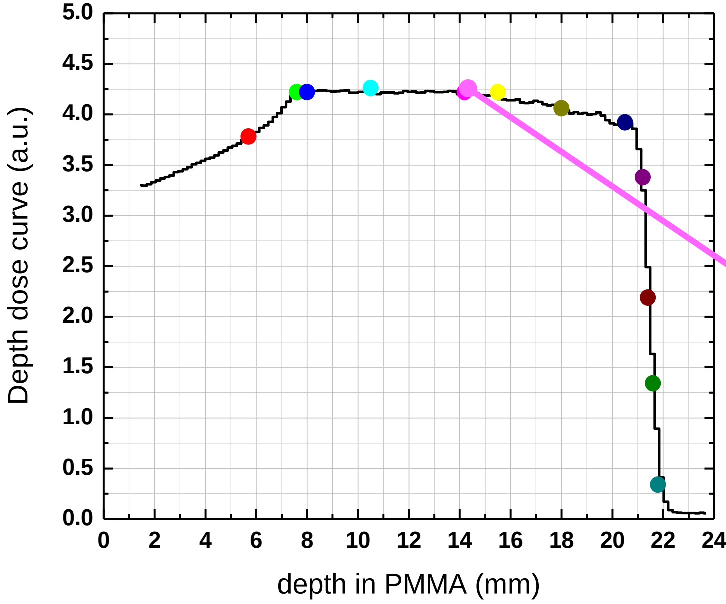

Constant TE scaling factor

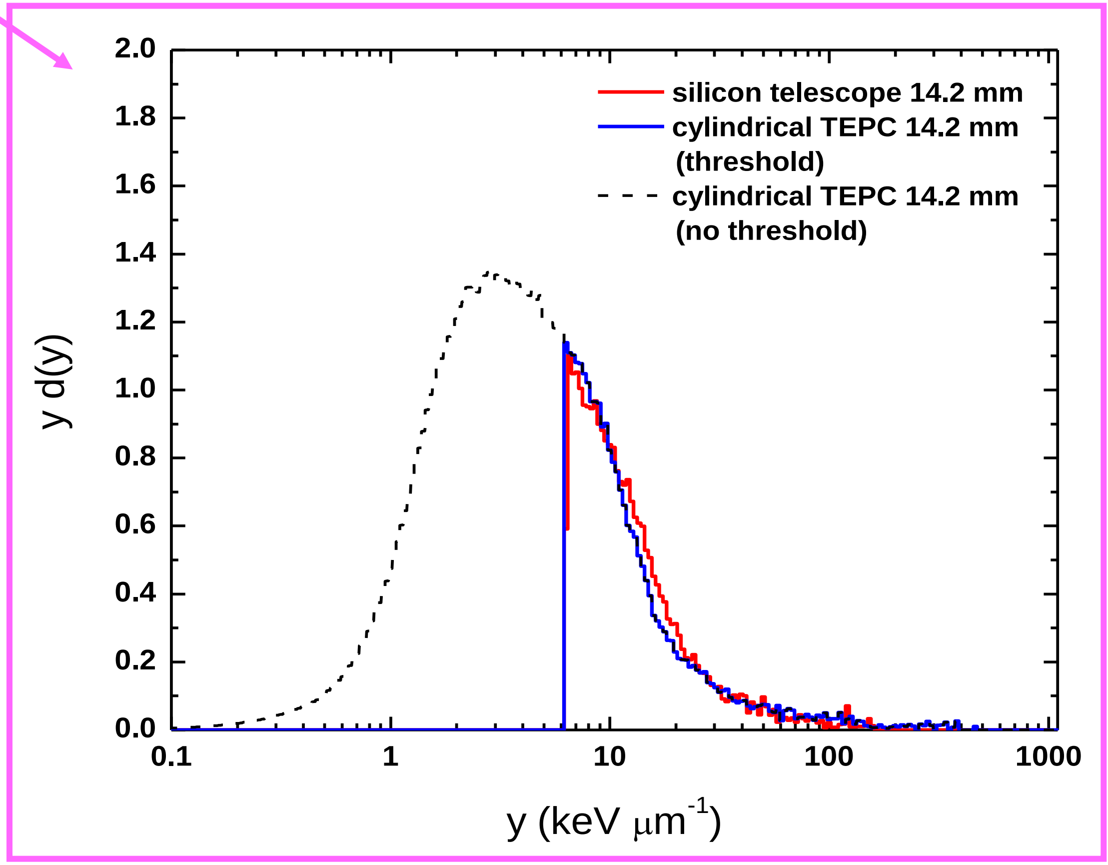

Comparison with cylindrical TEPC: proximal part of the SOBP

Constant TE scaling factor

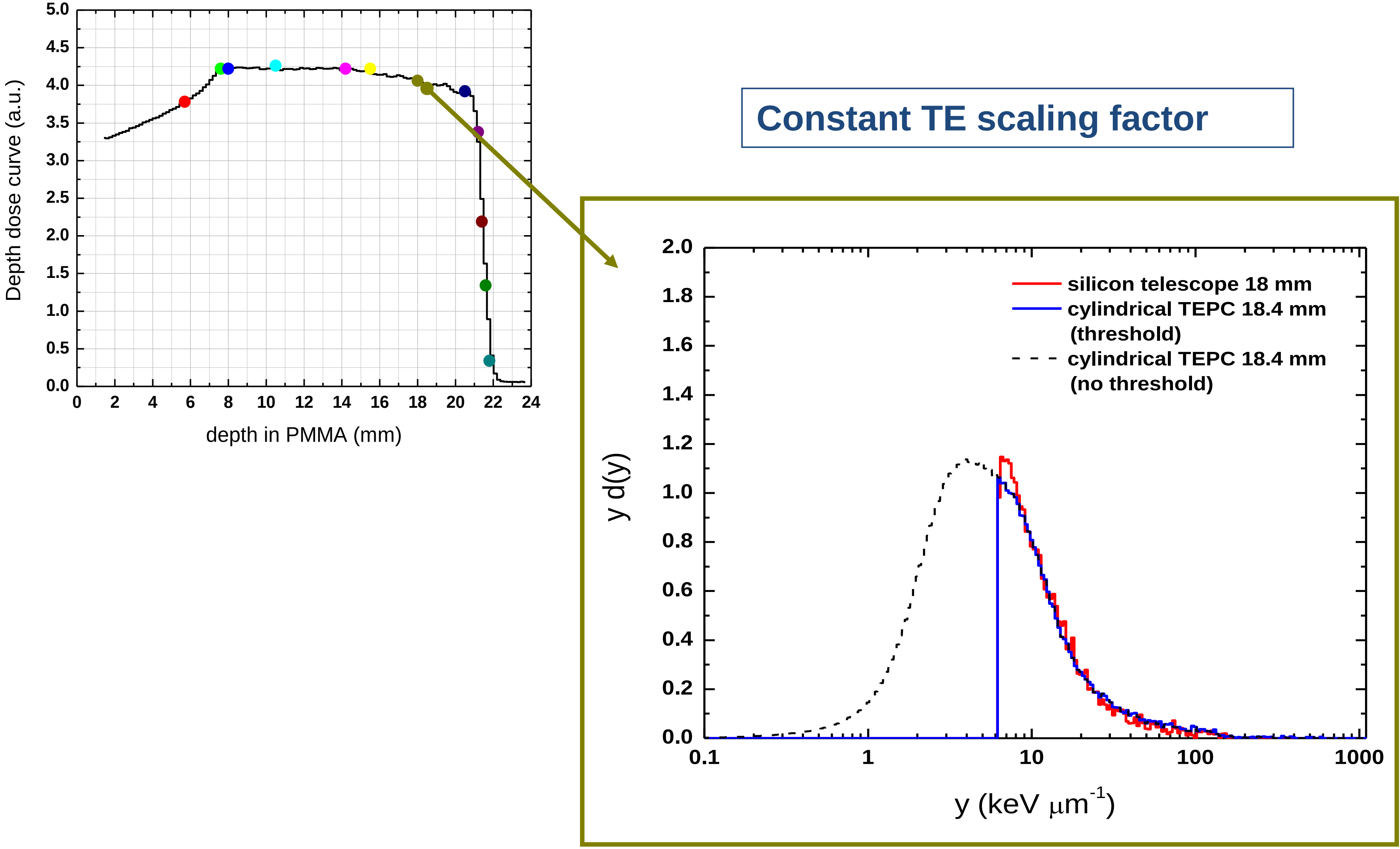

Comparison with cylindrical TEPC: proximal part of the SOBP

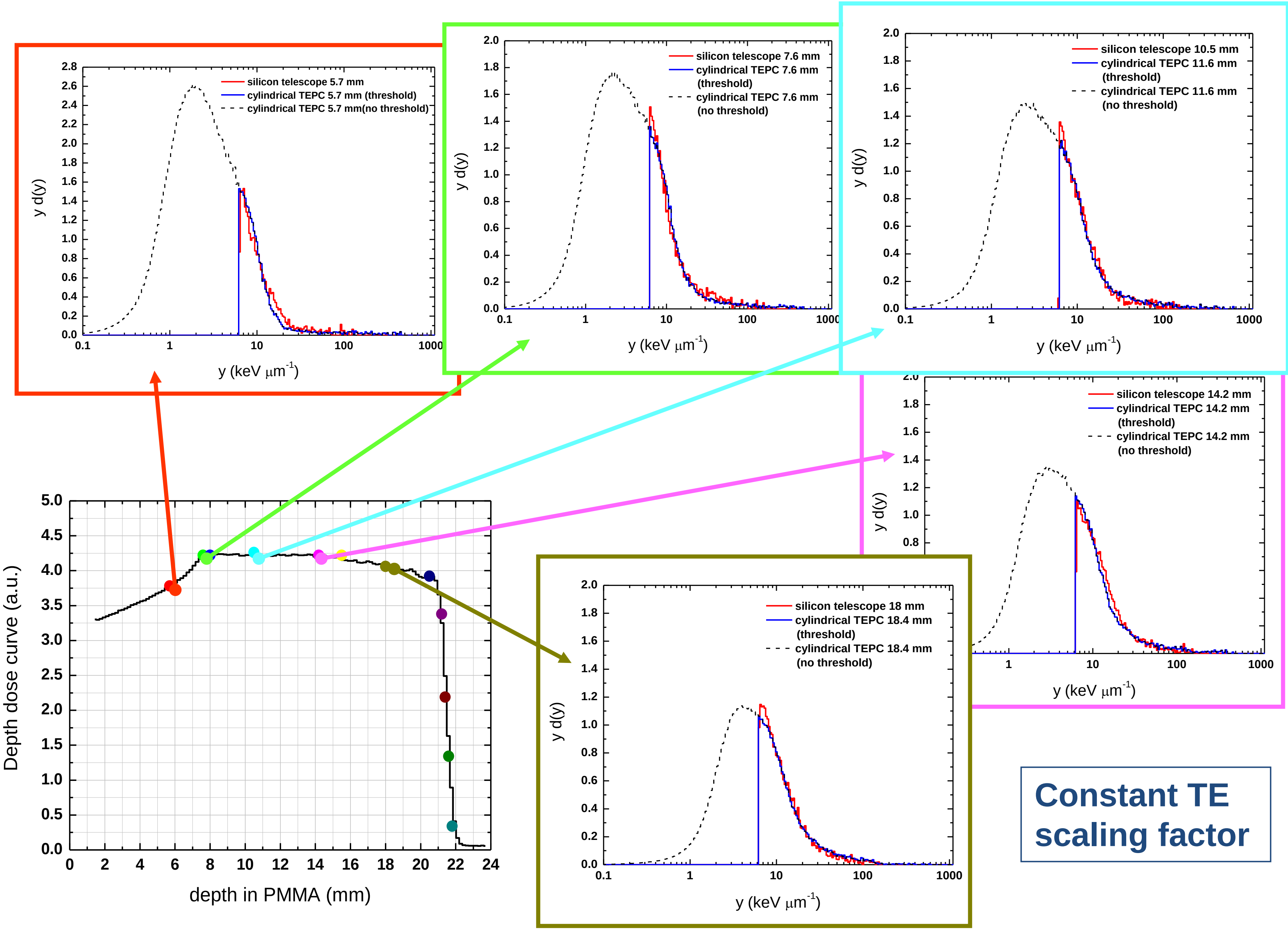

Constant TE scaling factor

Comparison with cylindrical TEPC: distal part of the SOBP

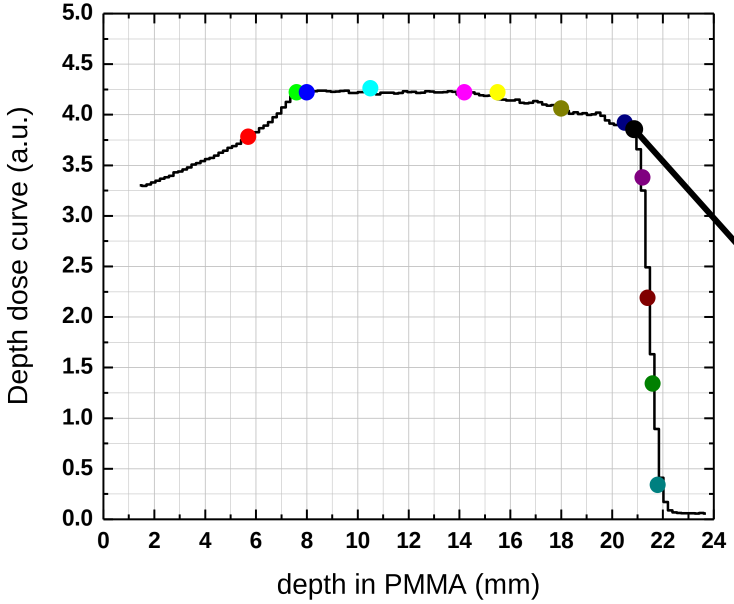

Constant TE scaling factor

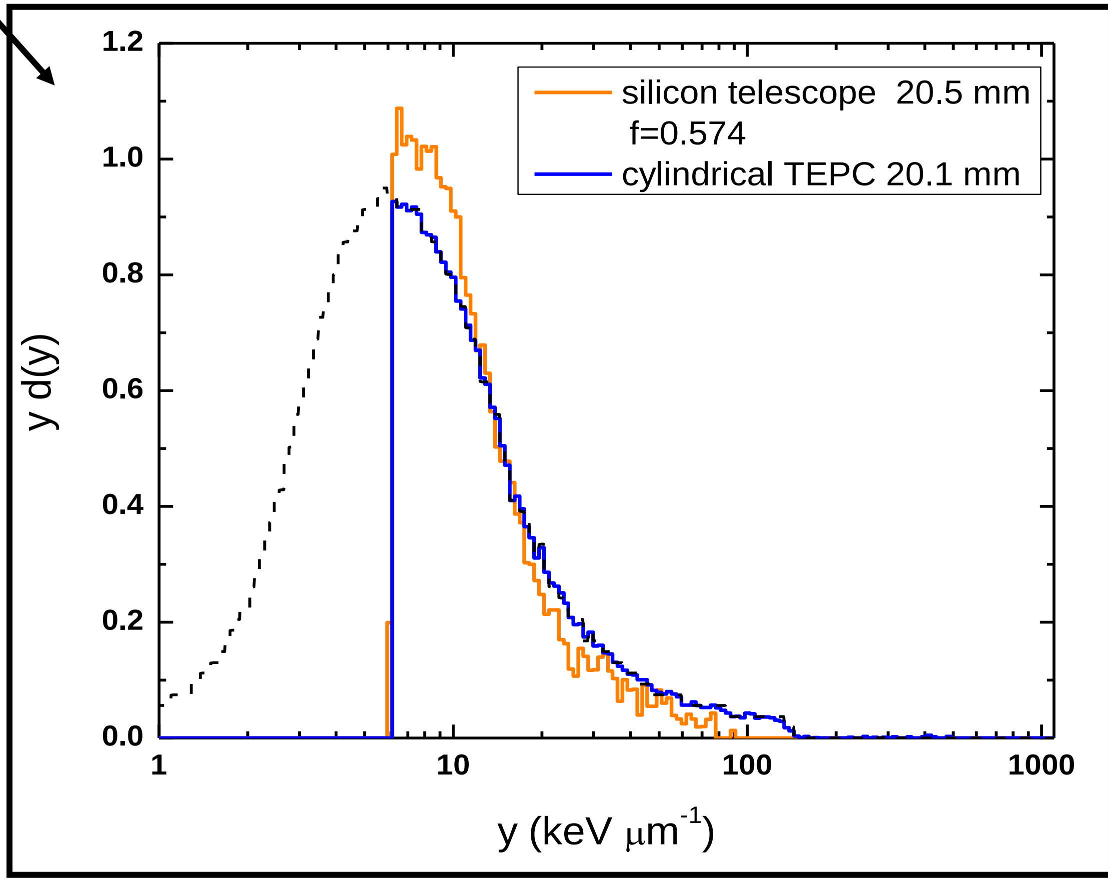

Comparison with cylindrical TEPC: distal part of the SOBP

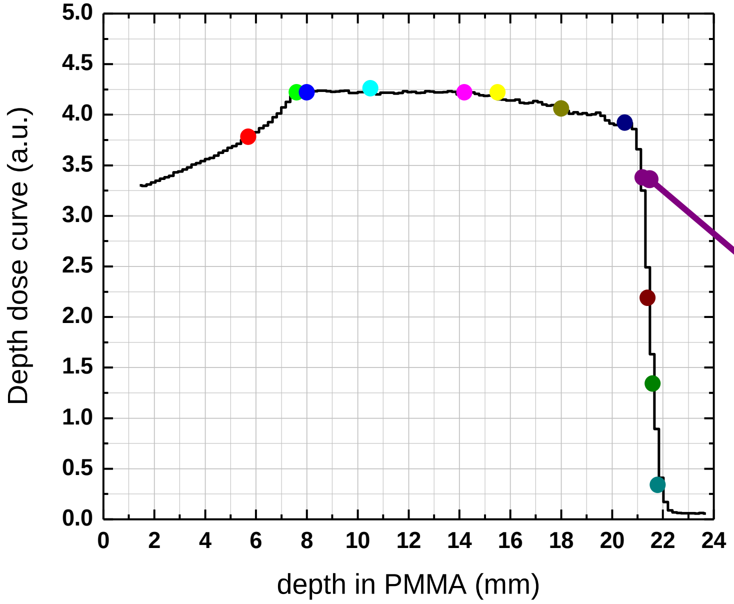

Constant TE scaling factor

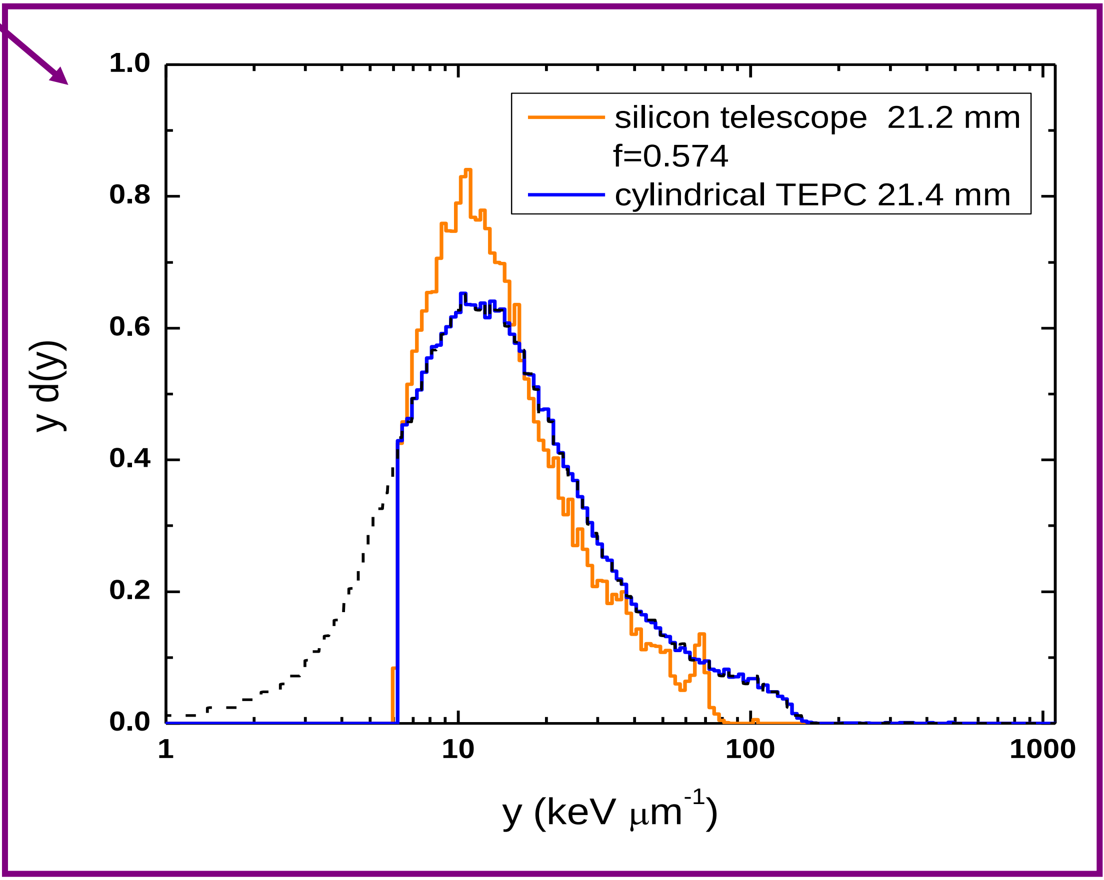

Comparison with cylindrical TEPC: distal part of the SOBP

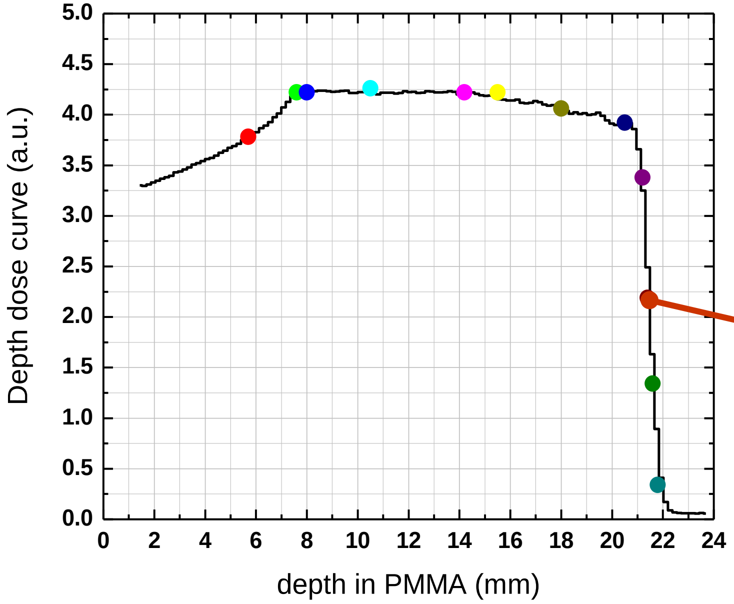

Constant TE scaling factor

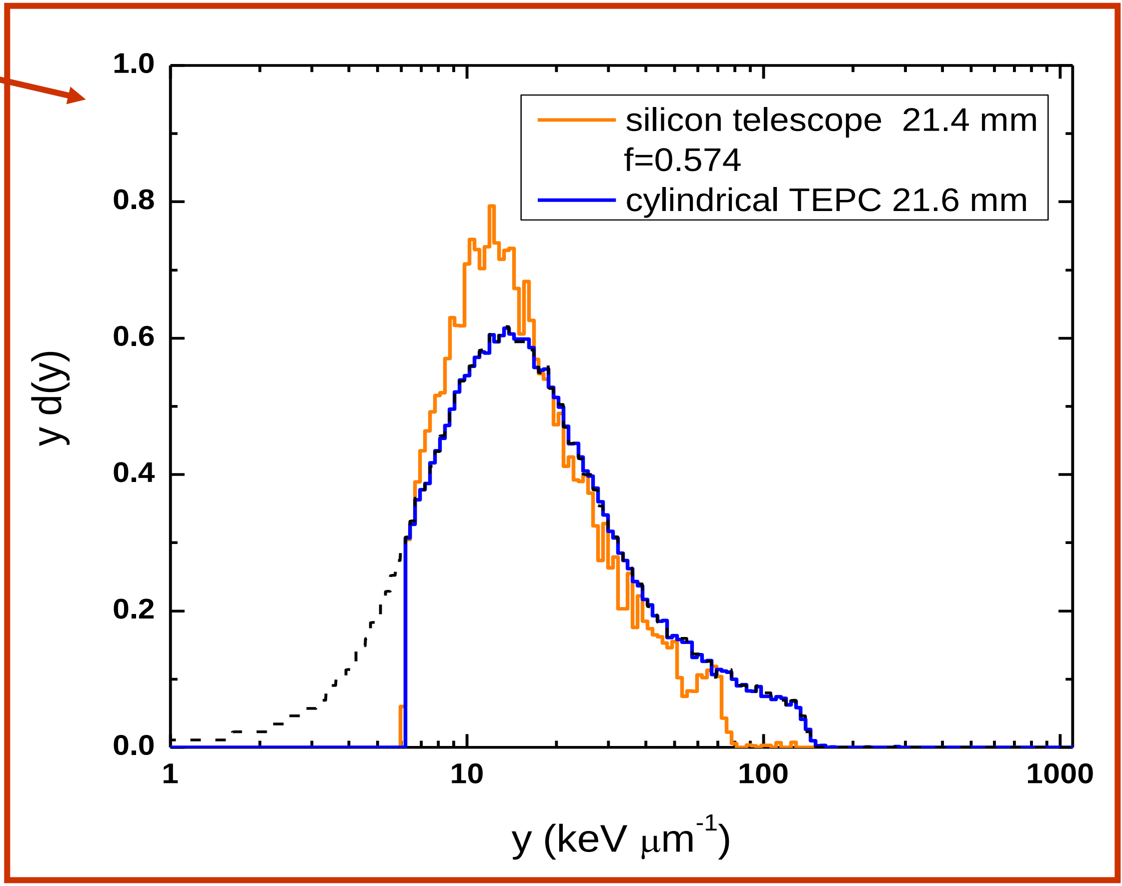

Comparison with cylindrical TEPC: distal part of the SOBP

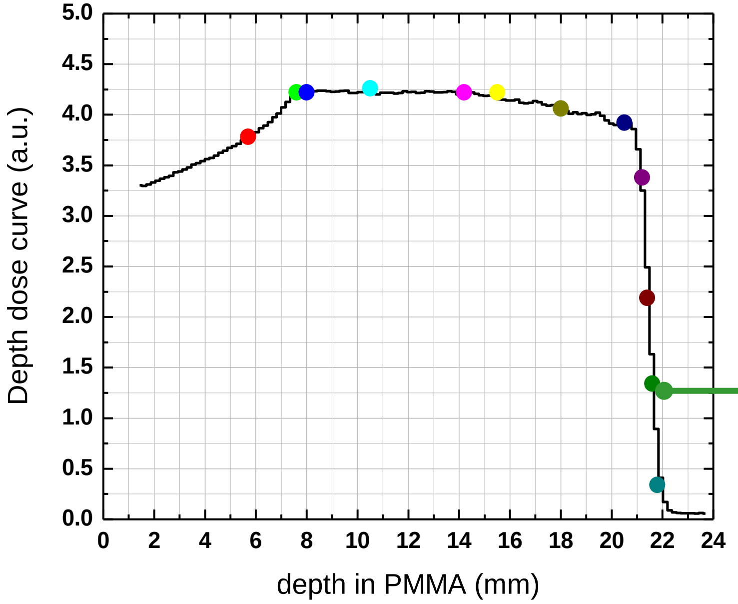

Constant TE scaling factor

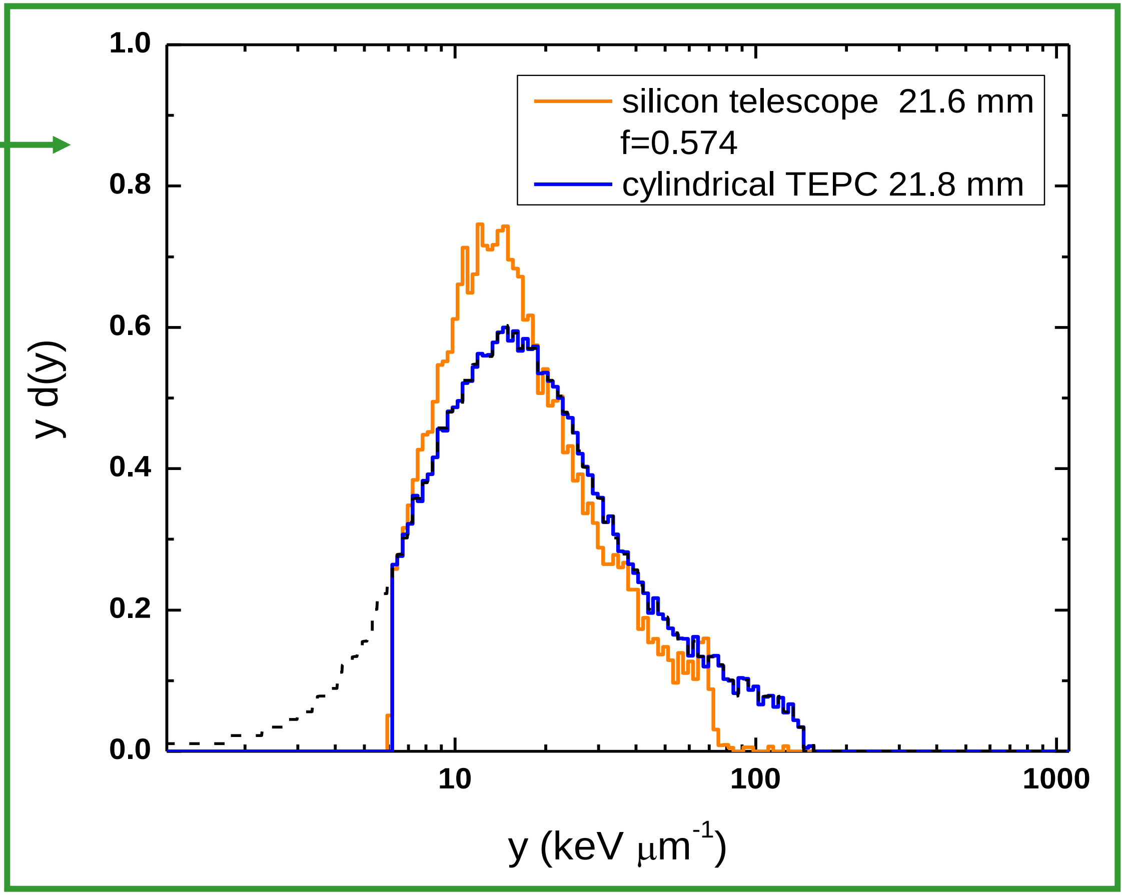

Comparison with cylindrical TEPC: distal part of the SOBP

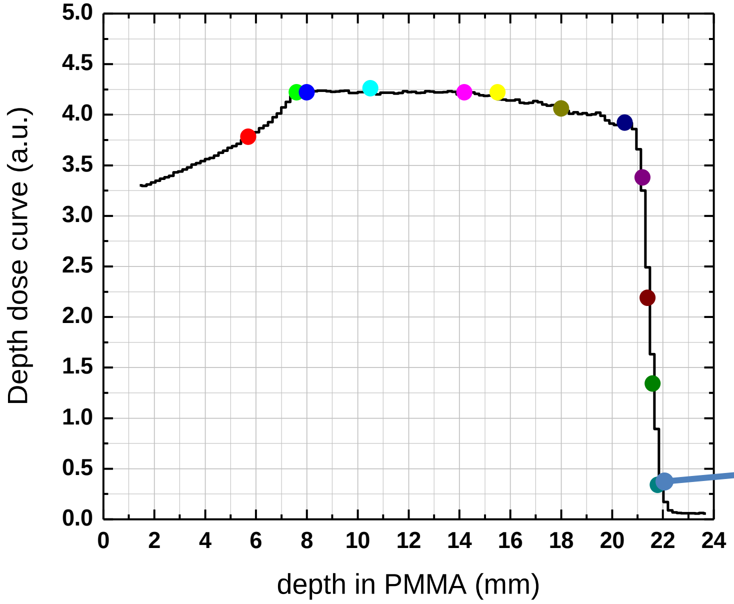

Constant TE scaling factor

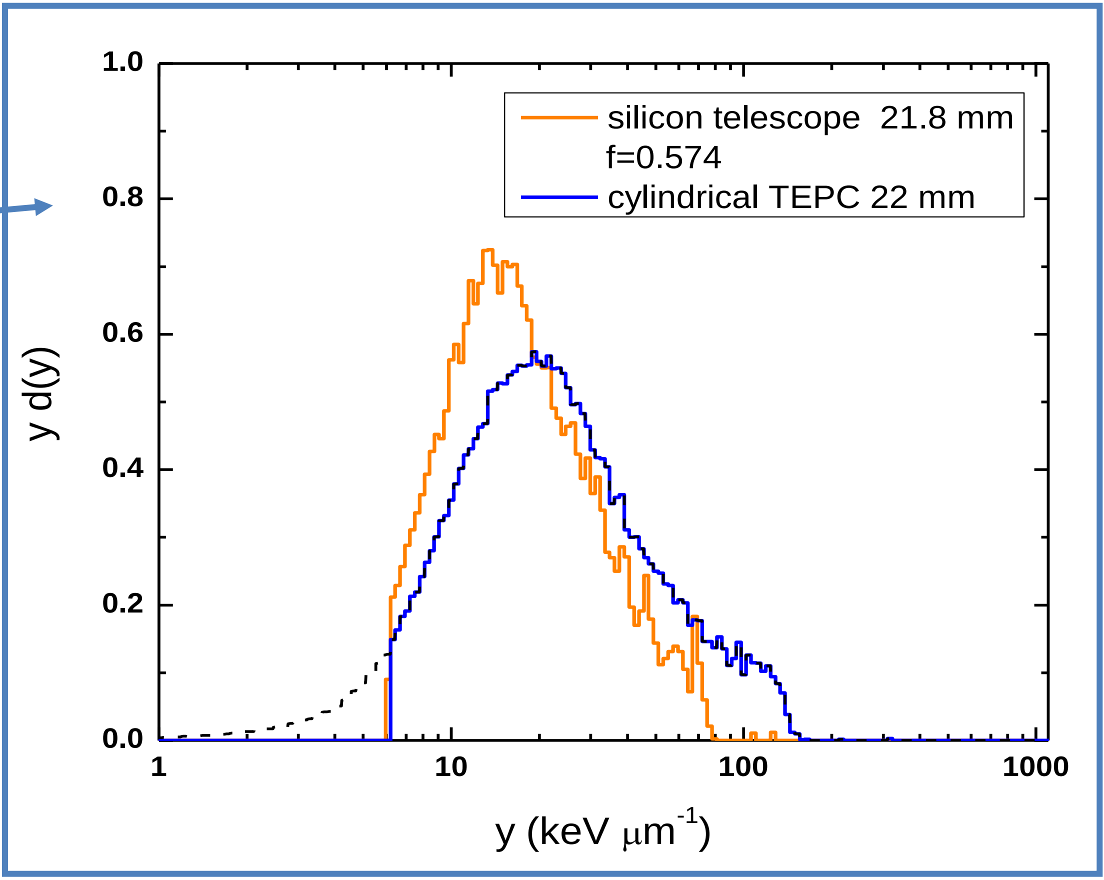

Comparison with cylindrical TEPC: distal part of the SOBP

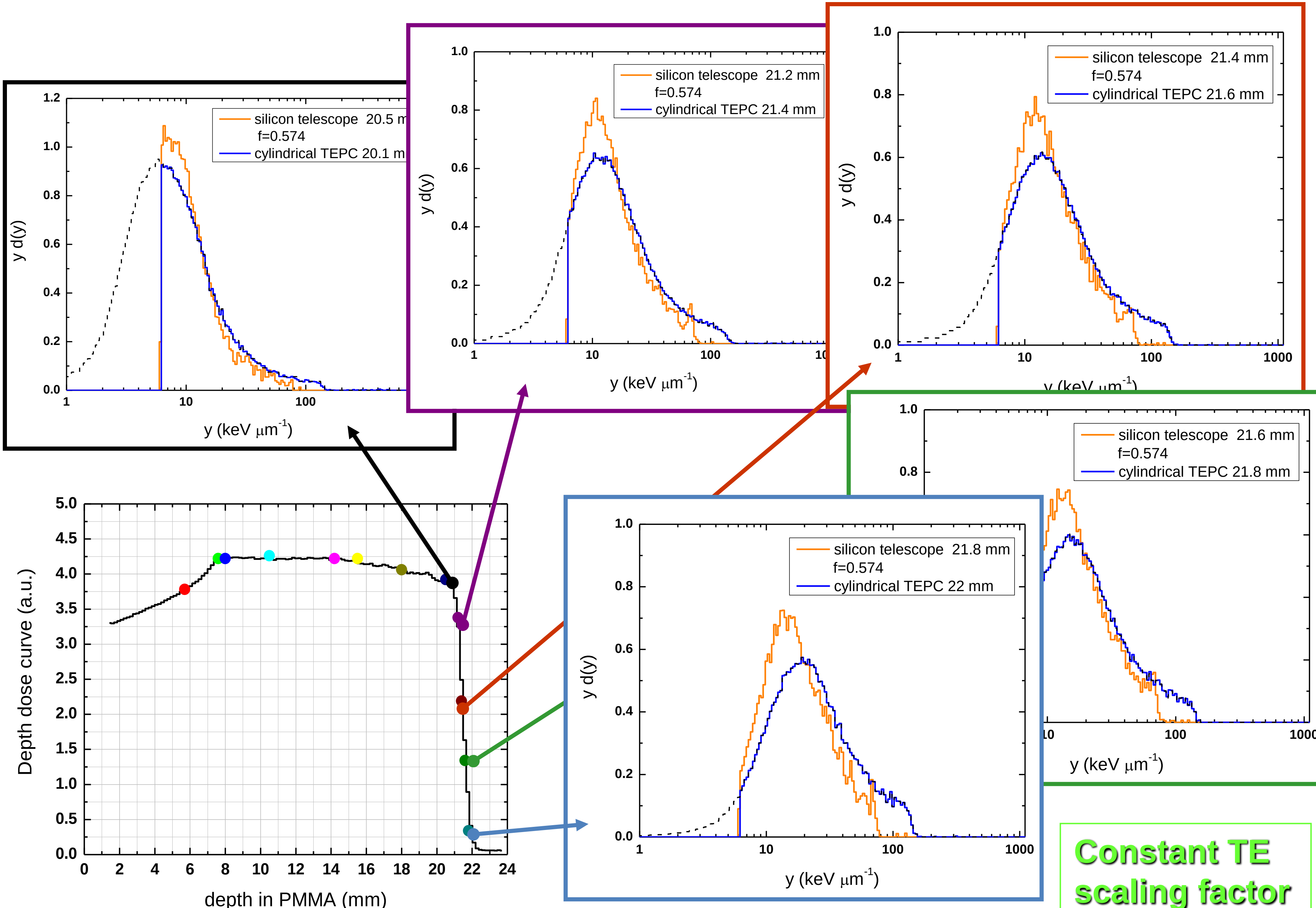

Constant TE scaling factor

But… in the distal part of the SOBP almost all protons stop within the E stage of the silicon detector.

An accurate tissue-equivalence correction can be applied by exploiting <u>event-by-event</u> the information given by the two stages

$$\varepsilon_{\Delta E}^{Tissue}(E) = \varepsilon_{\Delta E}^{Si}(E) \cdot \boxed{\frac{1}{E_{max}} \int_0^{E_{max}} \frac{S^{Tissue}(E)}{S^{Si}(E)} dE}$$

$$\varepsilon_{\Delta E}^{Tissue}(E) = \varepsilon_{\Delta E}^{Si}(E) \cdot \boxed{\frac{S^{Tissue}(E)}{S^{Si}(E)}}$$

where $$E \cong \varepsilon_{\Delta E}^{Si}(E) + \varepsilon_{E}^{Si}(E)$$

Comparison with cylindrical TEPC: distal part of the SOBP

Event-by-event TE correction!!!

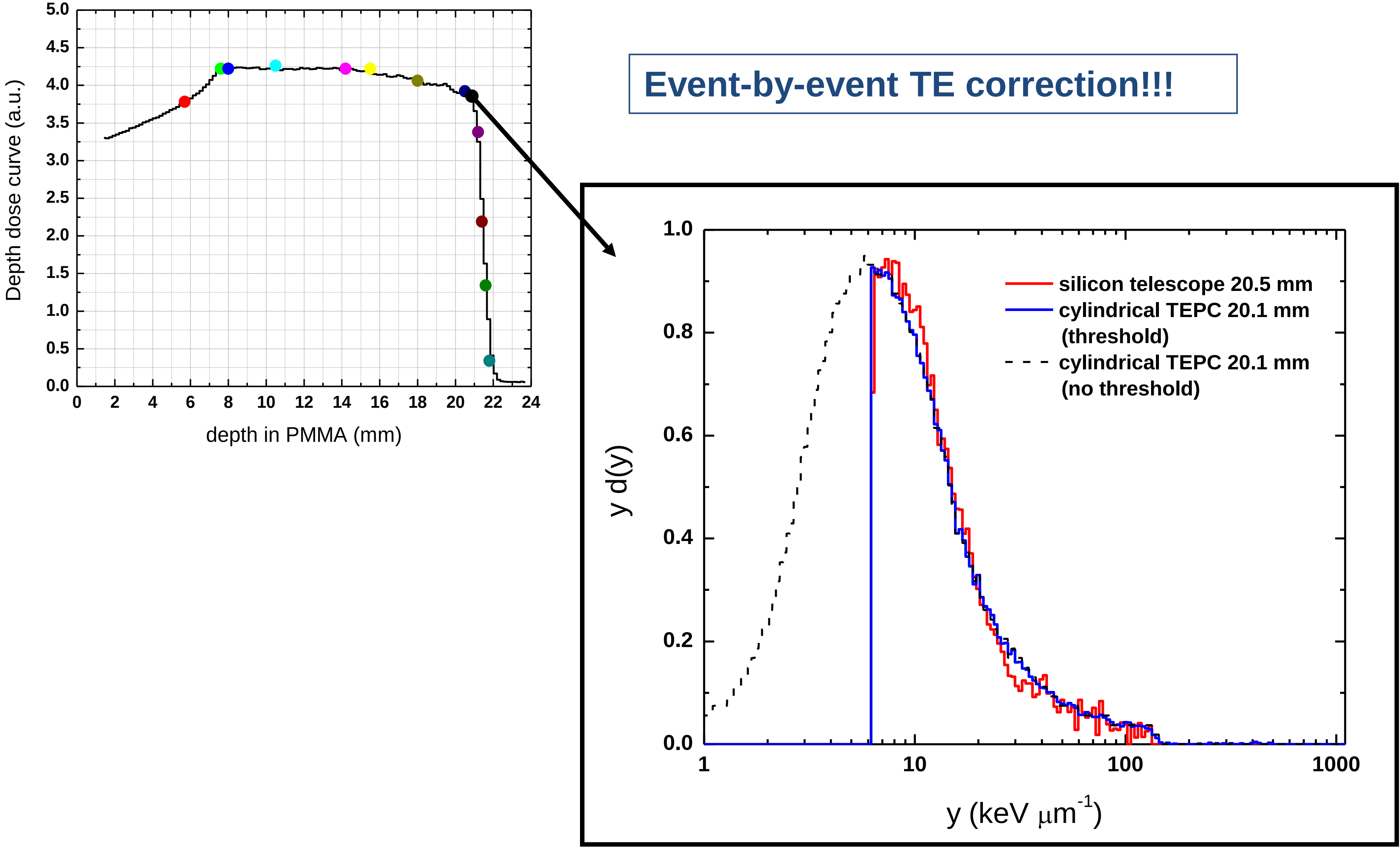

Comparison with cylindrical TEPC: distal part of the SOBP

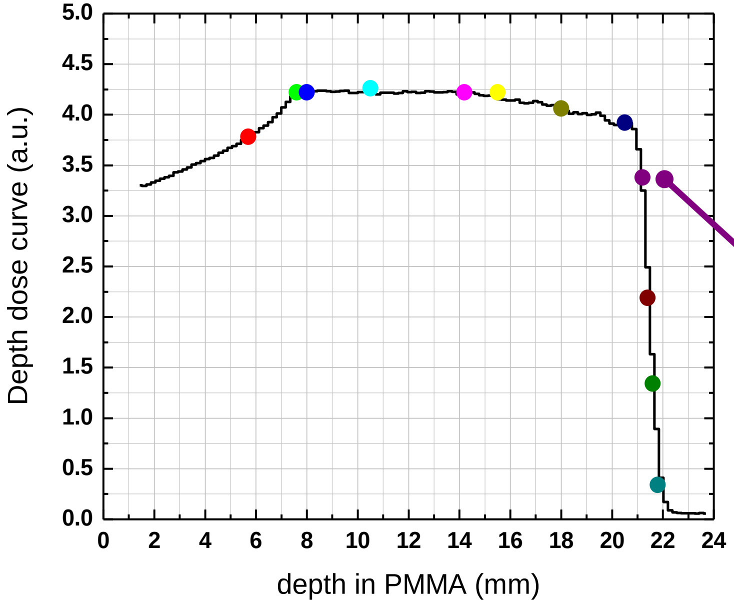

Event-by-event TE correction!!!

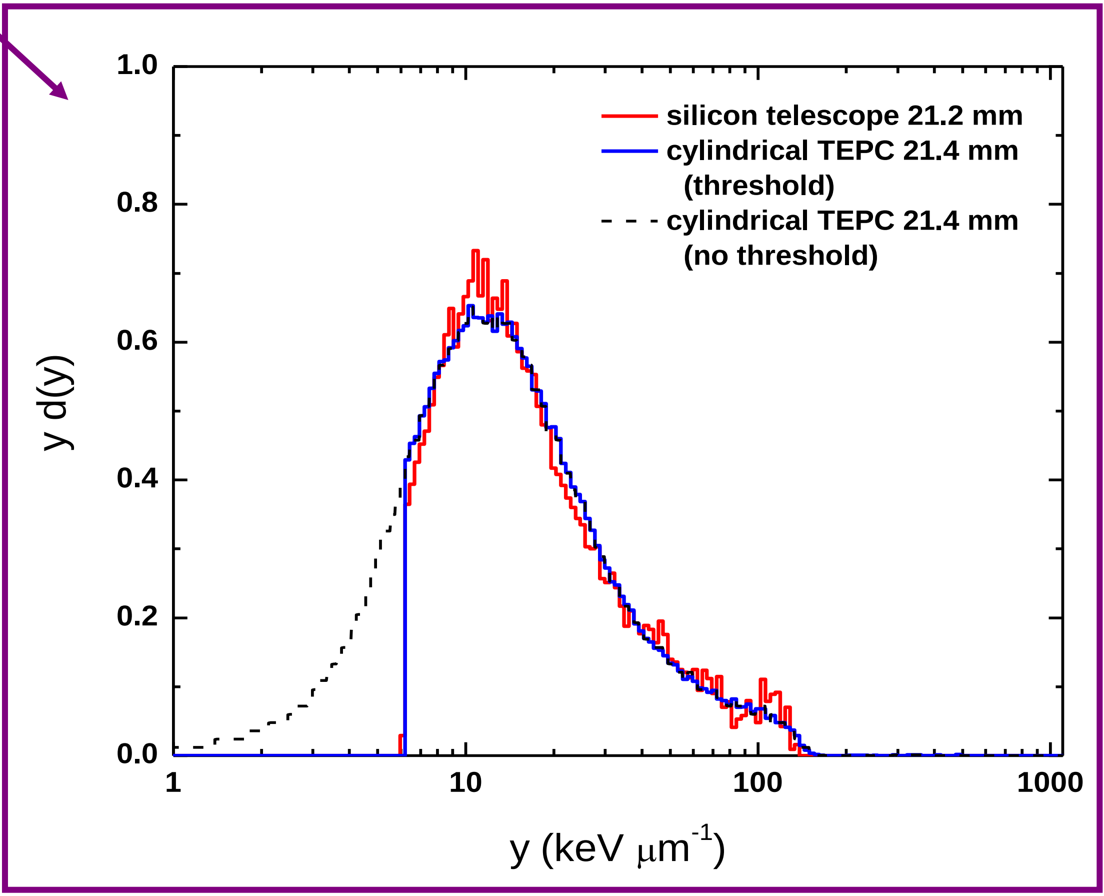

Comparison with cylindrical TEPC: distal part of the SOBP

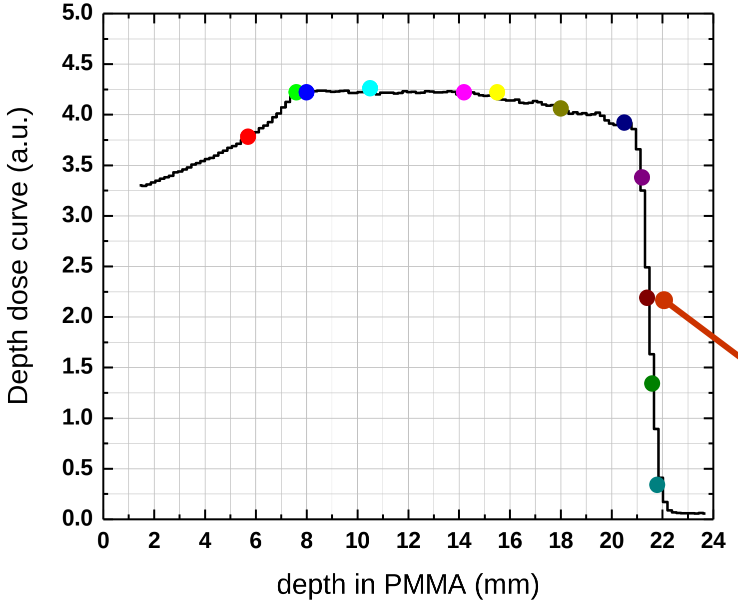

Event-by-event TE correction!!!

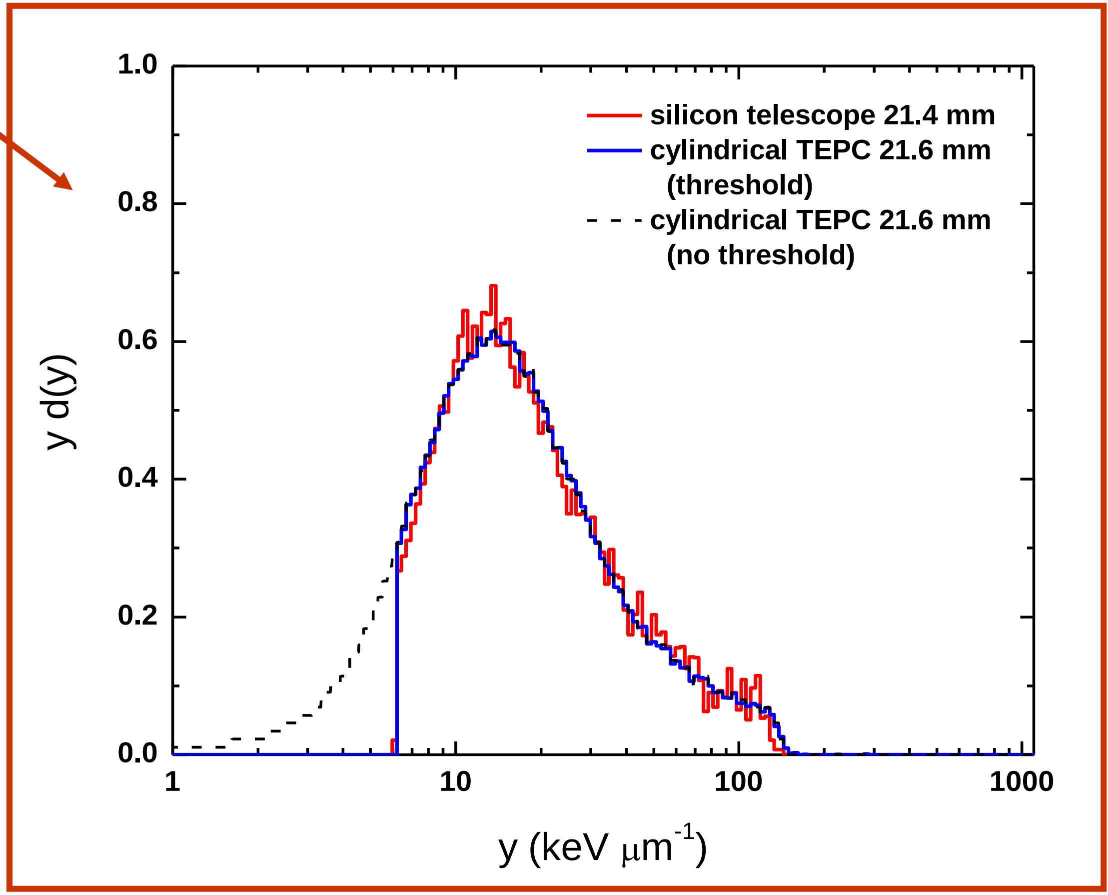

Comparison with cylindrical TEPC: distal part of the SOBP

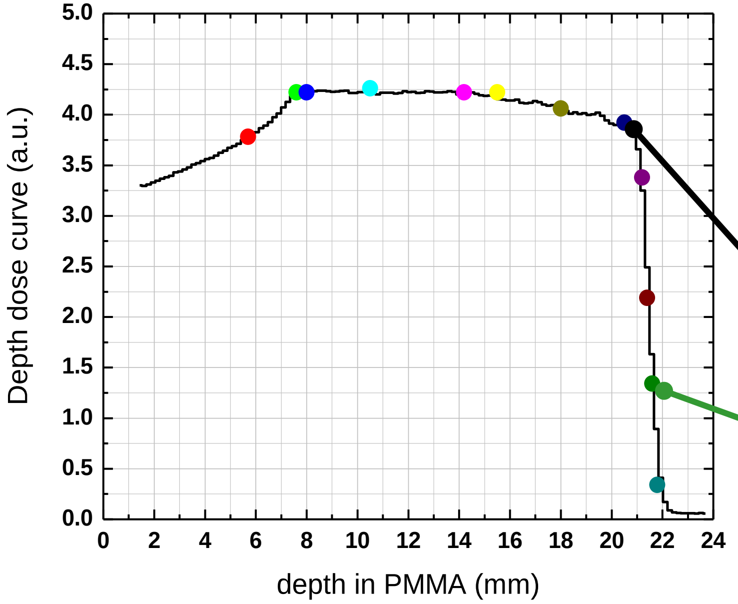

Event-by-event TE correction!!!

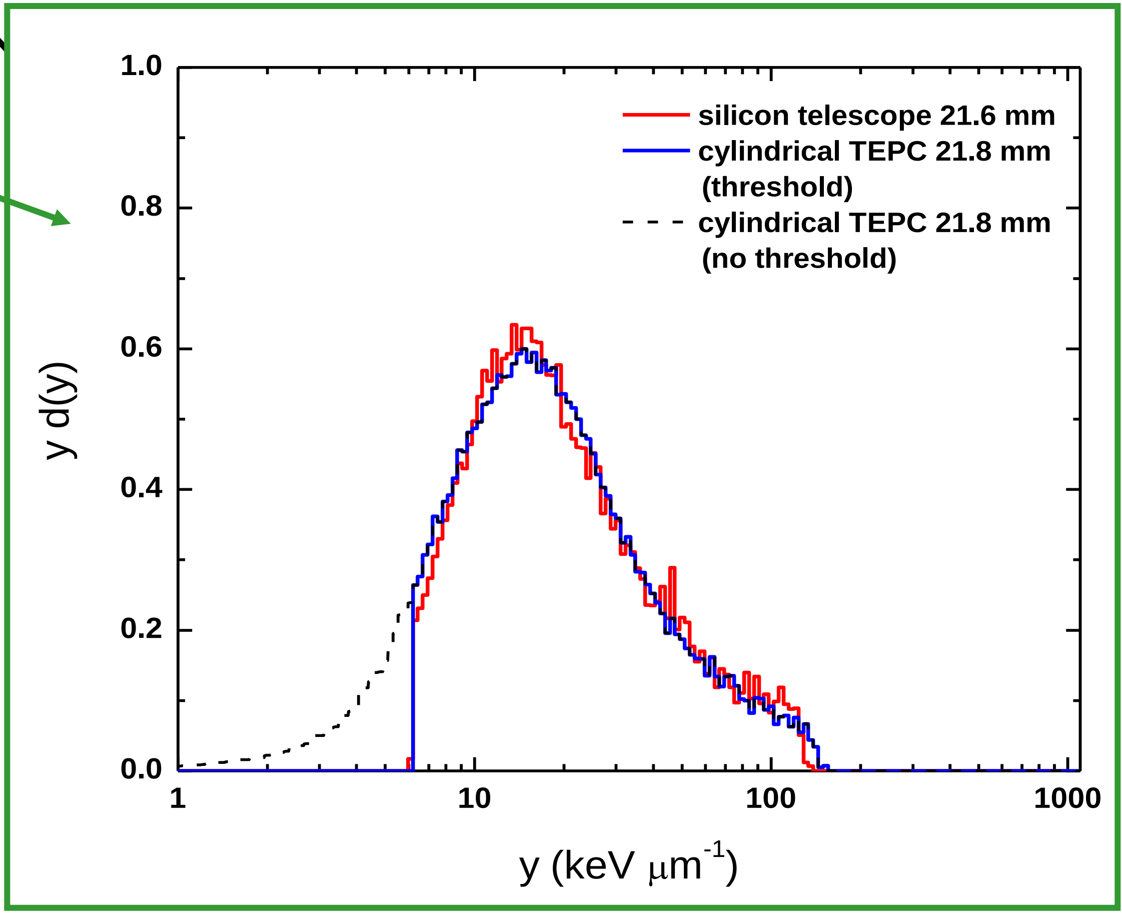

Comparison with cylindrical TEPC: distal part of the SOBP

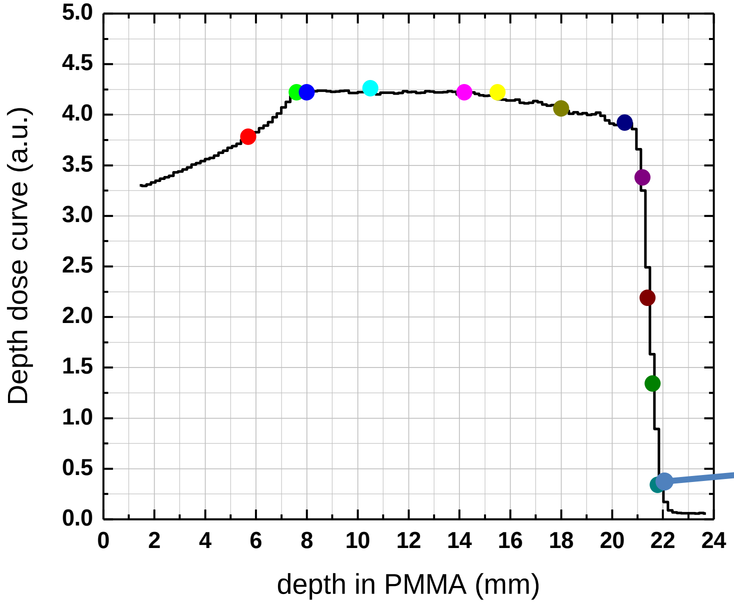

Event-by-event TE correction!!!

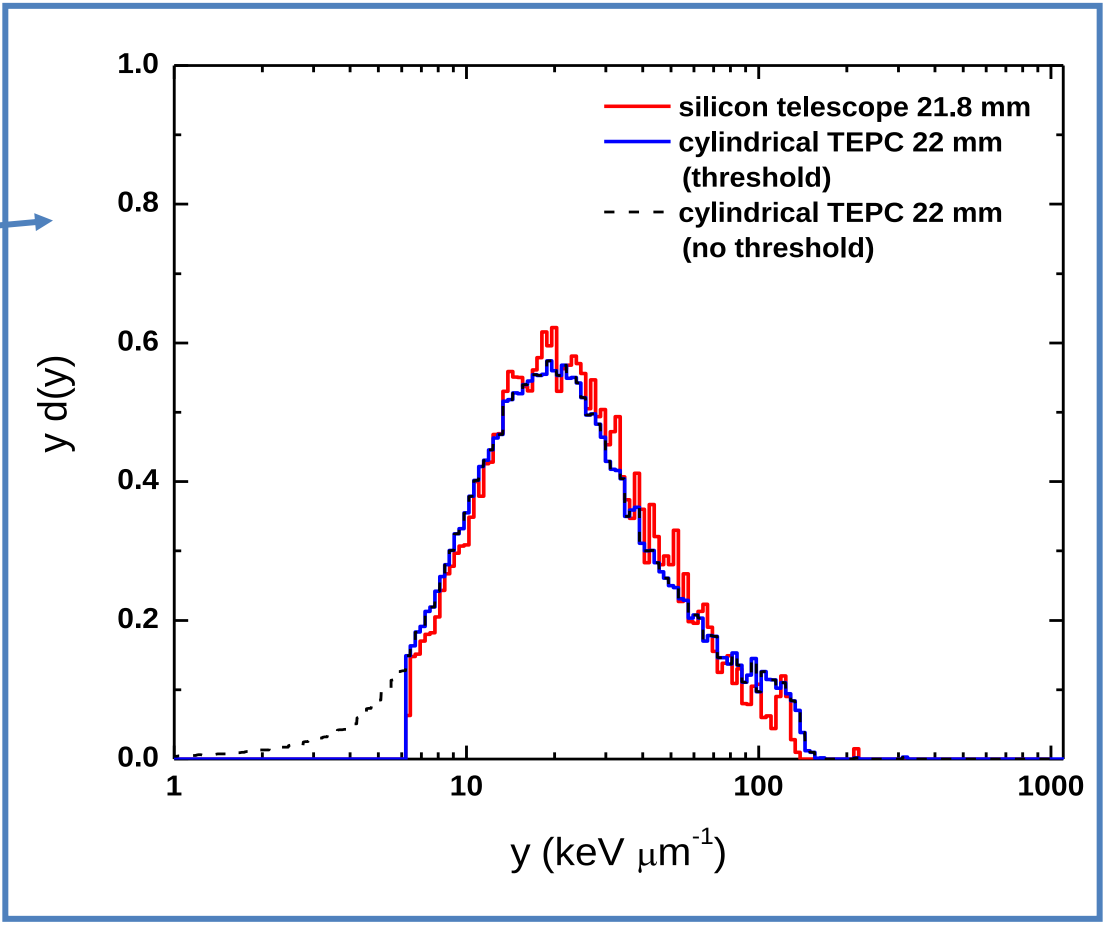

Comparison with cylindrical TEPC: distal part of the SOBP

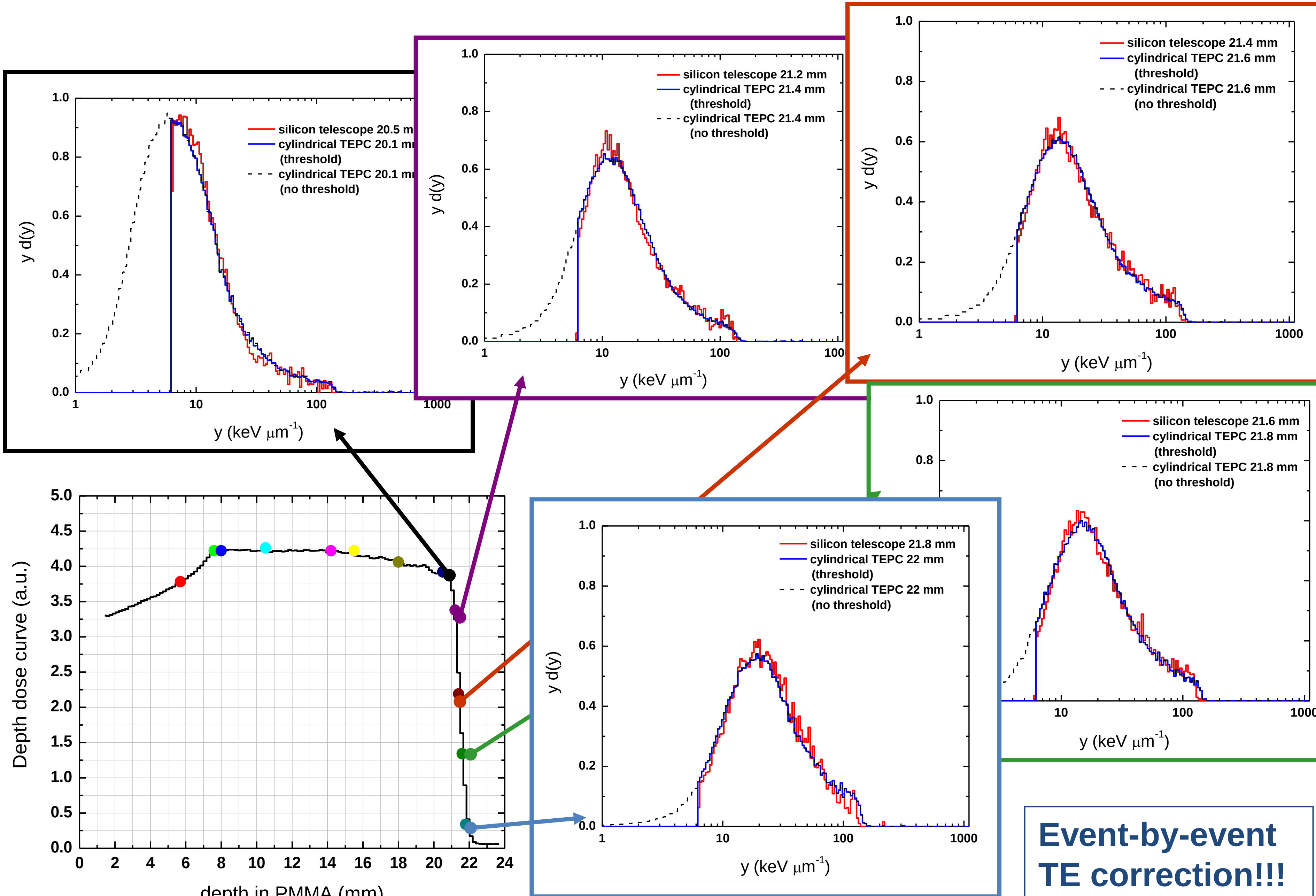

Event-by-event TE correction!!!

Characterization of the influence of the geometrical structure of ΔE detector on microdosimetric spectra: irradiations with 62 AMeV carbon ions

Preliminary irradiations with carbon ions

62 AMeV un-modulated carbon beam at the INFN-LNS cyclotron facility

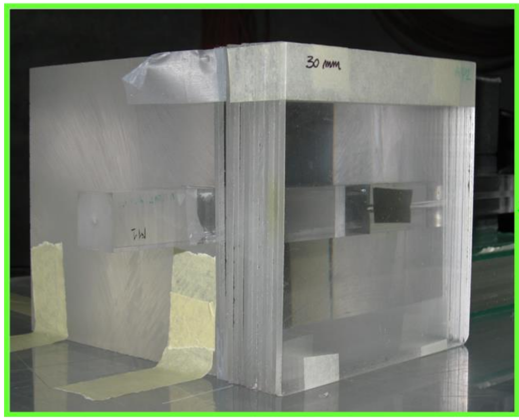

The device was inserted in a PMMA cube. At each measurement position, an adequate number of PMMA foils was located in front of the detector in order to reproduce the desired depth.

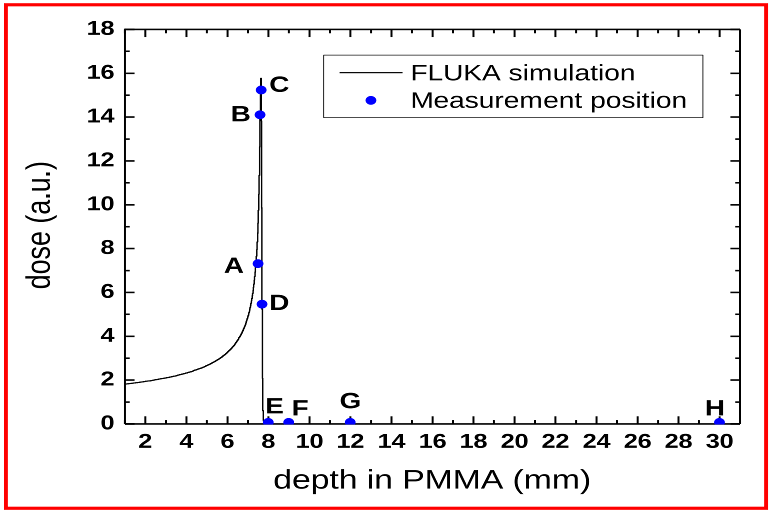

Experimental set-up

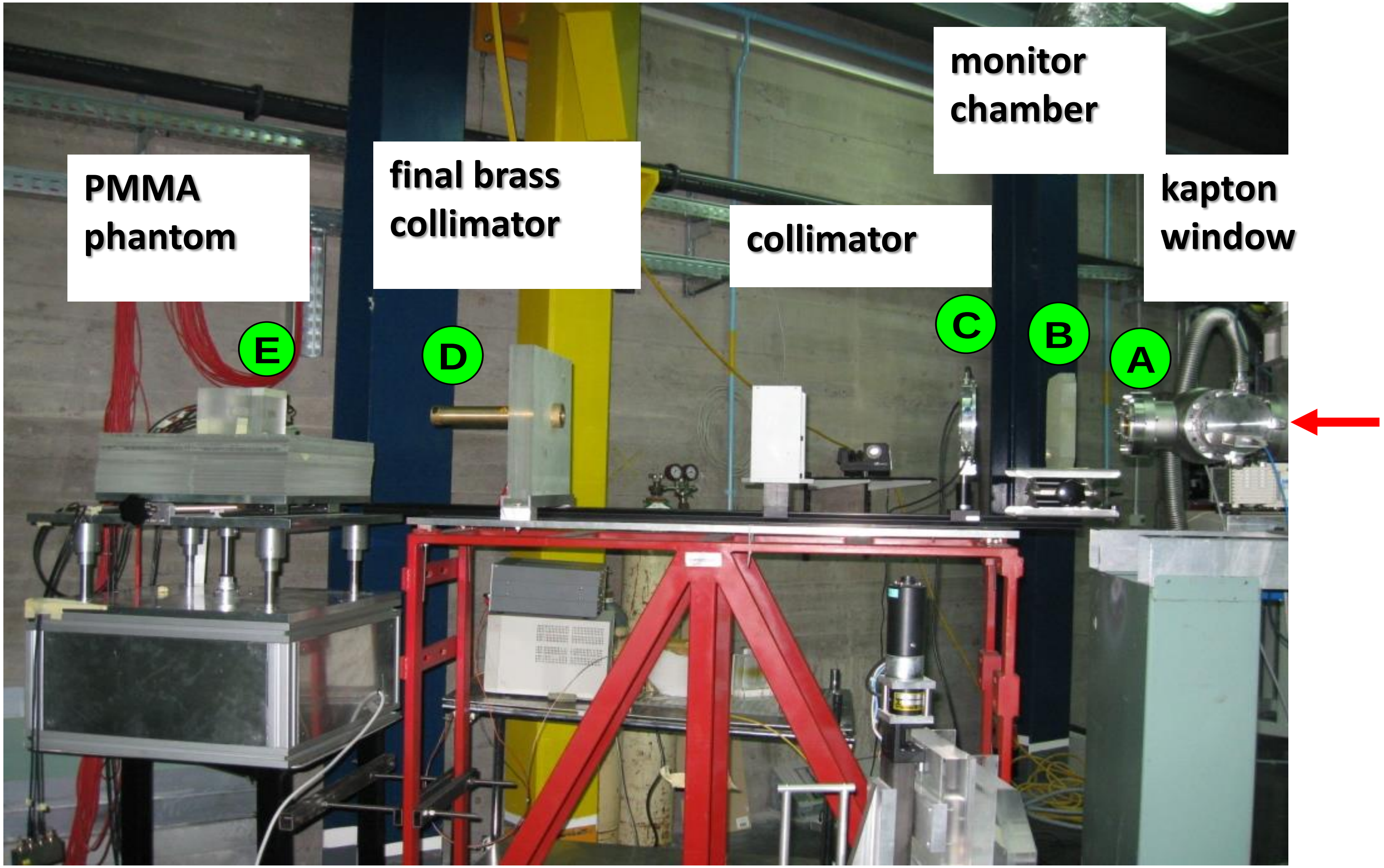

Measurements across the Bragg peak

ΔE-E scatter plots and lineal energy spectra

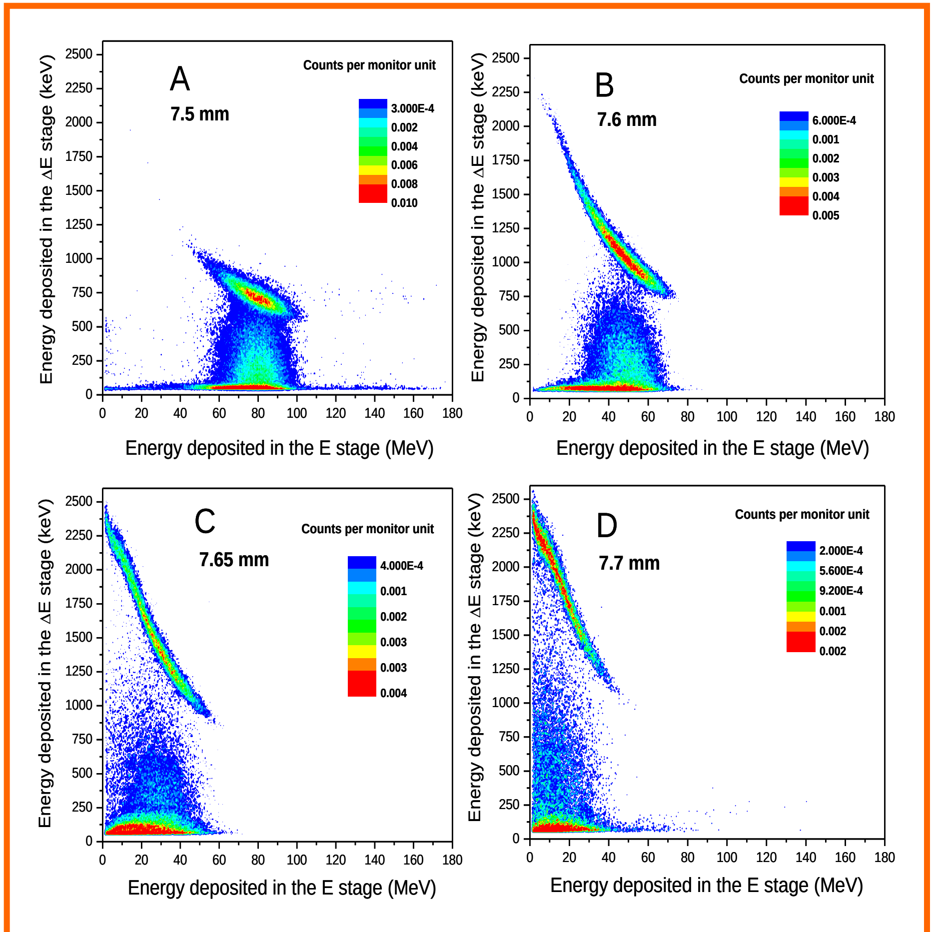

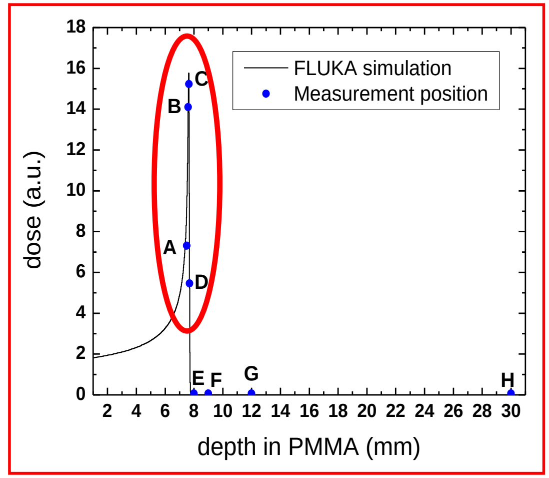

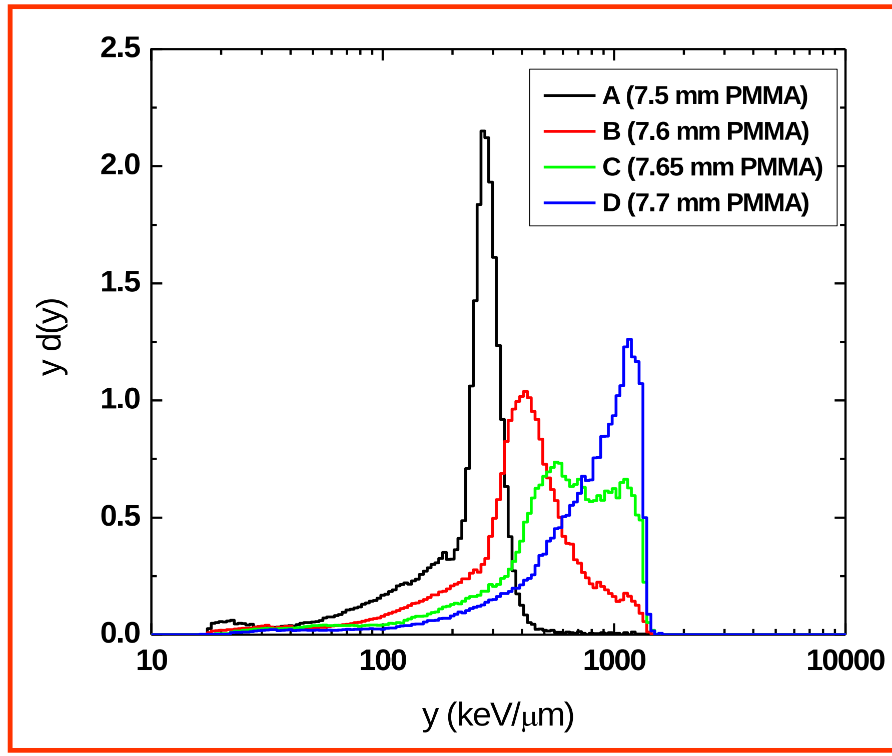

Measurements beyond the Bragg peak

ΔE-E scatter plots and lineal energy spectra

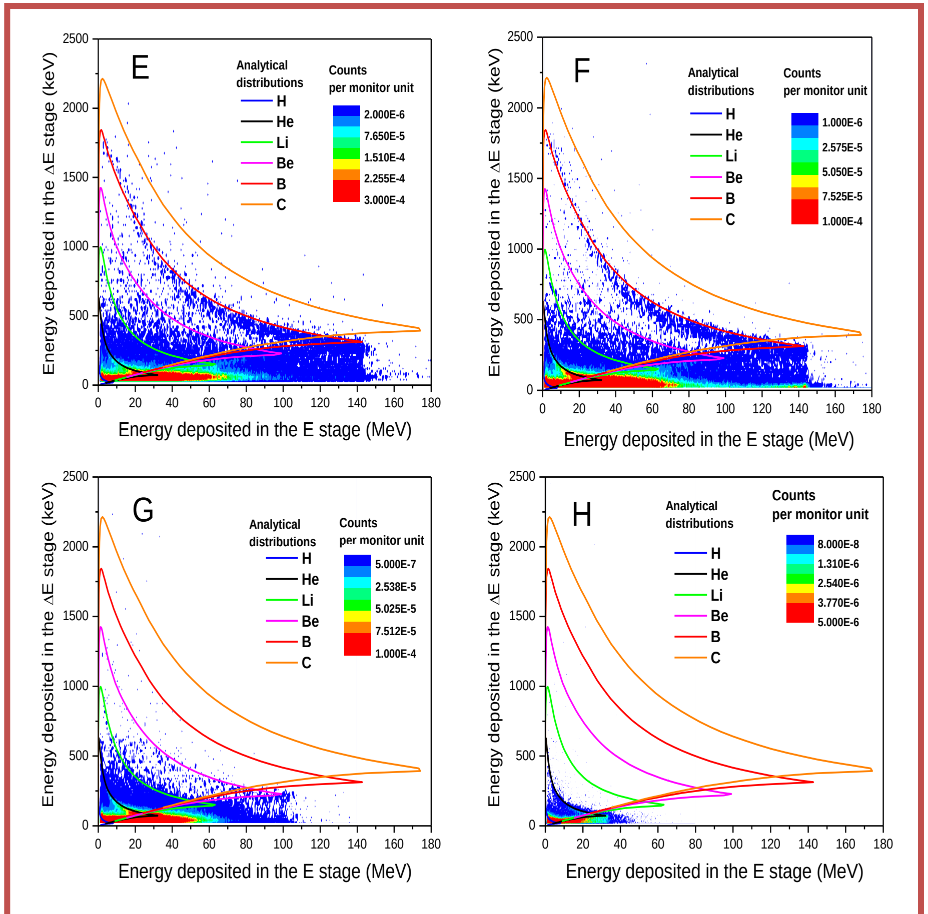

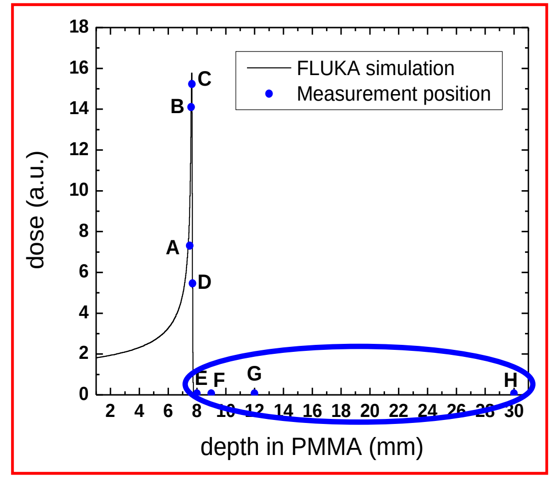

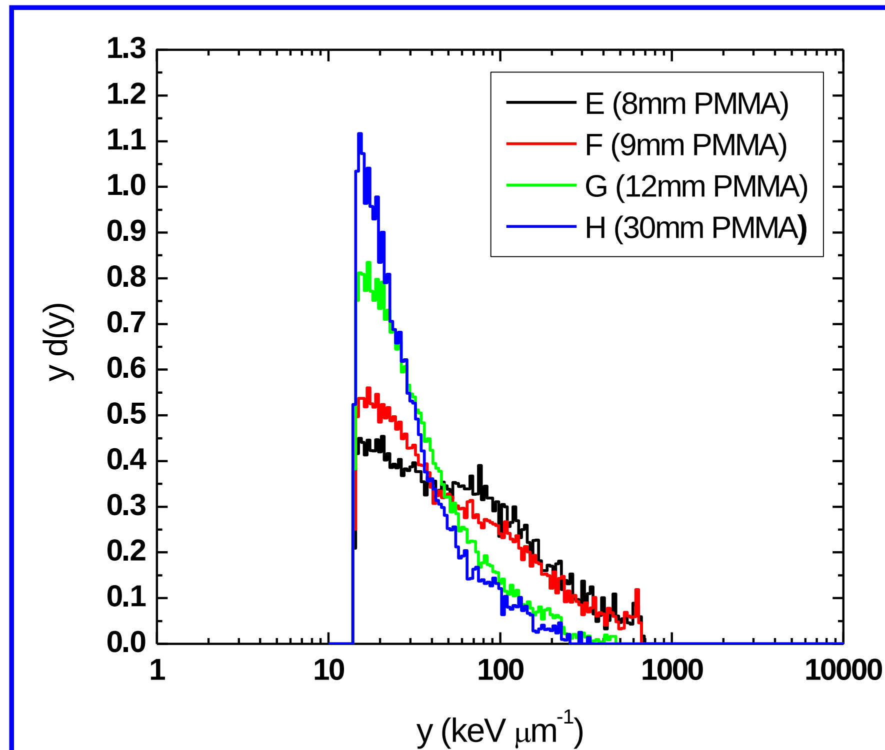

A silicon microdosimeter integrated into a nanodosimeter: BIOQUART and MITRA projects

Idea:

to substitute the nanodosimeter trigger detector with a silicon telescope in order to derive the nanodosimetric and the microdosimetric information event-by-event at same time

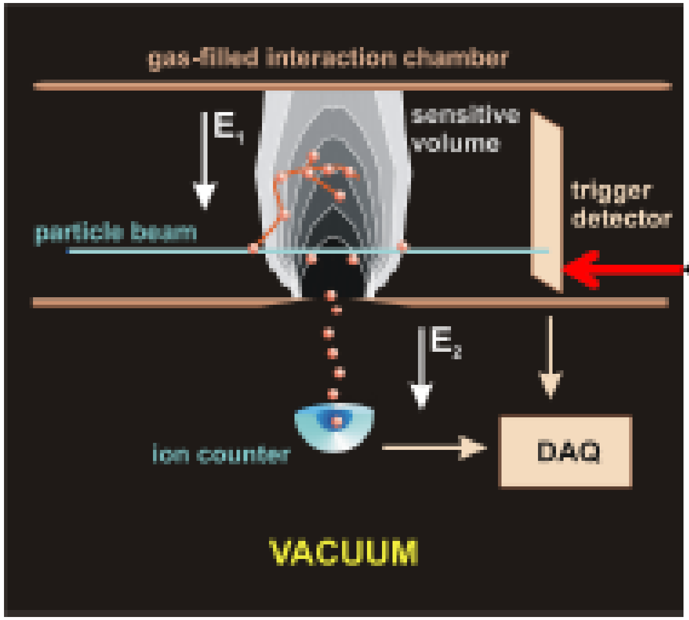

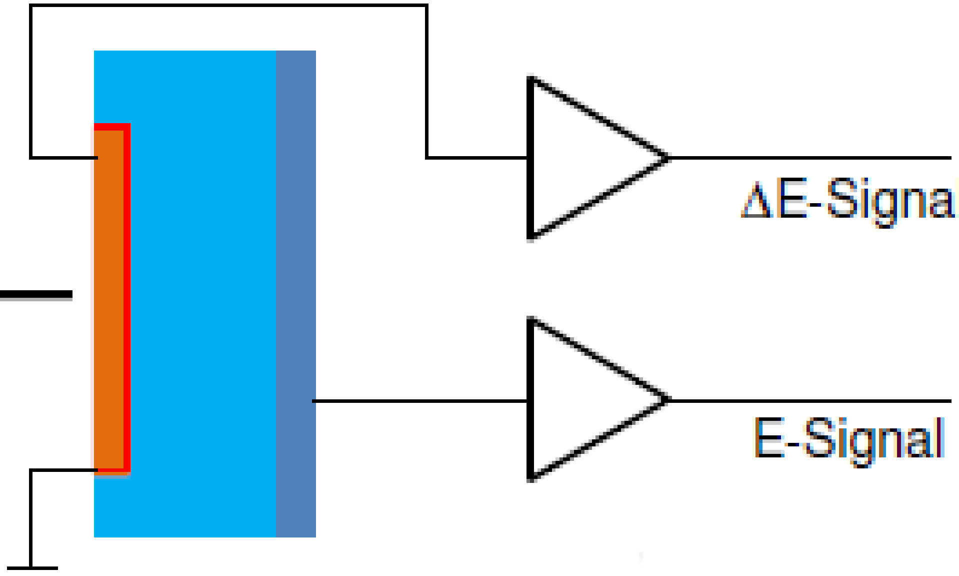

Irradiations with protons and alphas @ PTB: preliminary results

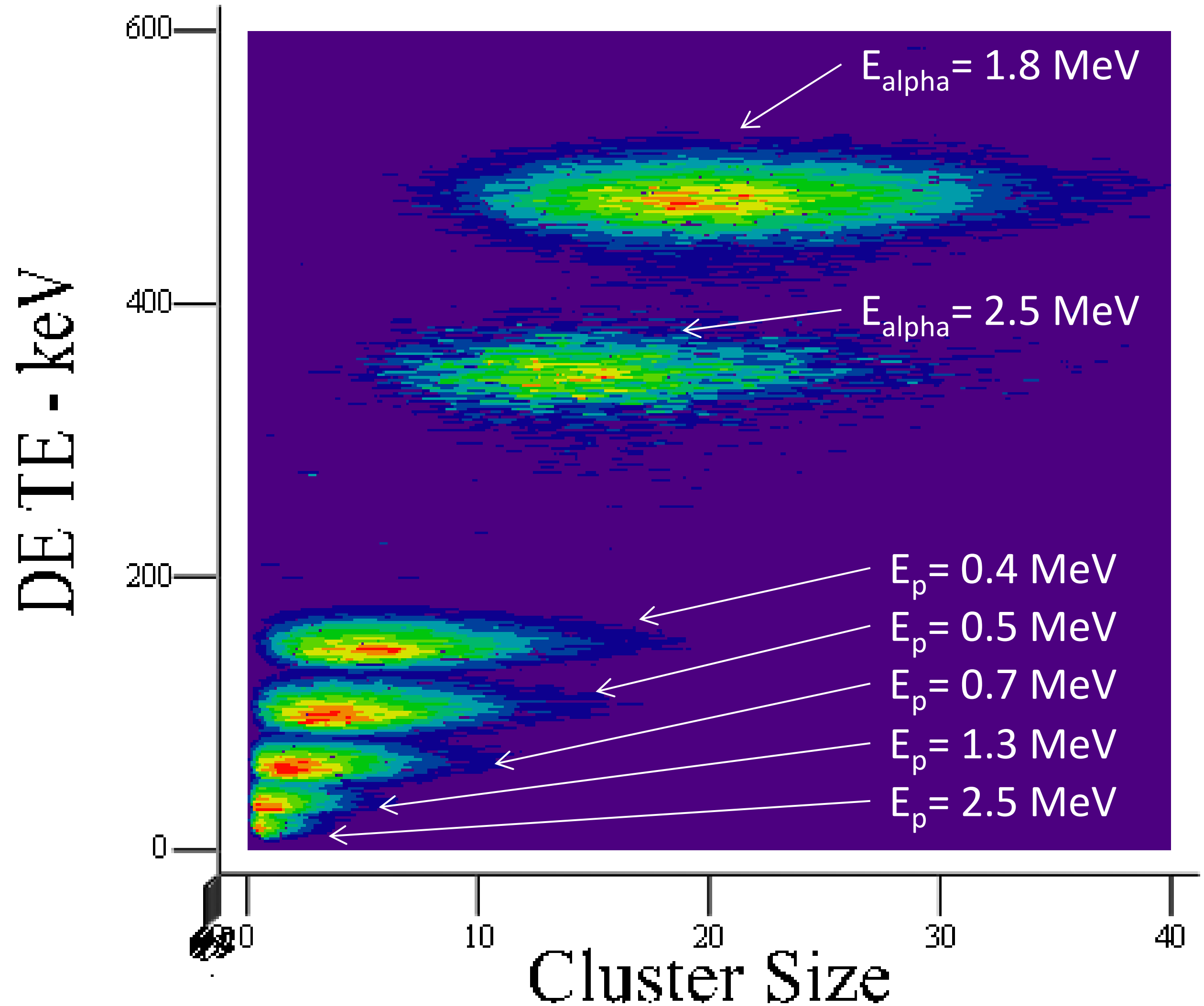

Limitations and open issues

- Radiation damage — protons and carbon ions @ clinical currents;
- Electronic noise — contribution of electrons to spectra;
- Dead layer — heavy recoils;
- Sensitive area ratio — E count rates much higher than those of ΔE;

- Detailed analysis of the charge collection process ;
- Study of behaviour in pulsed beams (sincrotrons);
- Set-up improvement


That's all Folks!

Conclusions

The monolithic silicon telescopes which differ in the geometrical structure of the ΔE detector were characterized with 62 AMeV carbon ions.

Microdosimetric distributions of the hadron beam were measured at different depths within a PMMA phantom

The experimental results were compared with those obtained by a numerical study based on Monte Carlo simulations (FLUKA code)

The comparison highlighted that events collected by the segmented telescope at low lineal energy values are not due to geometrical effects but probably to charge sharing between the ΔE electrode and the guard ring.

Further investigations are needed to better evaluate the charge sharing effect…

…, especially in view of the production of new devices in collaboration with ST-microelectronics

Measurement set-up

The measurements were performed by inserting two different sample detectors in a polymetilmetacrylate (PMMA) phantom at different depths

#1: single stage ΔE detector

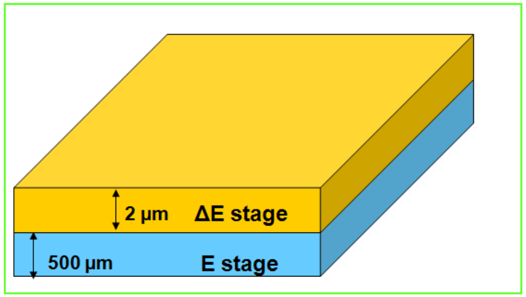

#2: segmented ΔE detector

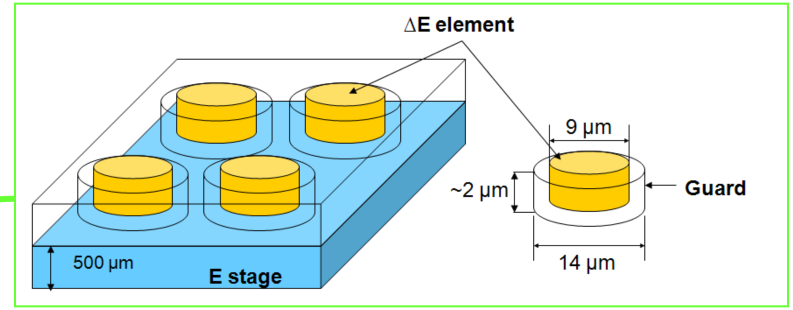

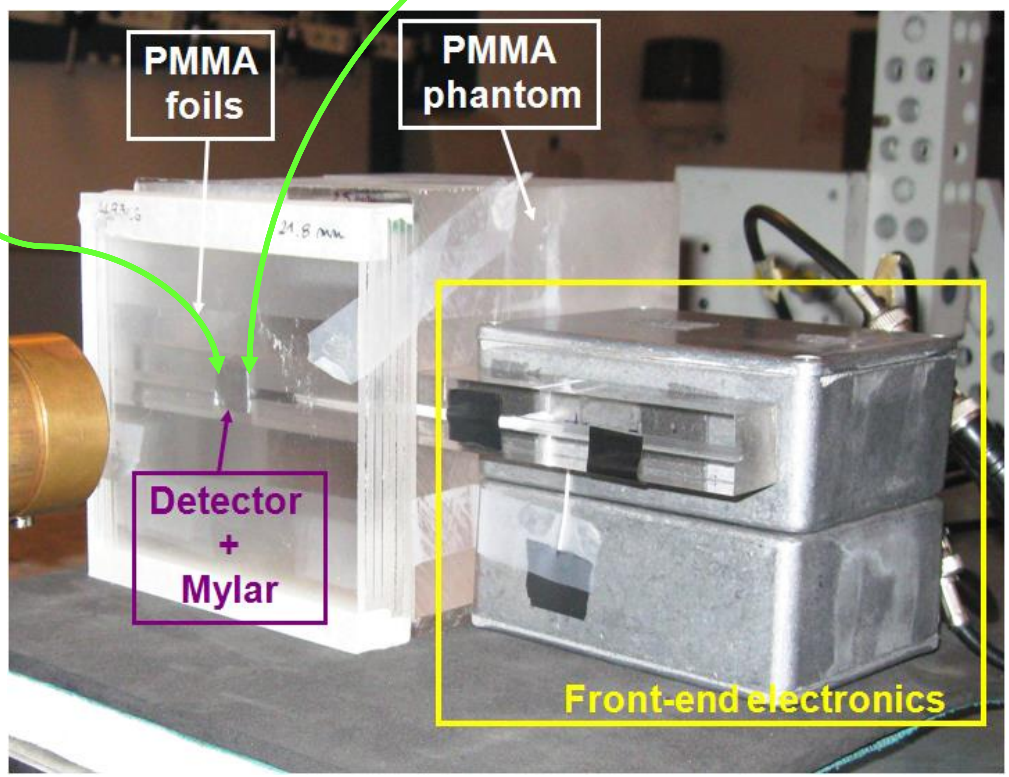

Experimental Results

The depth dose profile was characterized by a plane parallel advanced PTW Markus ionization chamber inserted in a water phantom. The measurement positions in a PMMA phantom were selected with respect to the reference profile obtained and by taking into account the difference in the phantom material.

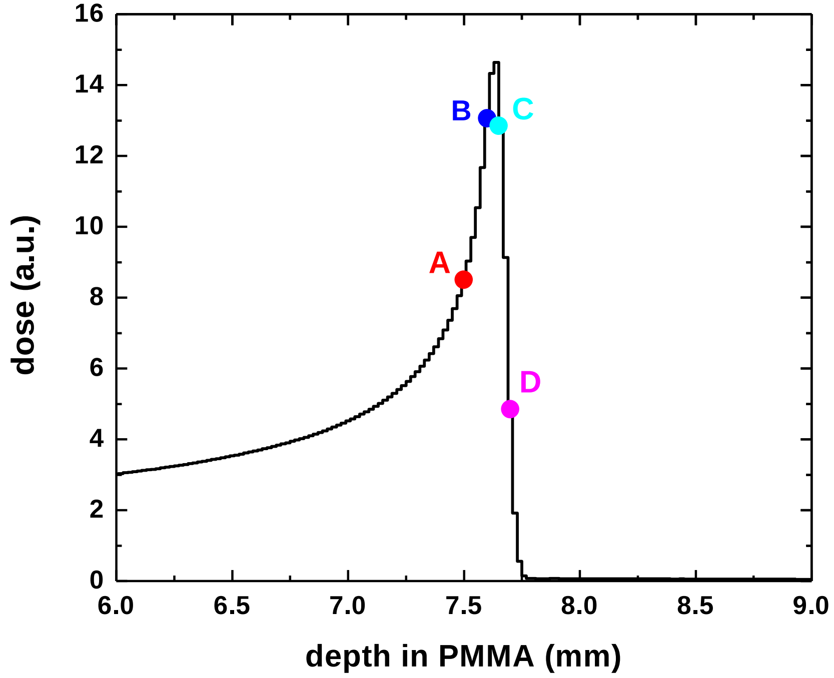

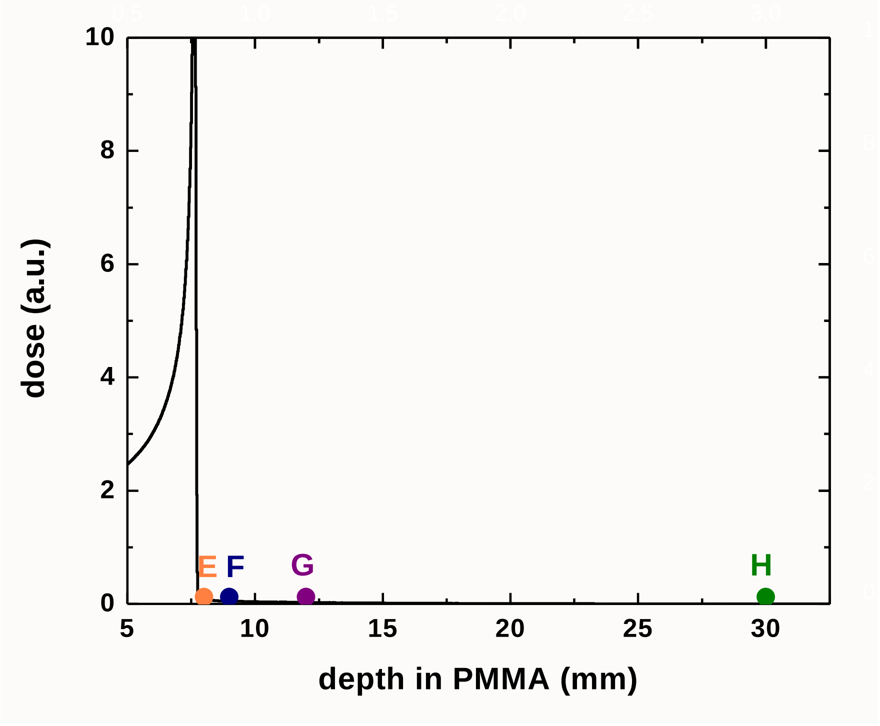

Experimental Results: measurements across the carbon Bragg peak

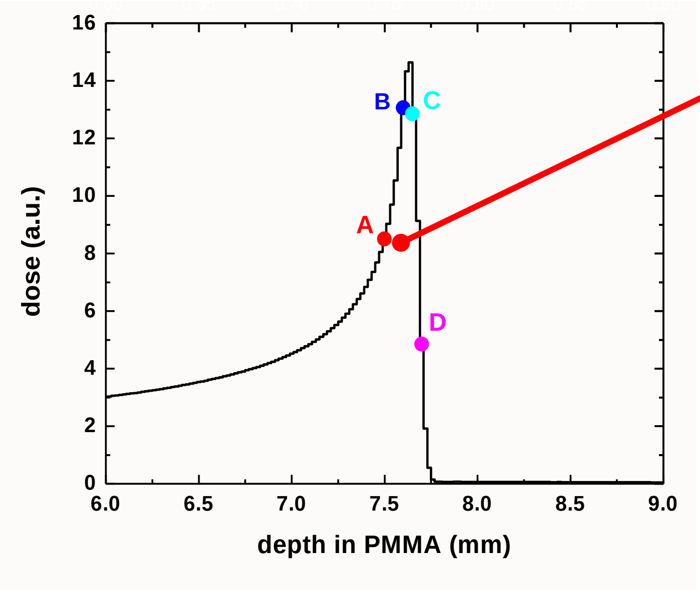

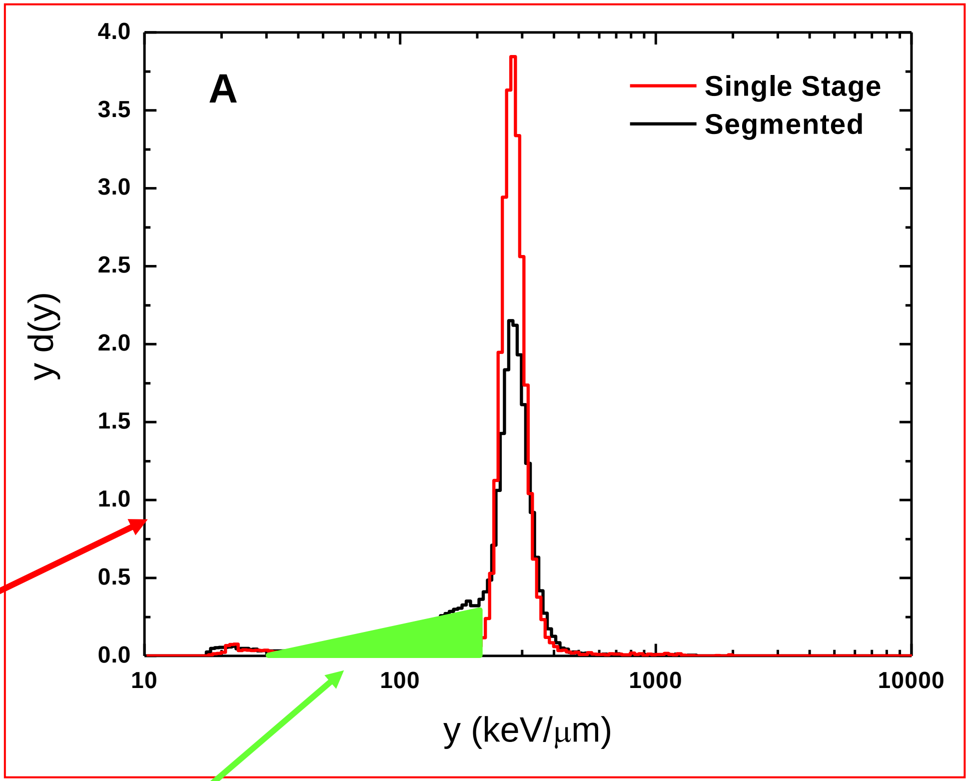

Tail ascribed to:

i) the track length distribution

ii) charge sharing

Experimental Results: measurements across the carbon Bragg peak

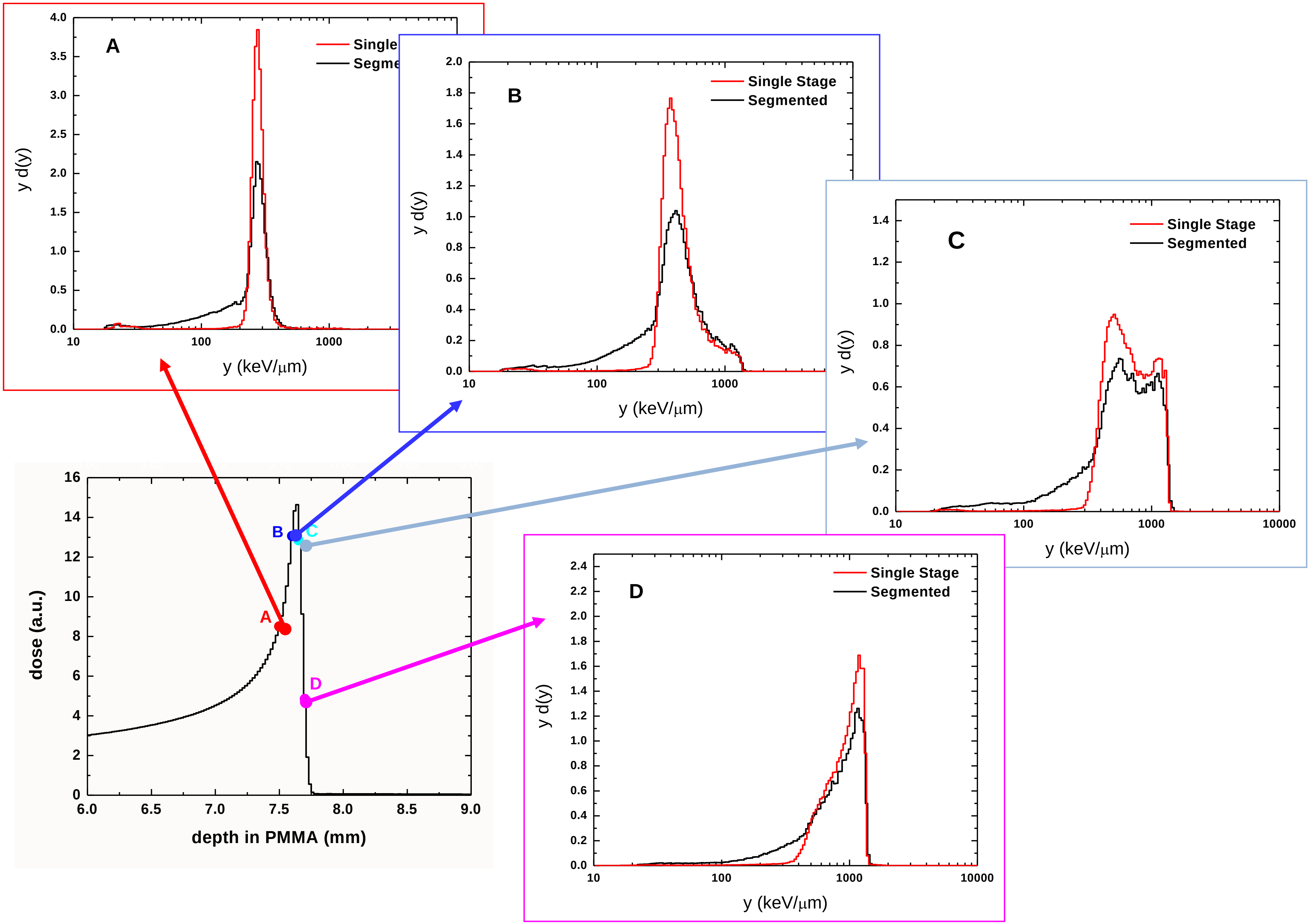

Experimental Results: measurements beyond the carbon Bragg peak

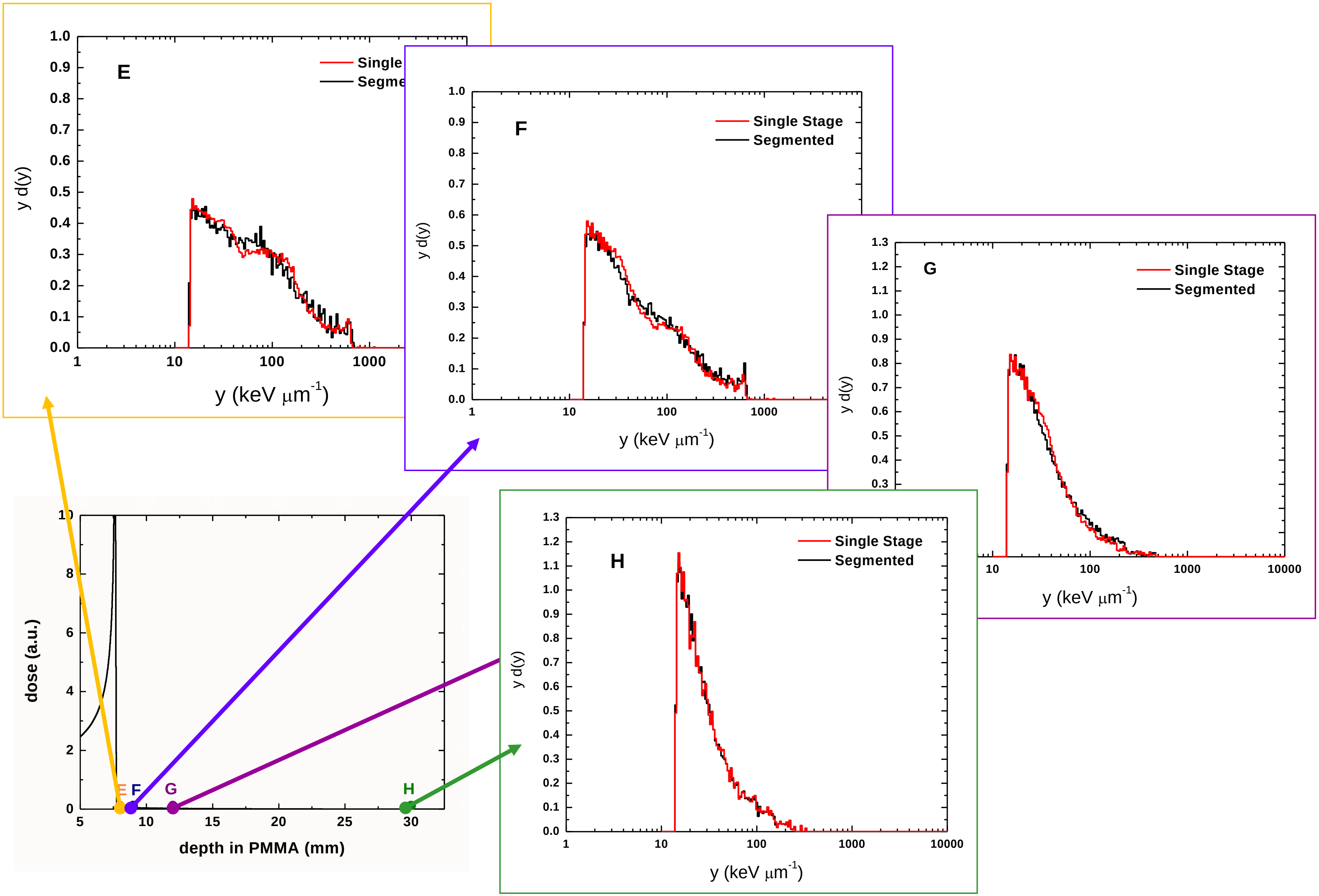

Numerical study: simulation with FLUKA Monte Carlo code

A detailed numerical study based on Monte Carlo simulations was carried out through the FLUKA code version 2012, a recent release able to transport heavy ions at energies lower than 100 AMeV (the older lower transport limit) by exploiting the new Boltzmann Master Equation model.

- **To optimize the calculation time, the transport of secondaries, especially electrons, was perform in details only in the detector and in a region of PMMA around it**

- **The energy imparted in the two detector stages at different depths in phantom was calculated on an event-by-event basis by multiple scattering transport.**

Numerical study: depth dose profile

Comparison between results of Fluka simulation and those obtained experimentally by a plane parallel advanced PTW Markus ionization chamber

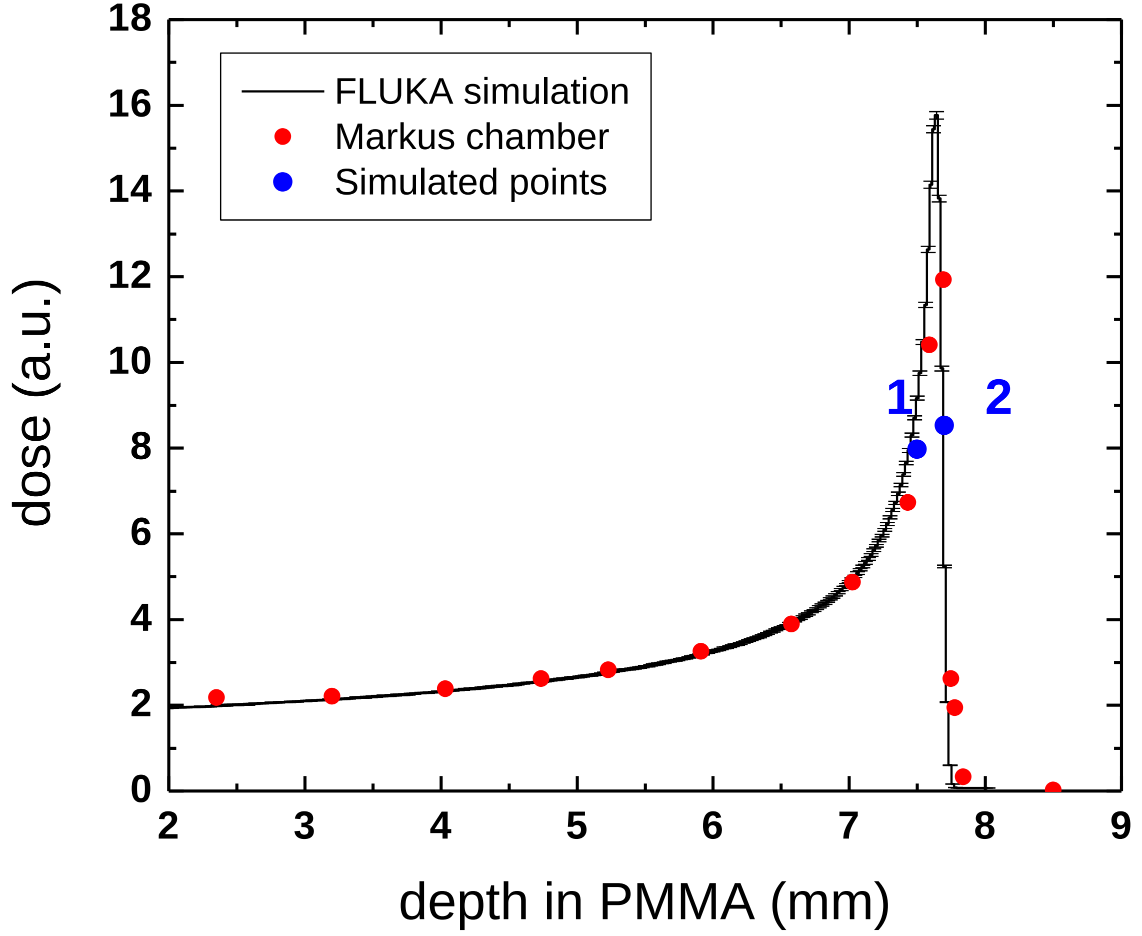

Numerical study: microdosimetric spectra

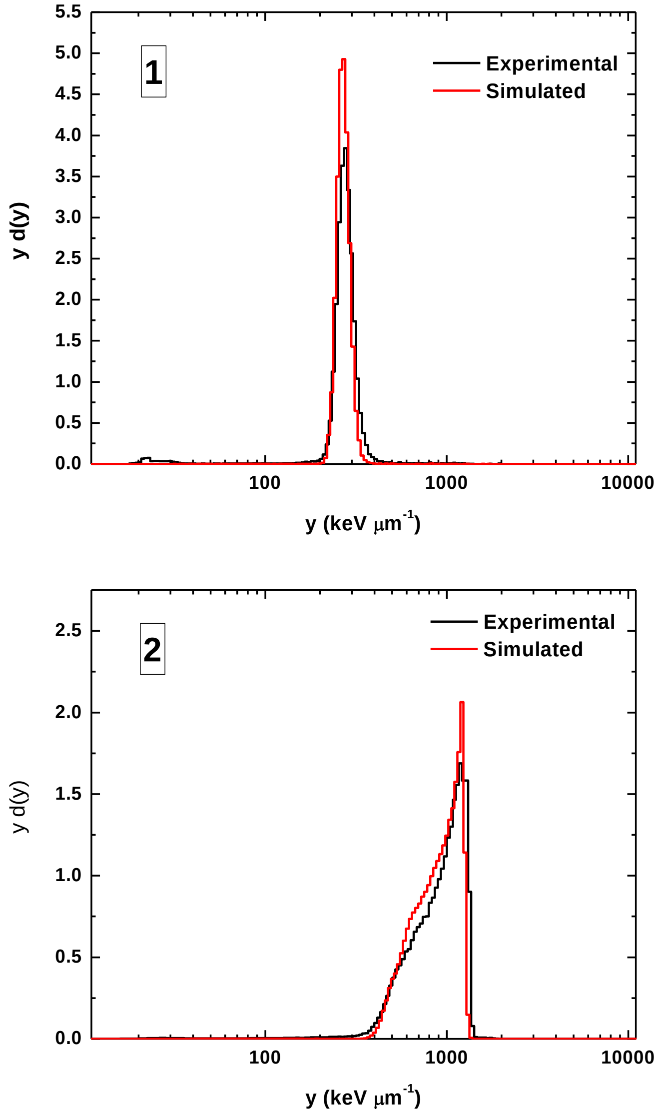

Segmented ΔE detector

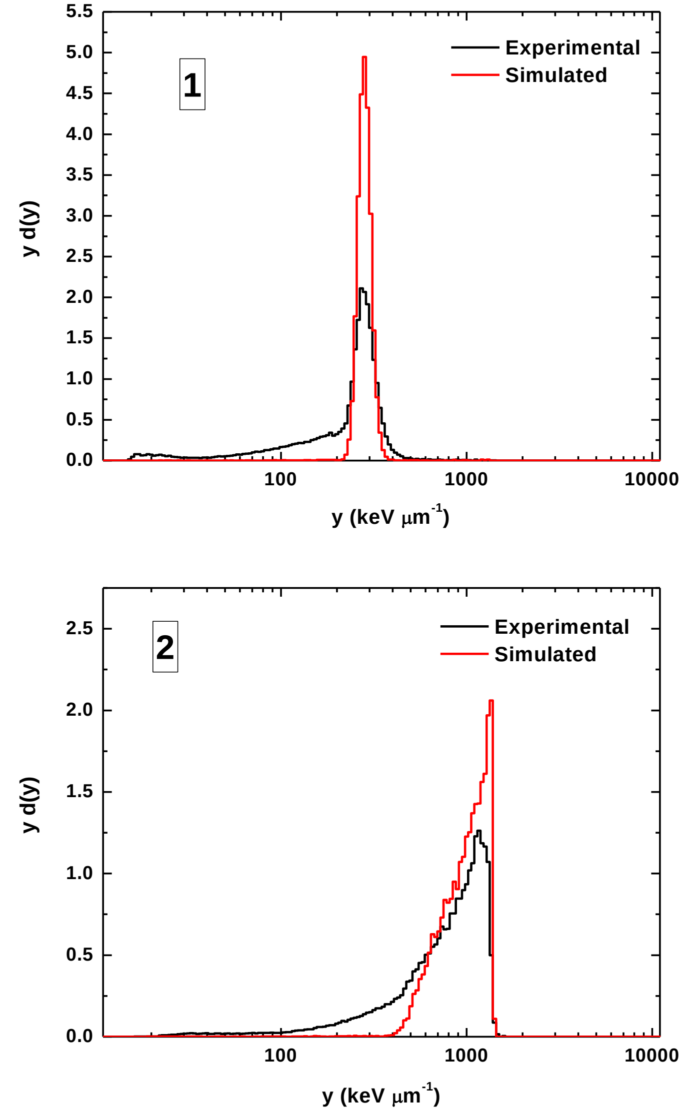

Numerical study: microdosimetric spectra

The simulated microdosimetric spectra do not change significantly by changing the detector geometry. In particular no events at low y values are foreseen…

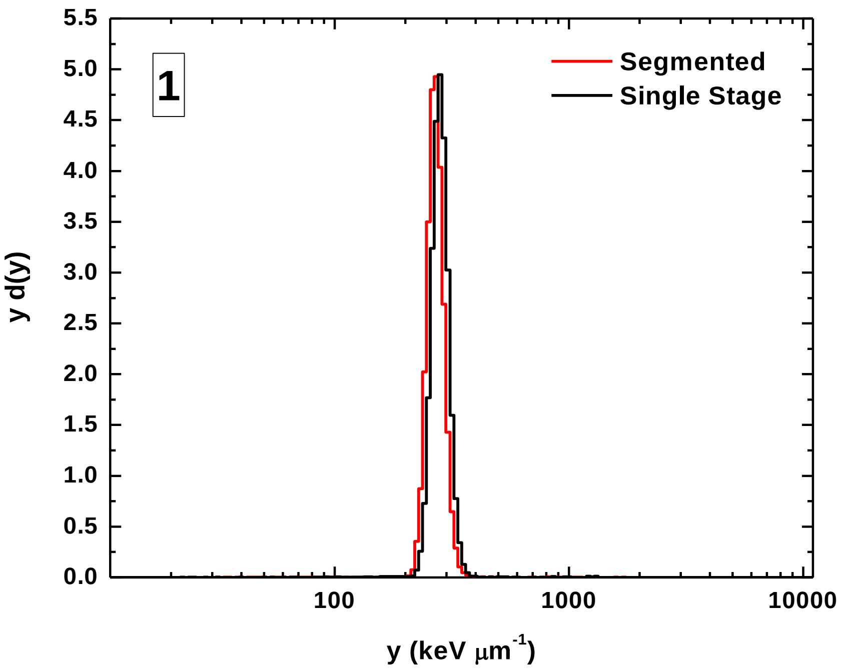

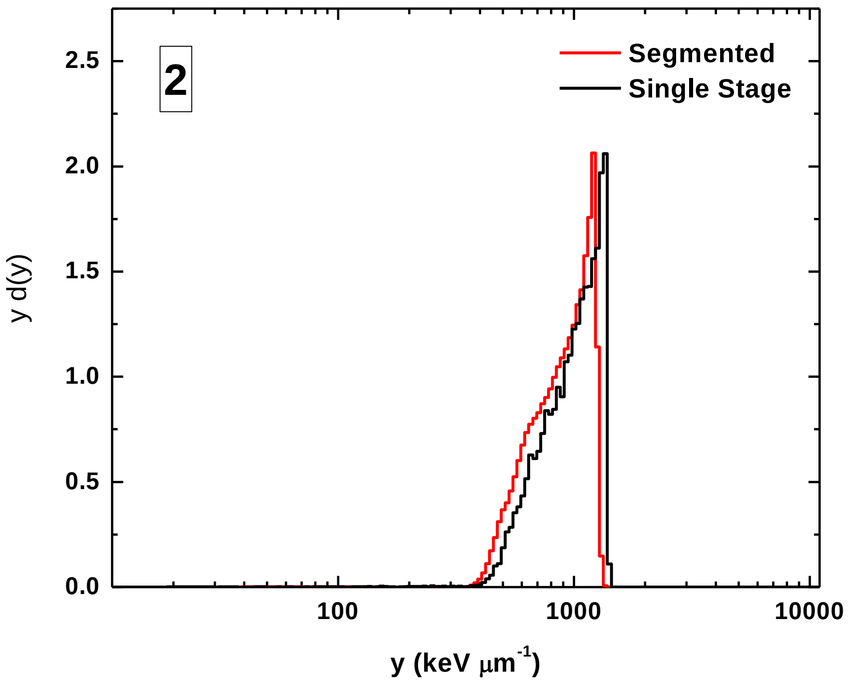

Discussion

The experimental behaviour of the segmented monolithic silicon telescope at low y values could be due to border effects, … in particular

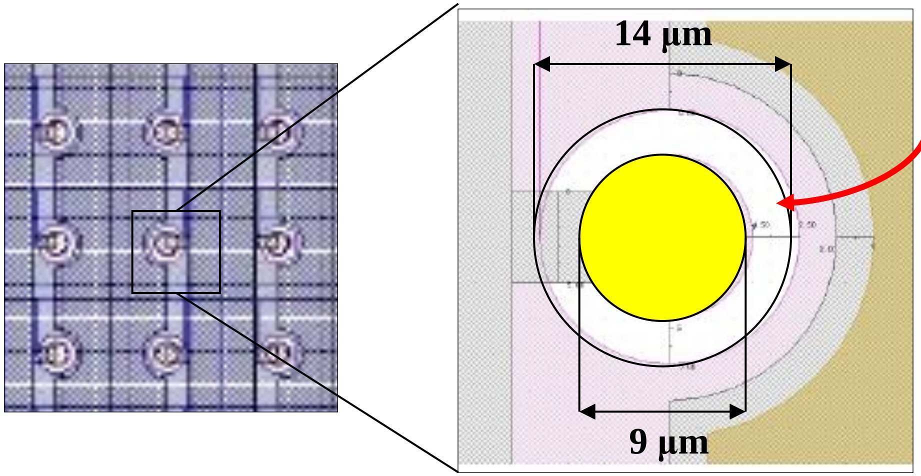

Charge sharing between the ΔE electrode and the associated guard ring which lead to partial charge collection

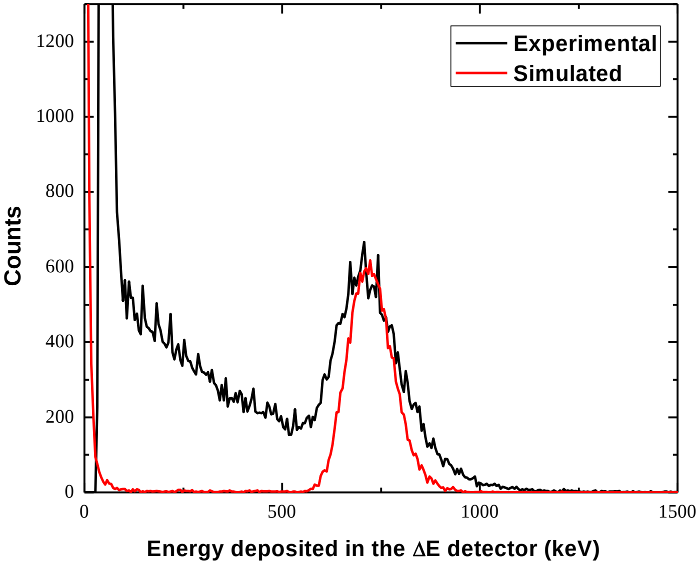

Events affected by partial charge collection are about 50% of total events

Electrode area: ≈ 64 µm²
Guard ring area: ≈ 154 µm²

The ratio of the areas is consistent with that of events

Test: ΔE detector with a volume shaped as a truncated cone